Prepared for the
AIR POLLUTION CONTROL OFFICE
by the
TENNESSEE VALLEY AUTHORITY
1971

PB 202 407

INVESTIGATION OF THE REACTIVITIES OF
LIMESTONE TO REMOVE SULFUR DIOXIDE
FROM FLUE GAS

INVESTIGATION OF THE REACTIVITIES OF LIMESTONE TO REMOVE SULFUR DIOXIDE FROM FLUE GAS

Reproduced by
NATIONAL TECHNICAL
INFORMATION SERVICE
Springfield, Va. 22151

4Y A

156

PB-202 407

BIBLIOGRAPHIC DATA SHEET

1. Report No. APTD-0699

2.

3. Recipient's Accession No.

4. Title and Subtitle
Investigation of the Reactivities of Limestone to Remove Sulfur Dioxide From Flue Gas

5. Report Date June 30, 1970

6.

7. Author(s) J. D. Hatfield, Y. K. Kim, R. C. Mullins, and G. H. McClellan

8. Performing Organization Rept. No.

9. Performing Organization Name and Address
Division of Chemical Development
Tennessee Valley Authority
Muscle Shoals, Alabama 35660

10. Project/Task/Work Unit No.

11. Contract/Grant No.
TV-29232A and
TV-30530A

12. Sponsoring Organization Name and Address
Air Pollution Control Office
Environmental Protection Agency
Post Office Box 12055
Research Triangle Park, North Carolina 27709

13. Type of Report & Period Covered

14.

15. Supplementary Notes DISCLAIMER - This report was furnished to the Office of Air Programs by Tennessee Valley Authority, Division of Chemical Development, Fundamental Research Branch, Muscle Shoals, Alabama 35660, in fulfillment of contract Nos. TV-29232A and TV-30530A.

16. Abstracts

An investigation has been conducted, concerning the properties of a limestone that are important in determining its effectiveness when injected into a combustion chamber to decrease the emission of SO_2 in the stack gas from burning sulfur-containing fuel in a power plant. To obtain this information, reactivities of thirty-five stones were measured and correlated with their mineralogical and crystallographic properties. Rates and capacities of sulfation were taken as measures of reactivity. The report is divided into three parts: reaction mechanisms and kinetics, properties of calcines and sulfated limestones, and evaluation of the reactivities of selected limestones toward SO_2.

17. Key Words and Document Analysis. 17a. Descriptors
Desulfurization
Flue gases
Limestone
Chemical reactivity
Reaction kinetics
Sulfation
Disproportionation
Calcines

17b. Identifiers/Open-Ended Terms
Calcination

17c. COSATI Field/Group 13B, 7D

18. Availability Statement Unlimited

19. Security Class (This Report) UNCLASSIFIED

20. Security Class (This Page) UNCLASSIFIED

21. No. of Pages 136

22. Price

FORM NTIS-35 (10-70)

USCOMM-DC 40329-P71

C

Tennessee Valley Authority
Division of Chemical Development
Fundamental Research Branch

INVESTIGATION OF THE REACTIVITIES OF LIMESTONE TO REMOVE SULFUR DIOXIDE FROM FLUE GAS

By

J. D. Hatfield, Y. K. Kim, R. C. Mullins, and G. H. McClellan

Muscle Shoals, Alabama 35660

INVESTIGATION OF THE REACTIVITIES OF LIMESTONE TO REMOVE SULFUR DIOXIDE FROM FLUE GAS

SUMMARY

To provide a guide for the selection of limestones for dry injection to absorb sulfur oxides from power plant combustion systems, the reactivities of thirty-five stones were measured and correlated with their mineralogical and crystallographic properties.

Rates and capacities of sulfation were taken as measures of reactivity. Both isothermal and polythermal measurements were made in a standard laboratory TGA apparatus that had an upper temperature limit of 940° C. The mineralogical and crystallographic properties were determined by petrographic and electron microscopy and by x-ray methods.

Calcination of the limestone proceeds from the outside surface toward the center of each particle. The rate of calcination is affected by the reaction temperature, the particle size of the stone, the crystallite size of the carbonate mineral in the stone, the relative amounts of magnesium and calcium in the stone, and the partial pressures of CO_2 and SO_2 in the furnace atmosphere. The reaction of CaO with SO_2 and O_2 at 915° C. is first order with respect to the partial pressure of SO_2 in the range 1 to 8.4% by volume, zero order with respect to the partial pressure of O_2 in the range 1 to 10% by volume, and zero order with respect to the loading of product until the layer of $CaSO_4$ completely

shields the available reaction surface. Below 640° C., the formation of sulfite predominates over that of sulfate, and the oxidation of sulfite to sulfate begins at about 720° C.; the sulfite also begins to decompose and to disproportionate in this temperature range. Disproportionation of sulfite at 880° C. is prevented by the presence of oxygen or CO_2, either of which promotes the formation of sulfate. The first-order specific rate constants for the decomposition of $CaSO_3$ and $CaSO_4$ and the loss of reactivity (dead-burning) of a high calcitic (Colbert) limestone were expressed in Arrhenius form.

Water vapor affects the rate of reaction of SO_2 with MgO but not with CaO; the reaction with MgO is too slow to be important under injection conditions. The direct substitution of SO_2 for CO_2 in the limestone also is too slow to be significant under injection conditions. The sulfation reaction occurs simultaneously with the calcination reaction when the rate of the calcination reaction is low; sulfation is most rapid, however, when there is a relatively large surface of unreacted CaO. The products of the sulfation reaction retard the calcination reaction when the two reactions occur simultaneously.

The physical properties of a calcine and its reactivity with SO_2 are influenced markedly by the texture of the parent limestone from which the calcine is formed. An Iceland spar, of mean crystallite size 7125 Å., calcined slowly below 950° C. because of its high thermal stability, and yielded a calcine with small pores and small crystallites of CaO. A very pure calcitic limestone, of mean crystallite size 3875 Å.,

yielded larger crystallites of CaO than did the Iceland spar under the same conditions, but the pore volume was larger and more favorably distributed among different sized pores for reaction with SO_2. Between 1000° and 1100°C. the calcines of both materials showed a minimum in pore volume, which was interpreted as the end of sintering and the beginning of recrystallization of the CaO. During sintering, small pores coalesce into larger pores with small changes in the crystallite size of the oxide; during recrystallization the crystallites grow into massive single crystals of CaO at rates proportional to the crystallite size of the original carbonate. The Iceland spar was less reactive with SO_2 than was the calcitic limestone under all the experimental conditions tested because of its slower calcination, its unfavorable pore-size distribution and pore volume, and its more rapid recrystallization. Electron microscope photographs of cleaved sulfated particles of these stones showed clearly the reaction zone between oxide and sulfate and the growth of the crystallites of sulfate at the outer surface.

A dolomite of mean crystallite size 2075 Å. was much superior to a calcite of mean crystallite size 3875 Å. in the absorption of SO_3 when calcined for 1 or 4 minutes at 1100° or 1225° C. The properties of the calcines that influence the absorption of SO_3 were affected by the time and temperature of calcination, by the particle size, and by the type of stone. Several interactions of factors affecting the various properties of the calcines were identified, including some three-factor interactions. It is shown that the temperature of calcination of the dolomite and the time of calcination of the calcite were the more critical factors that affect the SO_3 absorption capacity of the two stones.

Studies were made of the calcination, isothermal sulfation, and polythermal calcination-sulfation of 35 limestones, and the distinguishing characteristics of each reaction were correlated with the chemical and mineralogical properties of the stones. Six measures of the capacity and rate of reaction with SO_2 were correlated with the chemical and mineralogical properties of the stones, as well as with the reaction parameters. Multiple correlations of the capacity and rate parameters with the properties of the stones yielded equations from which the reactivity of a stone could be predicted from its chemical and mineralogical characteristics. The equations were tested with five stones considered for use in the Shawnee tests, using the reaction rate data at five temperatures obtained by Battelle in the dispersed-phase reactor. The prediction of the polythermal capacity for absorption of SO_2 from the chemical and mineralogical properties of the stones correlated well with the Battelle reaction rates at temperatures below 940° C. (1724° F.), but not at higher temperatures. No other predicted reactivity measure correlated significantly with the Battelle rate at any temperature.

The equations that express the polythermal capacity for absorption of sulfur oxides, w_3, mg. SO_3/50 mg. limestone, are

$$w_3 = -1.571z_4 + 5.685z_5 - 32.14z_6 + 3.603z_7 - 0.3280z_9 + 2.818z_{10}$$

$$\log w_3 = 0.05114z_2 - 0.06688z_4 + 0.2942z_5 + 0.1834z_7 - 0.01403z_9 + 0.1200z_{10}$$

where z_2 = (% rhombic carbonates)/(%CaO)

z_4 = microscopic grain size (coded)

z_5 = unit-cell length, a, of the carbonate mineral, Å.

z_6 = x-ray crystallite size of the carbonate mineral, microns

z_7 = log (Na_2O content of limestone, %)

z_9 = sum of contents of illite, montmorillonite, tremolite, limonite, feldspar, and muscovite, %

z_{10} = (% limonite)/(% total Fe_2O_3)

The best estimate of the value of w_3 is the arithmetic average of the values calculated from these two equations.

Although the data obtained at the temperatures accessible in this experimental study do not extrapolate well to the higher temperatures that are encountered in actual power-plant combustion chambers, the properties of stones that were shown to be desirable at low temperatures probably will be advantageous at the furnace temperatures also. Perhaps the major difference to be expected between the results obtained at low temperatures and those anticipated at high temperatures is the marked increase in the rate and extent of dead-burning at the high temperatures, as indicated by the results of the x-ray examinations. No way of avoiding the detrimental effect of rapid dead-burning at temperatures above about 1050° C. is indicated by our data. Our data indicate that stones that contain the smallest amounts of impurity minerals and whose rhombic carbonates are primarily calcitic and are present as the smallest crystallites will be the most effective for injection into the combustion chamber. Increasing the sodium content of the stone increases its reactivity, whereas iron, if present, should be in the form of limonite or goethite rather than in the lattice of the stone.

INVESTIGATION OF THE REACTIVITIES OF LIMESTONE TO REMOVE SULFUR DIOXIDE FROM FLUE GAS

CONTENTS

Page

Introduction 1

Reaction Mechanism and Kinetics 2

  Calcination 2

  Sulfation 6

    Effects of Loading and Composition of Gas 6

    Effect of Temperature 8

    Oxidation 10

  Disproportionation 10

    Decomposition of Sulfation Products 11

    Effect of Water Vapor on the Sulfation of CaO and MgO 11

  Dead-Burning 13

  Substitution 14

Properties of Calcines and Their Sulfated Products 19

  Effect of Texture of Calcites 19

  Electron Microscope Studies of Reaction Surfaces 43

  Properties of Calcite and Dolomite Calcines 48

    Absorption of SO_3 51

    Other Properties of the Calcines 60

Page

Comparison of Limestones 64

  Introduction 64

  Selection of Limestones 66

  Calcination 71

  Sulfation 73

    Isothermal 73

  Polythermal Calcination-Sulfation 73

  Correlations 76

  Multiple Correlations 95

  Application to Stones to be Used in Shawnee Tests 99

References 105

APPENDIX A: Mechanism of Calcination Reaction 107

APPENDIX B: Calculation of Kinetic Parameters for Calcination 109

APPENDIX C: Kinetic Interpretation of Differences Among Stones 111

APPENDIX D: Determination by Regression Analysis of the Significant Factors That Affect the SO_2 Absorption Properties of Limestone 115

APPENDIX E: Multivariate Analysis--A Look at Principal-Components Prediction 118

APPENDIX F: Relative Importance of Properties of Limestones For Reaction With Sulfur Oxides 122

APPENDIX G: The Textural Evolution of Limestone Calcines . .

TABLES

Page

I. Sorption of SO_2 by Lime 11

II. Statistical Summary of Pore-Size Distributions of Calcines 22

III. Bulk Densities of Calcines 28

IV. Properties of Sulfation Products 33

V. Properties of Calcines Under Different Calcination Conditions 50

VI. Analysis of Effects of Factors and Their Interactions on the Properties of Calcines 52

VII. Analysis of Variance for Partial Duplicates of Eight Absorption Samples Using the Average of Three Methods of Analyses 55

VIII. Chemical and Mineralogical Properties of Limestones . . 67

IX. Accessory Mineral Content of Limestones 69

X. Calcination and Isothermal Sulfation of Limestones . . . 74

XI. Polythermal Calcination and Sulfation of Limestones . . 77

XII. Capacity of Limestones for SO_2 and Rate of Sulfation . . 80

XIII. Intercorrelation of Chemical and Mineralogical Properties 83

XIV. Intercorrelation of Calcination and Sulfation Parameters 84

XV. Correlation of Calcination and Sulfation Parameters With Chemical and Mineralogical Properties of Limestones . . 87

Page

XVI. Correlation of Capacities and Rates of Reaction With Chemical and Mineralogical Properties of Limestones . . 88

XVII. Correlation of Capacities and Rates of Reaction With Calcination and Sulfation Parameters of Limestones . . . 88

XVIII. Correlation of Initial Reaction Rate With Chemical Properties and Texture of Limestones 91

XIX. Correlation of Combination Reaction Rate With Chemical Properties and Textures of Limestones 94

XX. Coefficients of Significant Factors in Multiple Correlation Equations 98

XXI. Predicted Reactivity Parameters of Limestones to be Tested at Shawnee 100

XXII. Correlation With TVA Results of Reaction Parameters Calculated From Battelle Data 102

XXIII. Changes in Limestone Properties Required to Produce Measured Changes in Reactivity 123

FIGURES

1. Kinetic Parameters for Calcination, $k = k_o \exp(-E/RT)$. 4

2. Effect of SO_2 and O_2 on Reaction Velocity at 915° C. With Minus 24- Plus 28-Mesh Colbert Limestone 4

3. Effect of SO_2 Concentration on Reaction Velocity 4

4. Effect of Temperature on the Absorption of SO_2 by Calcines of Minus 24- Plus 28-Mesh Colbert Limestone From Gas Containing 4.5% SO_2 9

5. Thermal Decomposition of Calcium Sulfite and Calcium Sulfate 9

Page

6. Effect of Water Vapor on the Sulfation of MgO and Limestone Calcine 12

7. Effect of Calcination Temperature on the Specific Rate of Loss of Reactivity With SO_2 12

8. Calcination and Sulfation at 890° C. Without CO_2 17

9. Calcination and Sulfation at 890° C. With 9.5% CO_2 . . . 17

10. Calcination and Sulfation at 855° C. With 16% CO_2 . . . 17

11. Mean Pore Size of 16-Hour Calcines 23

12. Frequency Distribution of Pores in 16-Hour Limestone Calcines 25

13. Frequency Distribution of Pores in 16-Hour Iceland Spar Calcines 25

14. Pore Volumes of 16-Hour Limestone Calcines 26

15. Pore Volumes of 16-Hour Iceland Spar Calcines 26

16. Mean Crystallite Sizes of 16-Hour Calcines 29

17. Crystallite Sizes of Calcines Heated Continuously at 6° C. per Minute 29

18. Surface Fractures on the Cleaved Surface of a Calcined Single Crystal of Calcite. 12,000X 45

19. Reaction Zone of Calcined Single Crystal of Calcite After Exposure to Sulfur Dioxide. 12,000X 46

20. Isopleths of SO_3 Absorption as Functions of the Time and Temperature of Calcination 58

21. Calcination and Sulfation of a Calcite, BCR 1679 72

Page

22. Calcination and Sulfation of a Dolomite, BCR 1690 . . . 72

23. Comparison of Calculated Reaction Parameters With Battelle's Apparent Reaction Rates 103

24. Relation Between Reduced Time and Degree of Calcination of Minus 24- Plus 28-Mesh Colbert Limestone 103

25. Effects of Amount of Injected Limestone and Kinetic Parameters on the Desulfurization of Stack Gas 114

26. Number of Roots Required to Explain Variations Among 13 Measured Properties of Limestones 120

INVESTIGATION OF THE REACTIVITIES OF LIMESTONE TO REMOVE SULFUR DIOXIDE FROM FLUE GAS

by

J. D. Hatfield, Y. K. Kim, R. C. Mullins, and G. H. McClellan

Division of Chemical Development
Tennessee Valley Authority
Muscle Shoals, Alabama 35660

INTRODUCTION

This investigation, conducted under APCO (formerly NAPCA) Contracts TV-29232A and TV-30530A, is concerned with the properties of a limestone that are important in determining its effectiveness when injected into a combustion chamber to decrease the emission of SO_2 in the stack gas from burning sulfur-containing fuel in a power plant. The report is divided into three parts: reaction mechanisms and kinetics, properties of calcines and sulfated limestones, and evaluation of the reactivities of selected limestones toward SO_2. This report covers work done during the period July 1, 1968, through June 30, 1970.

REACTION MECHANISMS AND KINETICS

In a study of the properties of limestones that determine their reactivities with sulfur oxides in flue gas, it was necessary to study and define the reactions that occur. The following is a summary of the reactions that occur when limestone is injected into a power plant combustion chamber to decrease the emission of sulfur dioxide in the stack gases.

Calcination

The reactions

$$CaCO_3 \rightarrow CaO + CO_2 \qquad (1)$$

$$MgCO_3 \rightarrow MgO + CO_2 \qquad (2)$$

occur when limestone is heated to a sufficiently high temperature. For most limestones, decomposition begins in the temperature range 600° to 700° C. (1100° to 1300° F.) and accelerates as the temperature is raised. The rate of calcination is affected by the temperature, by the particle size of the limestone, by the microscopic or x-ray crystallite size of the carbonate fraction, by the proportion of $MgCO_3$ and $CaCO_3$ in the limestone, and by the partial pressure of CO_2 in the calcining atmosphere. Sulfur dioxide, if present in the gas, also affects the rate of calcination.

Calcination is a phase-boundary reaction and proceeds from the outside surface into the center. The order of the decomposition reaction of a quite pure calcite is 2/3 when the particles are relatively large (minus 24- plus 28-mesh), as shown in Appendix A. The order of the decomposition reaction of calcium carbonate has been reported to be between zero and one for different preparations and under different experimental conditions; for this study we have used the value of 2/3 because of the demonstrated dependence of the rate of reaction upon the surface of the limestone in the particle size range used.

The details of calculating the kinetic parameters of calcination from polythermal thermogravimetric analysis (TGA) runs for the different limestones are given in Appendix B. The activation energy for calcination, E, of the stones ranged from 30 to 75 kcal./mole when their minus 24- plus 28-mesh fractions were calcined in a nitrogen atmosphere. The frequency factor, k_o, (sometimes called the pre-exponential term in the Arrhenius expression) was related to the activation energy for all calcites and dolomites by the expression

$$\log k_o = -1.233 + 0.2144E \quad (3)$$

The consistency of the data with this expression is shown in Figure 1.

The use of equation 3 to obtain a one-parameter characteristic of a given limestone may be somewhat misleading in the ordinary use of activation energy for reaction. Normally, a high activation energy indicates that a higher temperature is required to produce a given reaction rate than is needed for a lower activation energy. The change in the frequency factor, k_o, with the activation energy, however, overcomes this effect, and the stones with the higher activation energies decompose most readily. Van Heek and Jüntgen (14) showed the interrelationship between k_o, E, the order of the reaction, and the heating rate in affecting the decomposition of carbonates. Equation 3, therefore,

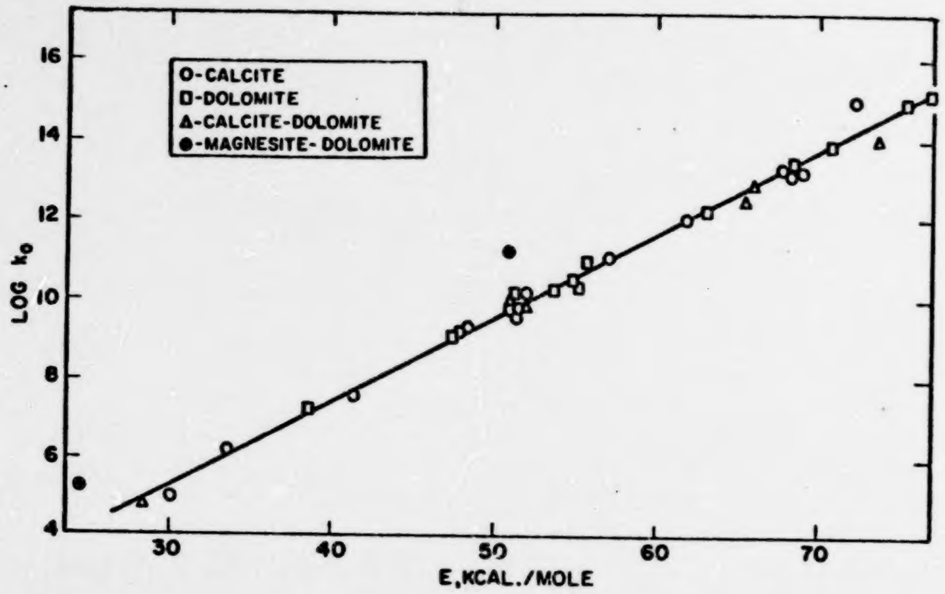

Figure 1. Kinetic Parameters for Calcination, $k = k_o \exp(-E/RT)$.

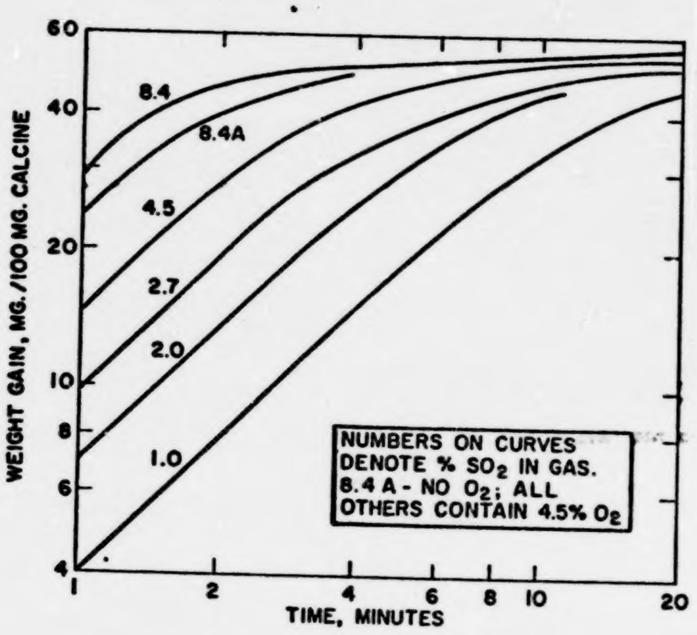

Figure 2. Effect of SO_2 and O_2 on Reaction Velocity at 915° C. with Minus 24- Plus 28-Mesh Colbert Limestone.

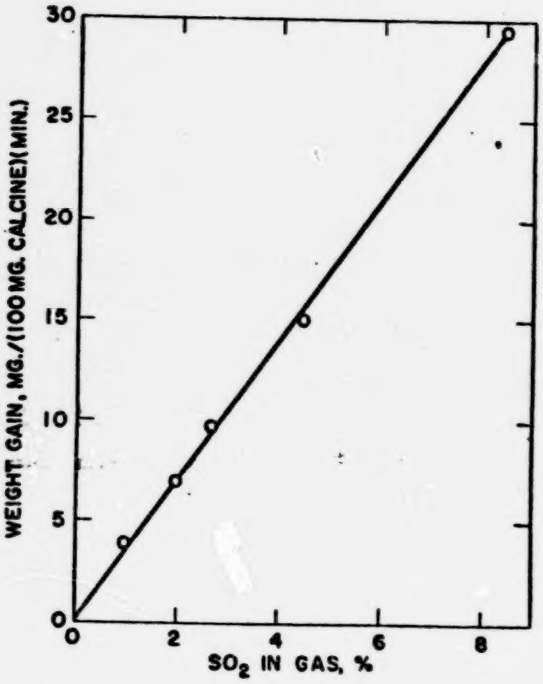

Figure 3. Effect of SO_2 Concentration on Reaction Velocity.

quantifies this relationship for limestones when the order is 2/3 and the heating rate is 5°C. per minute, the conditions used in this study.

Dolomite ideally contains $CaCO_3$ and $MgCO_3$ in equimolar amounts, with the two compounds in alternate layers in the structure. Magnesium carbonate decomposes at a lower temperature than does calcium carbonate, and it is possible to calcine the $MgCO_3$ portion of dolomite and leave the $CaCO_3$ unchanged. In most dolomites, however, calcium and other cations, such as Fe and Mn, are substituted for some of the magnesium in the magnesite layers, and there may also be substitution of magnesium for calcium in the calcite layers. These isomorphous substitutions affect the dimensions of the unit cells of both calcite and dolomite and also affect the grain size of the stones. The substitution of Mg for Ca in either dolomite or calcite is limited to about 5%, whereas that of Ca for Mg in dolomite can be as high at 20% (20). It is to be expected that a higher temperature will be required to complete the calcination of these substituted stones, and that both the maximum rate of decomposition and the temperature at which the maximum rate is obtained will be related to the relative amounts of Mg and Ca. The grain texture and the crystallite size within the grains of the stone also affect the rate of calcination and the temperature of its maximum rate, however, and the calcination parameters are complicated functions of the mineralogical and chemical properties of the stone.

Sulfation

The sulfation studies were made by TGA with minus 24- plus 28-mesh (Tyler) Colbert (high-calcium) limestone that had been calcined at 900°C. for 30 minutes. The calcined material was treated with gases containing different amounts of SO_2 and O_2 to determine the order of the reaction. The reactions are

$$CaO + SO_2 \rightarrow CaSO_3 \tag{4}$$

$$CaSO_3 + 0.5O_2 \rightarrow CaSO_4 \tag{5}$$

$$CaO + SO_2 + 0.5O_2 \rightarrow CaSO_4 \tag{6}$$

in which equation 6 is the sum of equations 4 and 5.

Effects of Loading and Composition of Gas: The kinetic equation from which is determined the order of reaction with respect to the partial pressure of SO_2, the partial pressure of O_2, and the loading or fraction sulfated is

$$\frac{1}{w_o}\frac{dw}{dt} = KP_s^{\ell}P_o^{m}w^{-n} \tag{7}$$

where w_o = initial weight of calcine

w = weight of calcine + absorbed sulfur compounds at time t

K = specific rate constant

P_s = partial pressure of SO_2

P_o = partial pressure of O_2

ℓ = order of reaction with respect to SO_2

m = order of reaction with respect to O_2

n = order of reaction with respect to loading

In each run P_s and P_o were kept constant so that the integrated form was

$$\log w = \frac{1}{n+1} \log w_1 + \frac{1}{n+1} \log t \qquad (8)$$

where w_1 is the weight gain at $t = 1$ minute.

Results for several combinations of SO_2 and O_2 contents in reactions with the calcine at 915° C. are shown in Figure 2; the results are plotted according to equation 8. In all the tests the slope $d \log w/dt$ was unity until a sufficiently thick layer was built up on the available reaction surface. This demonstrates that $n = 0$, or $1/(n+1) = 1$, for the first reaction stage, which is of primary (and perhaps only) concern when limestone is injected into a combustion chamber.

In the absence of oxygen, test 8.4A of Figure 2, the initial rate, as shown by the slope, was the same as that with oxygen (test 8.4), but the ratio of weight gains at $t = 1$ of runs 8.4 and 8.4A was the same as that of the molecular weights of SO_3 and SO_2. Hence, test 8.4A was proceeding according to reaction 4, but test 8.4 was proceeding according to reaction 6. It is postulated that reaction 4 occurs first and is the rate-limiting step; reaction 5 occurs at 915° C. at a relatively high rate when oxygen is present.

The order of the reaction with respect to the SO_2 content of the gas was determined by plotting the values of w_1 against the concentration of SO_2 in the gas, as shown in Figure 3. The linear relation indicates that $\ell = 1$ in the range of SO_2 concentration from 1 to 8.4%; Borgwardt (4) showed a similar relation in the range 0.0058 to 0.6% SO_2.

The value of m in equation 7 was determined by varying the O_2 content of the gas from 1 to 10% with the SO_2 content constant at 2%. The results of each test fell on the curve for 2% SO_2 in Figure 2, which indicates that the concentration of oxygen in this range has no effect, so that m = 0 in the range 1 to 10% O_2.

Effect of Temperature: A series of tests was made with gas containing 4.5% O_2, 4.5% SO_2, and 91% N_2 to determine the effect of temperature on the sulfation reactions; the results are shown in Figure 4. The data show a large increase in the extent of reaction as the temperature was raised from 392° to 635°C. and as the time was increased from about 2 to 10 minutes, a relatively small increase in the extent of the reaction between 635° and 717°C., and an increase in weight gain between 717° and 800°C. These phenomena are consistent with the assumption that the sulfite reaction predominates at low temperature and that there is a competition between the decomposition of sulfite and its oxidation as the temperature is raised. No detectable change in rate or extent of reaction was noted when the temperature was raised above 800°C., but this was due to equipment limitations.

The data in Figure 4 were evaluated kinetically by determining the activation energy for the overall reaction for the first 25% of reaction, and the instantaneous rate of reaction at 25% completion. This degree of reaction was selected because initial slopes could not be measured precisely, whereas the times and slopes at 25% completion could be determined with considerable precision. The activation energies were 15.6 kcal/mole for the overall first quarter of reaction and 17.8 kcal./mole for the instantaneous reaction at 25% completion. It is

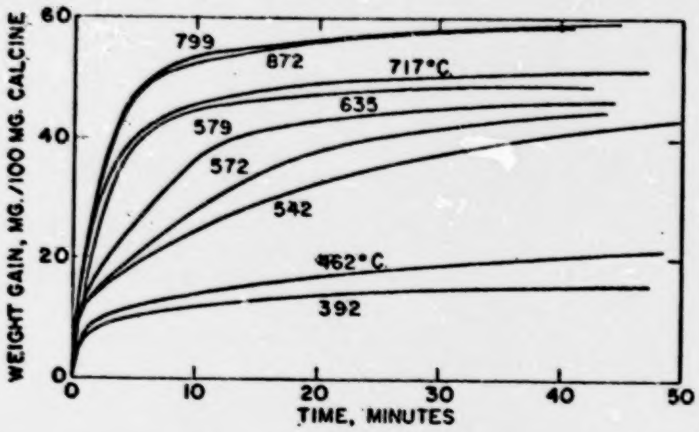

Figure 4. Effect of Temperature on the Absorption of SO_2 by Calcines of Minus 24- Plus 28-Mesh Colbert Limestone From Gas Containing 4.5% SO_2.

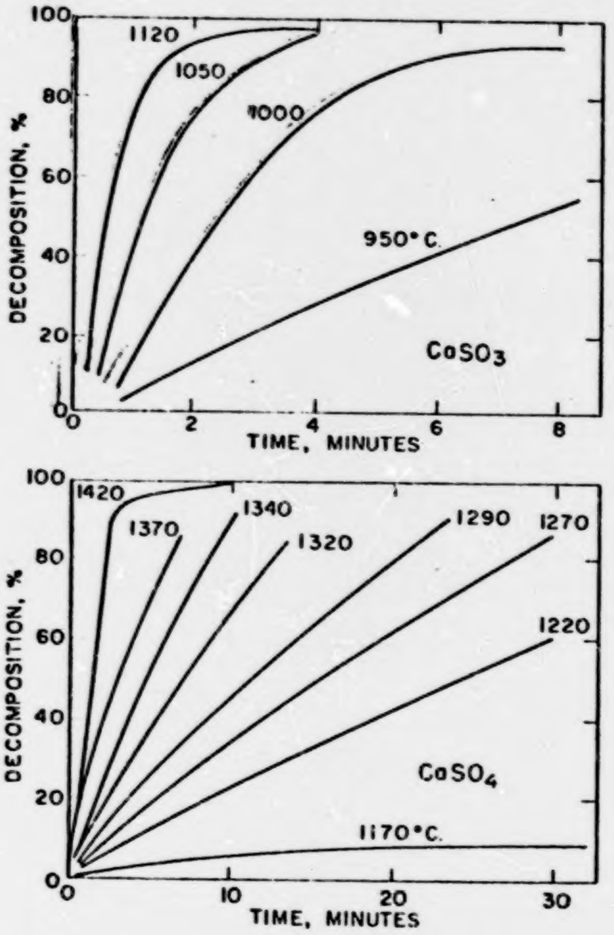

Figure 5. Thermal Decomposition of Calcium Sulfite and Calcium Sulfate.

probable that the activation energy for the initial reaction between SO_2 and CaO for this particular limestone will be lower than those determined at 25% completion.

Oxidation: An effort was made to study the oxidation of calcium sulfite, reaction 5, by thermogravimetric analysis, but the weight gain at the low temperatures used was not large enough to indicate any significant reaction; at high temperature the calcium sulfite decomposed and complicated evaluation of the kinetics.

Disporportionation

The disproportionation of calcium sulfite

$$4CaSO_3 \rightarrow 3CaSO_4 + CaS \qquad (9)$$

was studied at 880° C. (1615° F.) and is summarized in Table I. Lime was treated with SO_2 alone and in mixtures with O_2, CO_2, or both, and the distribution of the sorbed sulfur was determined by chemical analysis. In the presence of oxygen, only calcium sulfate was formed; when no oxygen was present, considerable amounts of sulfite and sulfide appeared in the product. In the presence of carbon dioxide but no oxygen, less sulfide was formed than when both carbon dioxide and oxygen were absent, indicating that carbon dioxide oxidizes both sulfite and sulfide to sulfate. The last two tests of Table I show that sulfide, if formed by disproportionation, does not persist in the presence of oxygen even at low temperatures. The increase in sulfite content as the temperature was raised from 580° to 635° C. indicates that the reaction of lime with SO_2 increases faster in this temperature range than does the oxidation reaction.

TABLE I

Sorption of SO_2 by Lime

Temp., °C.	Compn. of gas, %			Distribution of S, %		
	SO_2	O_2	CO_2	SO_4^{--}	SO_3^{--}	S^{--}
880	0.5	3	15	>99	<0.05	<0.05
	0.5	0	0	71	2	27
	0.5	0	15	93	1	6
	0.5	3	0	>99	<0.05	<0.05
635	0.5	3	0	58	42	<0.01
579	0.5	3	0	75	25	<0.01

Decomposition of Sulfation Products: The decomposition of $CaSO_3$ and $CaSO_4$

$$CaSO_3 \rightarrow CaO + SO_2 \qquad (10)$$

$$CaSO_4 \rightarrow CaO + SO_2 + 0.5O_2 \qquad (11)$$

was studied by analysis of samples that had been heated at constant temperature for different times. The results are shown in Figure 5, and the rate constants for the first-order decomposition reactions are expressed in Arrhenius form as

$$CaSO_3\text{:}\quad k = 1.3 \times 10^9 \exp(-67{,}500/RT)\ \text{sec}^{-1} \qquad (12)$$

$$CaSO_4\text{:}\quad k = 6.1 \times 10^6 \exp(-69{,}500/RT)\ \text{sec}^{-1} \qquad (13)$$

Effect of Water Vapor on the Sulfation of CaO and MgO: A sample of Colbert limestone that had been calcined at 900° C. was compared with reagent powdered $Mg(OH)_2$ that had been calcined at 610° C. to form MgO. Each oxide was treated at 900° C. with a gas containing 6% SO_2, 4% O_2, and either zero or 10% water vapor. As shown in Figure 6, water vapor did not affect the first stage of the reaction of lime with SO_2, but the second stage was promoted slightly. The MgO did not react with SO_2 in the absence of water, and its rate of reaction in the presence of

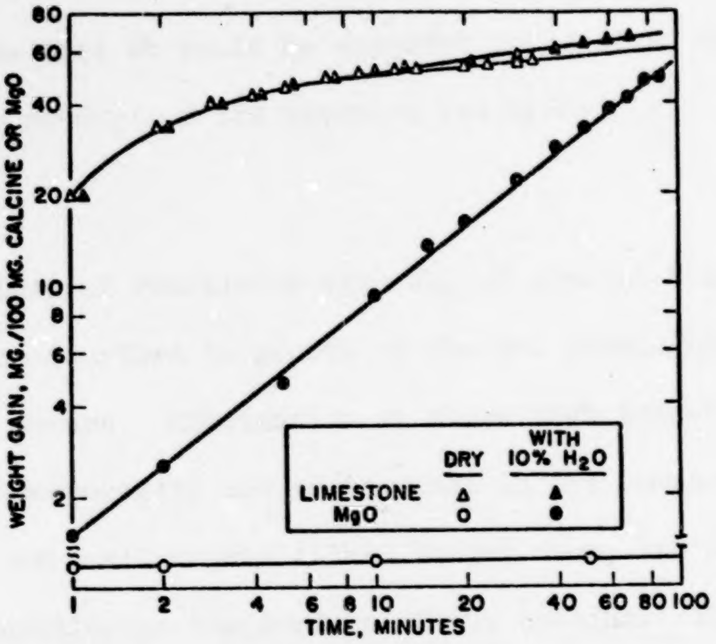

Figure 6. Effect of Water Vapor on the Sulfation of MgO and Limestone Calcine.

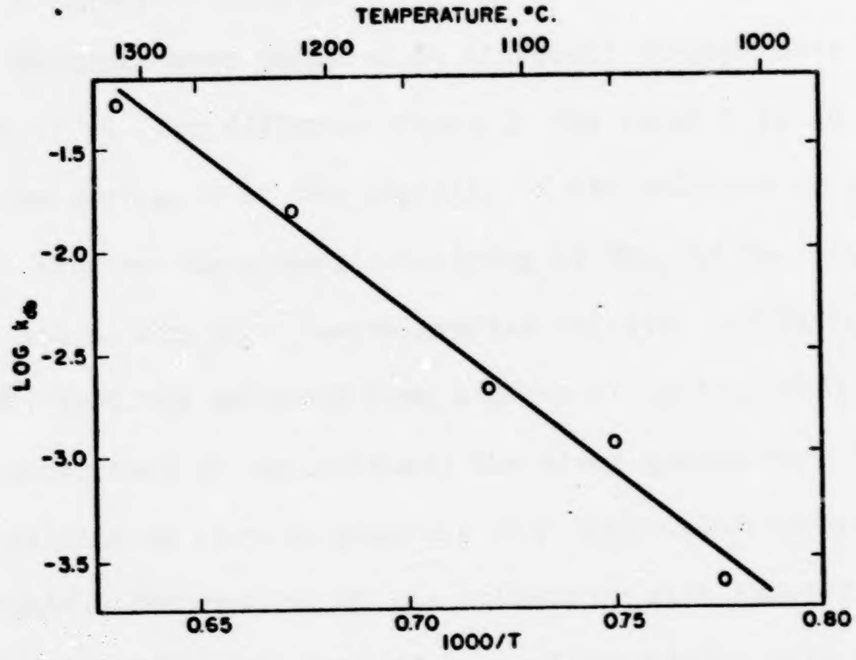

Figure 7. Effect of Calcination Temperature on the Specific Rate of Loss of Reactivity with SO_2.

water was so low that it would be expected to be of no value under injection conditions; the product of the reaction was $MgSO_4$.

Dead-Burning

The loss of reactivity with SO_2 of lime at temperatures above the optimum has been ascribed to growth of the CaO crystallites and to the sintering that occurs. Calcination at these high temperatures results in a decrease in the porosity and an increase in the compactness of the calcine, in combination of small crystals into larger ones, and in formation of a film of certain impurities on the surface of the calcine. The reaction may be indicated as

$$CaO \rightarrow (CaO) \qquad (14)$$

where the parentheses indicate a less reactive species from whatever cause.

Calcines were prepared at different temperatures in the range 1117° to 1317° C. for different times in the range 1 to 30 minutes, and measurements were made of the capacity of the calcines to absorb SO_2 at 920° C. from an atmosphere containing 4% SO_2, 4% O_2, and 92% N_2. The limestone was a very pure coarse-grained calcite, 99% $CaCO_3$, designated sample 89C, that was selected from a group of agricultural stones obtained from the Department of Agriculture; the clear grains were handpicked to obtain a calcite as free as possible from impurities already present in small amounts. The results of the sulfations were treated as those of a first-order reaction--the rate of loss of reactivity with SO_2 was assumed to be proportional to the remaining reactivity. The reactivity and capacity of a soft calcine at 900° C. in an atmosphere containing 15% CO_2 and 85% N_2 were arbitrarily taken as the maximum reactivity and total capacity of the stone. The degree of dead-burning or loss of reactivity, ϵ, was defined as

$$\epsilon = \frac{Gg - G_{T,t}}{Gg} \tag{15}$$

where Gg = SO_2 capacity of soft calcined (900° C.) stone

$G_{T,t}$ = SO_2 capacity of stone calcined at T° C. for t minutes

At each constant temperature, the plot of log $(1 - \epsilon)$ against time was a straight line, as the integrated first-order model predicts, as in the expression

$$\ln (1 - \epsilon) = k_{db}t \tag{16}$$

where $\underline{k}_{db}$ is the specific rate constant for dead-burning of this particular stone.

An Arrhenius plot of the logarithm of the dead-burning constant against the reciprocal of the absolute temperature is shown in Figure 7, from which is obtained, for this particular limestone,

$$k_{db} = 3.3 \times 10^8 \exp (-71{,}000/RT) \text{ sec}^{-1} \tag{17}$$

Substitution

The reaction

$$CaCO_3 + SO_2 \rightarrow CaSO_3 + CO_2 \tag{18}$$

in which the CO_2 of calcite is replaced by SO_2 is thermodynamically favorable at temperatures below those of the decomposition of calcite, but TGA is not sufficiently sensitive to detect any weight change until decomposition is pronounced. Van Heek (15) found a significant substitution reaction before calcination began and found that the extent of the substitution reaction was influenced greatly by the supply of SO_2 and varied among limestones and powdery precipitated carbonates. Coutant (5) also demonstrated an interaction of sulfation with calcination and a correlation between the degree of calcination of the stones and the fraction of sulfite sulfur in the product after short times of exposure. When the temperature is high enough, however, calcination of the limestone proceeds rapidly in the presence of SO_2. A given loss in weight is obtained at a higher temperature in the presence of SO_2 than in an inert atmosphere. There is considerable reaction with SO_2 during calcination when the heating rate is 5° C. per minute, but the proportions formed by substitution, equation 18, and by reaction with the calcine, equation 4, are unknown. It is probable that the bulk of the product, $CaSO_3$ and eventually $CaSO_4$, originates from reaction with the calcine, both simultaneously with and subsequent to the calcination reaction.

To test the relative degrees of sulfation and loss of CO_2 from the limestones, several series of runs were made with minus 24-plus 28-mesh Colbert limestone at two temperatures, 855° and 890° C. The CO_2 content of the input gas ranged from 0 to 16%, but the SO_2 and O_2 contents were kept constant at 5% and 3%, respectively. The limestone sample, 166 mg., was distributed evenly in a 80-mg. plug of quartz wool that was placed in a Gooch crucible that had been cut off to form a container 20 mm. in diameter and 8 mm. high. A perforated cover was placed on the container to permit ingress and egress of gases. The assembly was placed in the TGA apparatus in a CO_2 atmosphere, and the furnace, preheated to the desired temperature, was elevated into position. When thermal equilibrium was established (there was no loss or gain of weight in the CO_2 atmosphere), the reaction tube was evacuated abruptly and the flow of simulated stack gas was started. At the end of a predetermined time of exposure, the sample container was removed from the heating zone and swept with an atmosphere of CO_2 to quench the calcination and sulfation reactions; this treatment, however, led to some unavoidable recarbonation of the unsulfated lime. The sample was analyzed for sulfur and CO_2, and the degrees of sulfation and calcination were calculated from the TGA weight change.

A similar procedure was used to determine the change in weight on calcination in the absence of SO_2; the SO_2 in the simulated stack gas was replaced by N_2. When calcination was complete the composition of the stack gas was changed to the proper proportions of CO_2, SO_2, O_2, and N_2, and measurements were made of the sulfation reaction.

In the absence of CO_2 at 890° C., Figure 8, the rate of calcination in the presence of SO_2 was almost the same as that in its absence, but the product of the sulfation reaction prevented complete calcination. Some sulfation occurred during calcination and continued after calcination ceased. Precalcination had only a slight effect on the rate of sulfation because calcination was much more rapid than sulfation.

The addition of 9.5% CO_2 to the simulated stack gas retarded both calcination and sulfation reactions, Figure 9. Calcination was only 85% complete in the presence of SO_2, and the sulfation reaction was affected also. At 855° C. in an atmosphere of 16% CO_2, Figure 10,

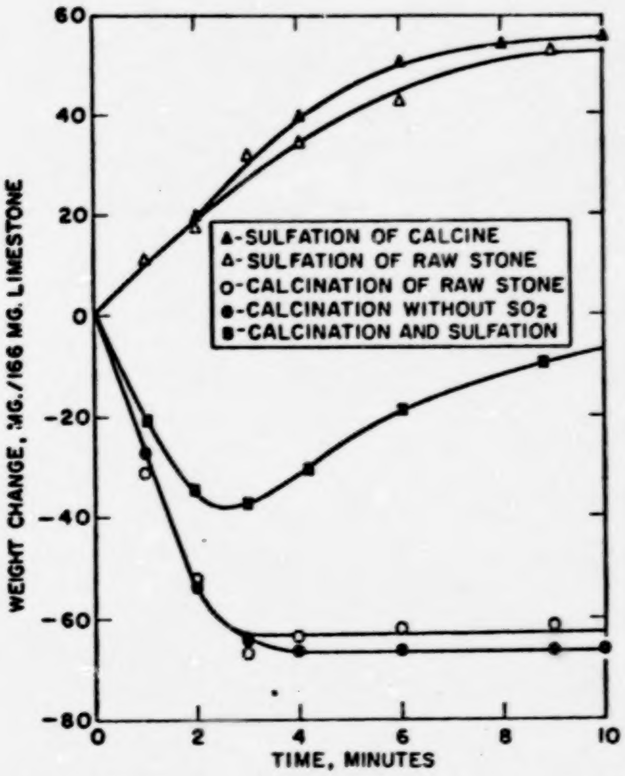

Figure 8. Calcination and Sulfation at 890°C. Without CO_2.

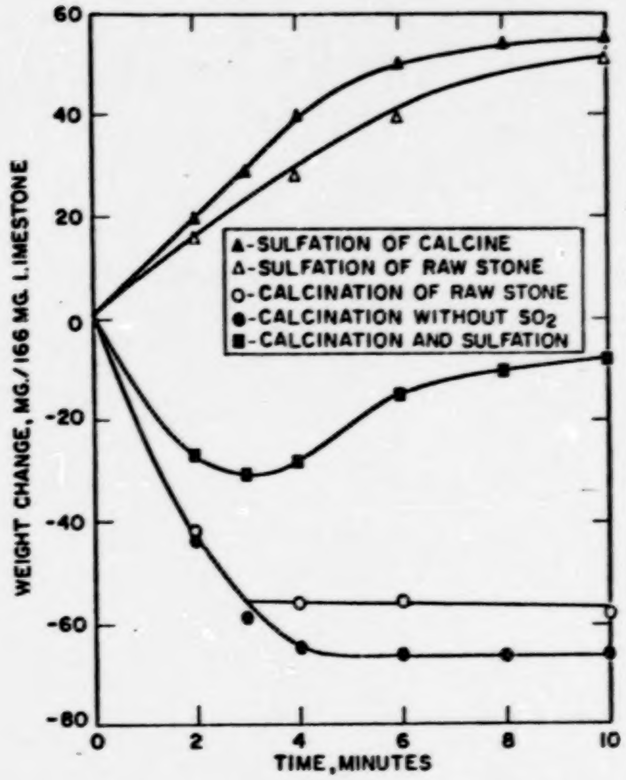

Figure 9. Calcination and Sulfation at 890°C. With 9.5% CO_2.

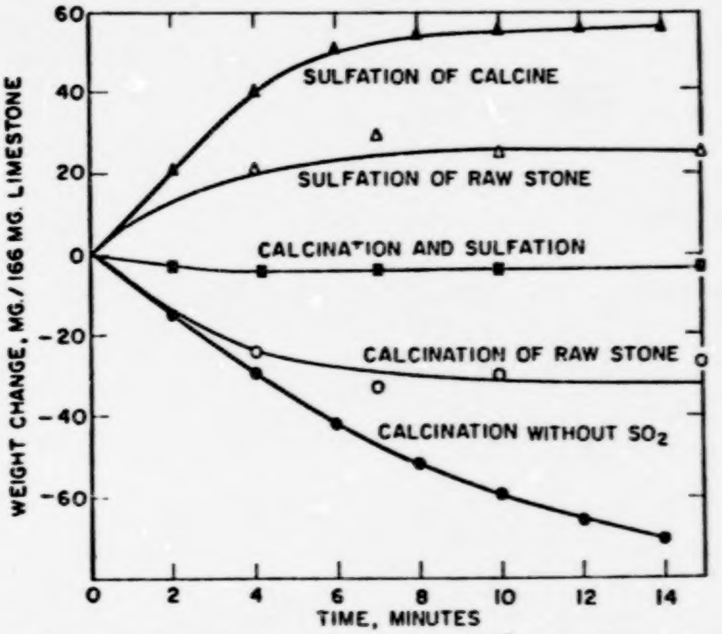

Figure 10. Calcination and Sulfation at 855°C. With 16% CO_2.

the rate of calcination was considerably lower in the presence of SO_2 than in its absence, and the calcination leveled off at about 50% completion in the presence of SO_2. The sulfation reaction was also much slower and only 50% of the calcine was sulfated. The net weight change in this test was very small.

While these results are not conclusive as to the relative importance of the substitution reaction, it is obvious that both the rate and the amount of sulfation depend heavily upon the availability of calcine to react with the SO_2. It is possible that in polythermal heating SO_2 replaces a small amount of CO_2 before calcination begins, but it is evident that when conditions are such that calcination is slow in the absence of SO_2, sulfation also is slow in the presence of SO_2. Under otherwise identical conditions, increasing the amount of calcine increases the sulfation reaction. The retardation of calcination by SO_2 may reflect the formation of a shell of product on the surface that hinders the escape of CO_2 in the surface-controlled phase-boundary reaction.

PROPERTIES OF CALCINES AND THEIR SULFATED PRODUCTS

In this section the properties of calcines and their sulfated products are compared on the basis of texture and type of stone. Results of x-ray, electron microscope, and porosity studies of two calcites of different texture are described that show the differences in the physical properties of their calcines and their reactivities with SO_2. Results of electron microscope studies of reaction surfaces of single crystals are presented to demonstrate the unreacted core mechanism and to describe the reaction front. The effects of the time and temperature of calcination and the particle size of the initial stone on the properties of the calcines of a pure calcite and a rather pure dolomite are described also.

Effect of Texture of Calcites

In the study of the effects of the crystallite size of the raw material on its calcination and sulfation, the calcites studied were a high-purity calcitic limestone (USDA Reference Sample 89) and clear crystals of Iceland spar (Ward's Natural Science Establishment, Inc.). Both materials were crushed and screened to produce a minus 20- plus 24-mesh fraction from which samples were handpicked to minimize the effect of minor accessory minerals. The cell constants of both materials showed that there had been no significant isomorphism, and that both materials were pure calcites as defined by Goldsmith and Graf (9).

A 3-gram sample of each calcite was calcined in a platinum boat for 16 hours at a constant temperature in the range 750° to 1300° C. The samples were inserted into the preheated furnace to effect initial shock calcination; the long retention time was sufficient for complete calcination at each temperature.

The calcined samples were placed immediately in a drying oven at 110° C. to prevent hydration and recarbonation. Samples for study by x-ray diffraction at room temperature were ground to minus 200-mesh under nitrogen in a dry box. The samples for electron microscopy were replicated immediately upon removal from the drying oven. All the electron micrographs were prepared by two-step replication that yielded platinum-shadowed carbon replicas. Each sample was replicated in triplicate to minimize sampling and observational errors.

A series of calcination studies was made on minus 200-mesh samples of each material with a high-temperature x-ray diffractometer furnace which permits the examination of hot calcines. The results were compared with those obtained with the shock-calcined samples.

The degree of calcination of the samples was determined by x-ray examination, which can detect residual or uncalcined calcium carbonate. The mean crystallite size was determined by the x-ray line-broadening technique. Only the relative sizes of crystallites are important in these studies, and the values reported may not have real physical significance.

This study was primarily an electron microscope investigation of the evolution of small pores during calcination and the correlation of x-ray data with observations made from a large number of electron micrographs (Appendix G). Some mercury porosimetry measurements were made as an independent check on these methods.

The statistical summary of the results of the pore size distributions of the calcined calcitic limestone and Iceland spar that were determined by electron microscopy are shown in Table II. All the statistical values were calculated by the methods described in the ASTM Manual on Quality Control of Materials (STP 15c) except for the *t*-test for comparing the means of data from arrays of different sizes. The value of *t* was calculated from the expression described by Snedecor (23)

$$t = (\bar{x}_1 - \bar{x}_2)\sqrt{\frac{n_1 n_2 (n_1 + n_2 - 2)}{(n_1 + n_2)\Sigma x_2}} \qquad (19)$$

where $\underline{\bar{x}}_1 - \underline{\bar{x}}_2$ is the difference between the groups means and $\Sigma \underline{x}^2$ is the pooled sum of squares. All the data show positive skewness coefficients, indicating that the data tail off in the direction of large pores.

The change in mean pore size with rising temperature of calcination is shown in Figure 11. The mean pore size of the calcitic limestone increases irregularly to a maximum at about 1000° C. and then decreases at higher temperatures. The mean pore sizes of the Iceland spar apparently change in a different manner. The mean pore size initially is larger than that of the limestone and increases at approximately the same rate as that of the limestone between 750° and 950° C. A small

TABLE II

Statistical Summary of Pore-Size Distributions of Calcines

(Prepared by shock calcination and heating for 16 hours;

pore sizes determined by electron microscopy)

Calcination Temperature, °C.	Mean pore size, Å.	Standard deviation, Å.	Median pore size, Å.	Mode of pore size, Å.	Number of pores measured	Skewness	*t*-Value[a]
			Calcitic limestone				
750	635	269	600	400	246	2.19	-
850	1188	627	1100	1300	252	0.97	12.78
900	1194	588	1100	1100	253	1.05	0.11
950	1404	658	1300	1300	210	1.17	3.63
1000	2183	1183	2000	2100	250	1.55	8.52
1050	1998	920	1800	1500	250	0.90	1.96
1100	1958	963	1800	1500	201	0.87	0.44
1200	1655	1021	1400	1300	254	1.19	3.23
1300	1489	837	1300	1300	254	1.13	2.02
			Iceland spar				
750	720	349	600	400	251	1.12	-
850	1291	645	1200	1300	254	1.04	12.38
900	1238	623	1200	1300	252	0.92	0.95
950	1744	1093	1500	1300	253	1.72	6.40
1000	1602	897	1500	1700	250	1.21	0.69
1050	1775	971	1500	1300	257	1.25	1.11
1100	1882	1069	1700	1700	251	1.58	1.19
1200	3102	2224	2600	3400	98	2.90	6.91
1300	2974	1931	2500	2500	96	1.56	0.43

---

[a] Value for comparing confidence between means of arrays of different sizes; applicable only to pairs of adjacent arrays (750° *vs*. 850° C., 850° *vs*. 900° C., etc.).

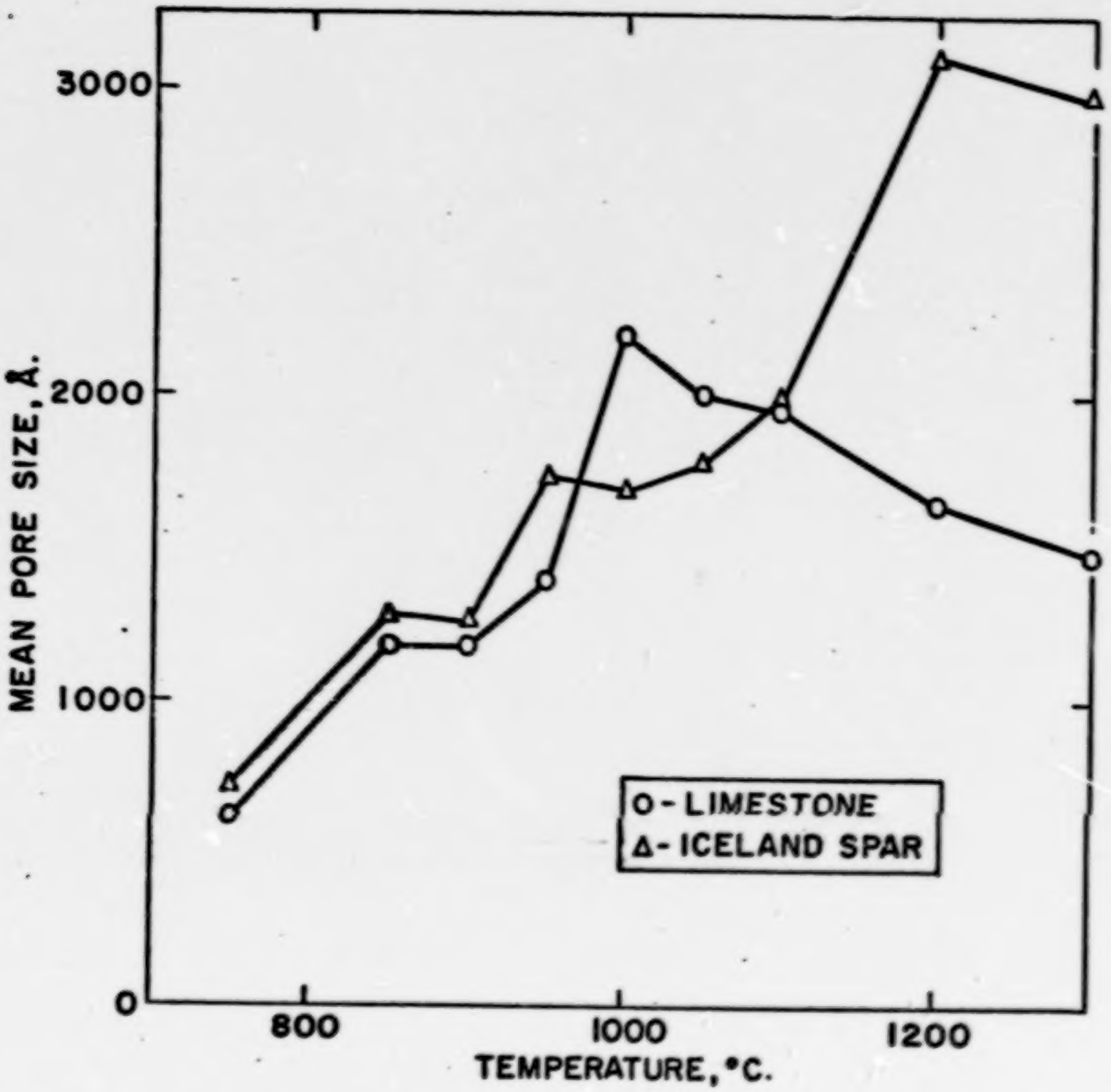

Figure 11. Mean Pore Size of 16-Hour Calcines.

inflection in the curve between 950° and 1100° C. indicates a change in the rate of growth of the mean pore size of the Iceland spar. The mean pore size of the calcines of the Iceland spar increases between 1100° and 1200°C., after which a decrease begins such as that observed with the limestone.

Selected cumulative frequency curves for the pore sizes of calcines of the limestone and Iceland spar are shown in Figures 12 and 13. The data in Figure 12 show changes in pore size of the limestone calcines as indicated in the statistical summary of these data. Between 750° and 1000° C. there is a general increase of pore sizes with rising temperature, but at temperatures above 1000° C. this trend is reversed and the fraction of small pores increases with rise in calcination temperature. This trend in the formation of pores was unexpected and in marked contrast with the behavior of Iceland spar.

The development of pores in the Iceland spar calcines, Figure 13, shows a continuous increase in pore size with rising temperature of calcination. The data are grouped around three temperature ranges and indicate a soft burn below 900° C., a medium burn below 1100° C., and a hard burn above 1100° C. The observed decrease in porosity is consistent with the observations of Hedin (13) who calcined Iceland spar at different temperatures.

The distribution of pores in some of the calcines was determined by mercury porosimetry. Raising the temperature of calcination of the limestone decreased the total pore volume and shifted the distribution toward larger pores in all the limestone calcines except that made at 1100° C. (Figure 14). This sample showed a higher pore volume and a

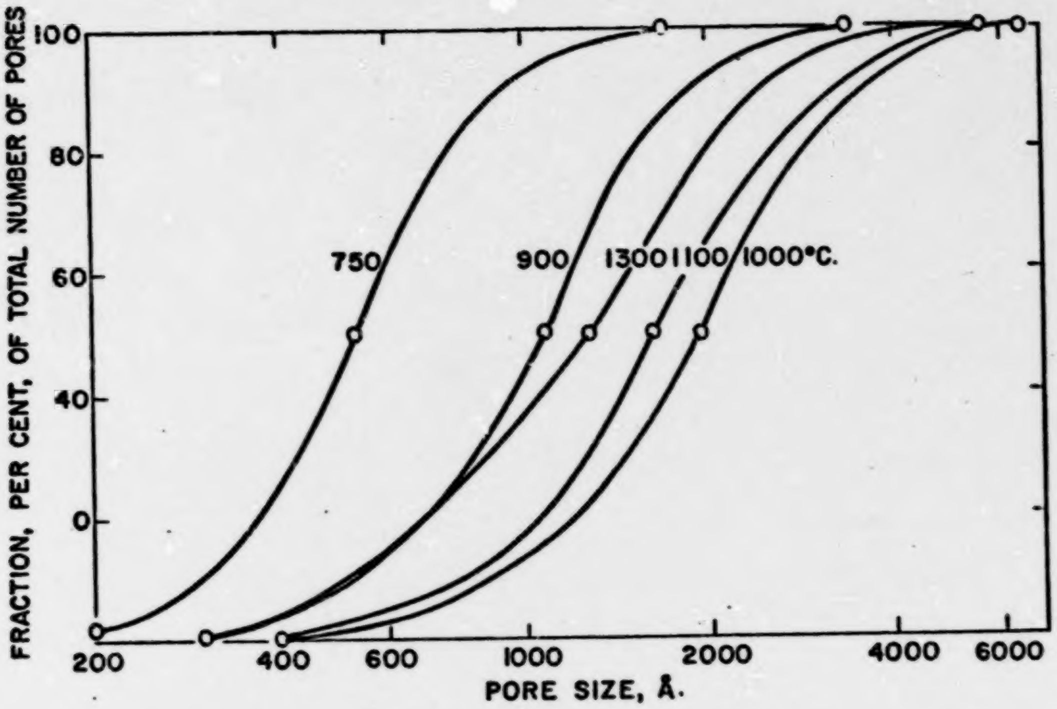

Figure 12. Frequency Distribution of Pores in 16-Hour Limestone Calcines.

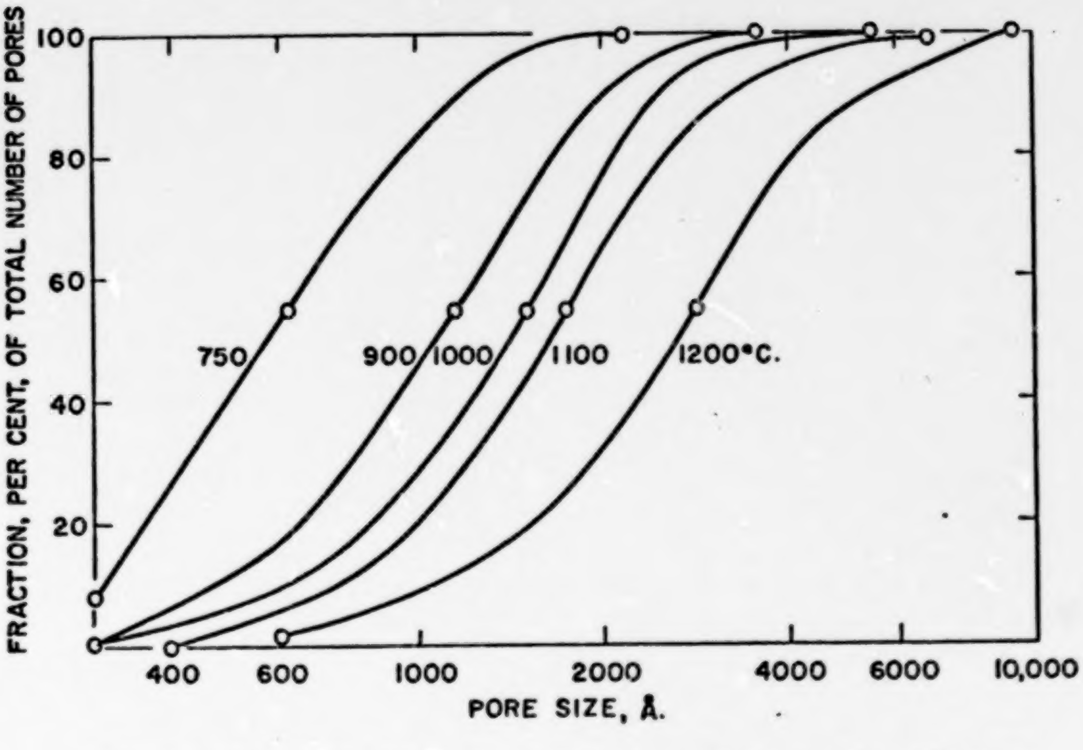

Figure 13. Frequency Distribution of Pores in 16-Hour Iceland Spar Calcines.

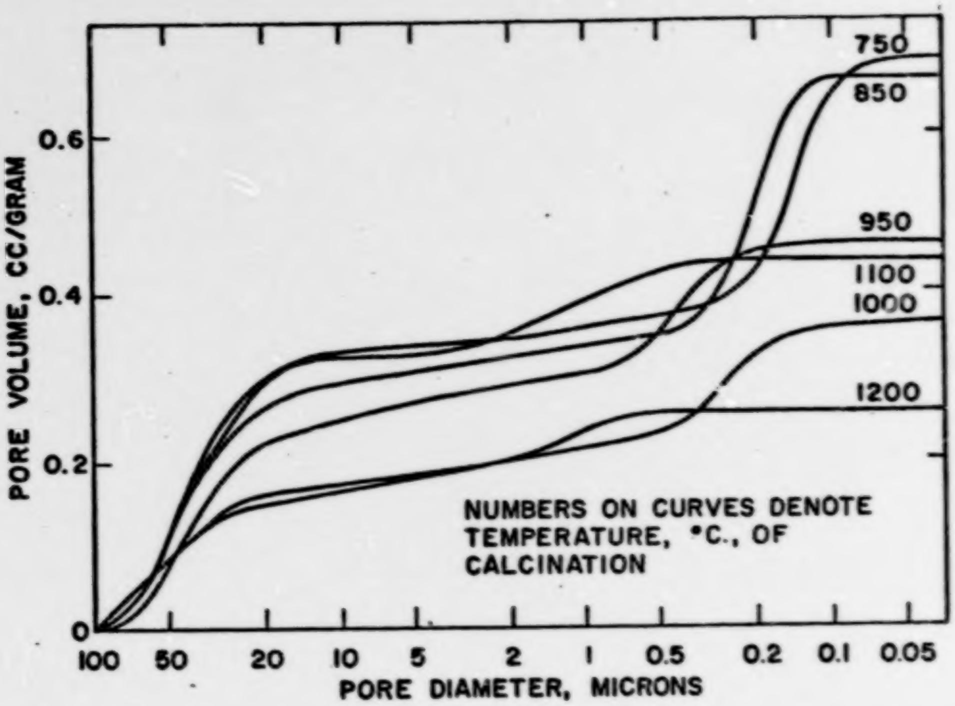

Figure 14. Pore Volumes of 16-Hour Limestone Calcines.

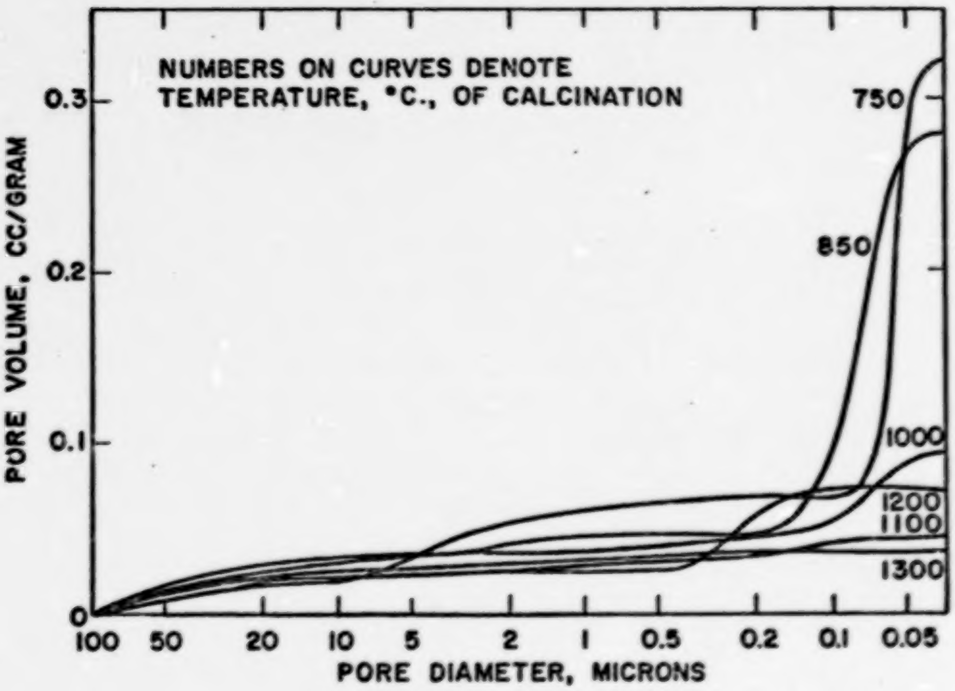

Figure 15. Pore Volumes of 16-Hour Iceland Spar Calcines.

more even distribution of pores in the 17.5- to 0.175-micron region than the 1000° C. calcine. The Iceland spar data (Figure 15) show less than half the total pore volume of limestone calcines prepared at the same temperatures, and almost all the pores in the 750° and 850° C. calcines are smaller than 0.2 micron. The total pore volume of the spar calcines decreases and the pore distribution shifts toward larger values with rising calcination temperature, except for the 1200° C. calcine. The total pore volume of this calcine was larger than that of the 1100° C. spar calcine; this may have resulted from the mechanism that caused the larger pore volume in the 1100° C. limestone calcine. The bulk densities determined by mercury displacement are presented in Table III..

The crystallite sizes determined by x-ray of the shock calcines that were quenched in air are shown in Figure 16. The limestone calcines had larger CaO crystallites than the spar calcines at temperatures below 950° C. Between 950° and 1050° C. both materials show a decrease in crystallite size with a minimum at 1000° C. Further rise in calcination temperature causes the expected increase in crystallite size; the crystallite size of the spar calcines reaches a maximum at 1100° C. and then decreases, whereas that of the limestone calcines increases up to 1200° C. before decreasing. Mayer and Stowe (17) studied a lime prepared in a rotary kiln at 1350° C. and found that the crystallite size of the calcium oxide ranged from 0.1 to 100 microns (10^3 to 10^6 Å.).

TABLE III

Bulk Densities of Calcines

(Prepared by shock calcination and heating for 16 hours. Bulk density determined by mercury displacement with all pores larger than 17.5 microns filled with mercury)

Calcination temperature, °C.	Density, g./cc., of calcine from indicated calcite	
	Calcitic limestone	Iceland spar
750	1.50	1.66
850	1.51	1.69
950	1.96	-
1000	2.02	2.68
1100	2.32	3.06
1200	2.56	2.64
1300	-	3.03

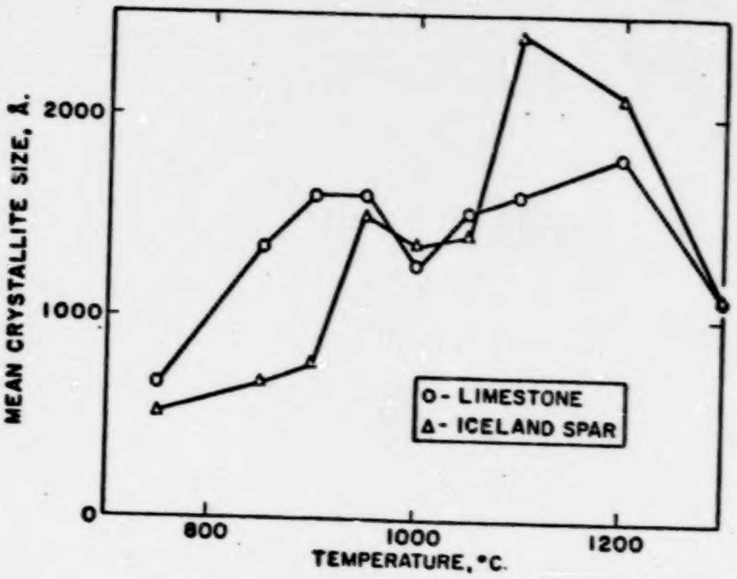

Figure 16. Mean Crystallite Sizes of 16-Hour Calcines.

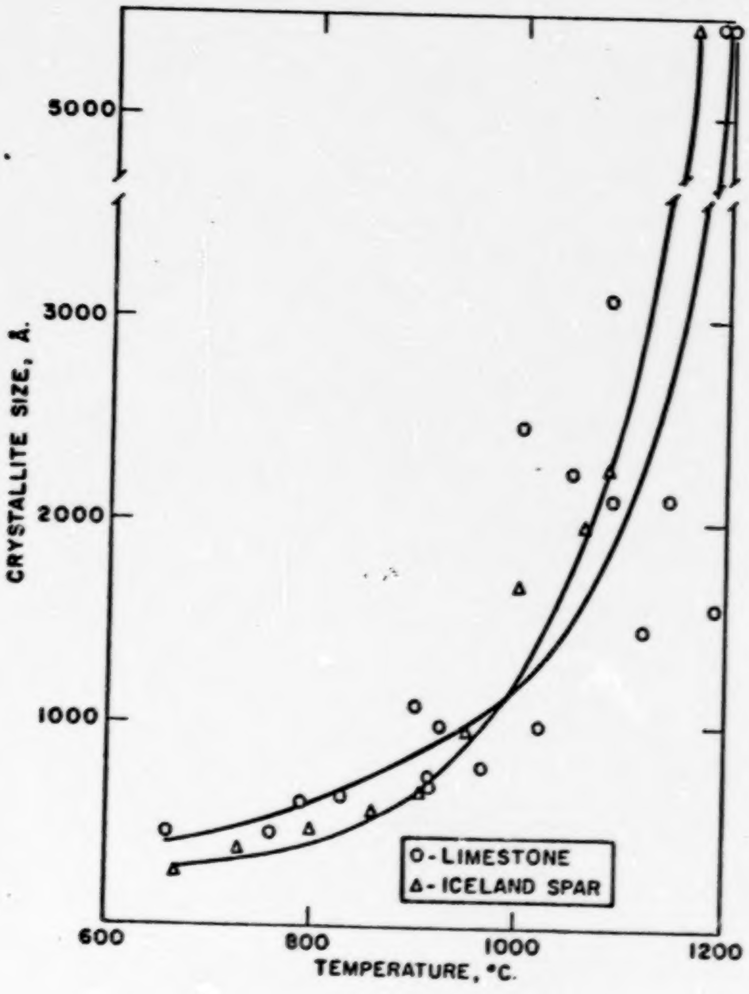

Figure 17. Crystallite Sizes of Calcines Heated Continuously at 6° C. per Minute.

The decrease in crystallite size of the shock-calcined materials at temperatures above 1200° C. was considered a result of the experimental procedure of quenching the heated samples. Samples of both materials were then heated in a high-temperature diffractometer furnace over the same temperature range so that the phase changes and crystallite growth could be studied without quenching the samples. Several samples of each material were ground to minus 200-mesh and a portion of each sample was placed on the stage, heated rapidly to 600° C., and held there for 1 hour. The temperature programmer then was started, and the sample was heated at 6° C. per minute to 1400° C. with continuous recording of the diffraction maxima from which the crystallite sizes were determined. The results in Figure 17 show that the continuously rising temperature caused a continuous increase in crystallite size when there was no quenching, from which it was concluded that either the shock calcination or the rapid air quenching after heating for 16 hours shattered or at least highly strained the crystals. The effects of shock calcination are not well known, and they are difficult to reproduce for direct x-ray study. The long period of calcination after rapid dissociation should effectively anneal the sample. Quenching, however, probably had a major effect on the crystallite size, and attempts were made to evaluate its importance. A sample of each material was heated to 1400° C. with the temperature programmer and held there for 4 hours, by which time crystallite growth had ceased. The power was turned off and each sample was cooled to room temperature in less than 4 minutes. The x-ray maxima of the undisturbed sample after cooling showed the same relative decrease in crystallite size as in Figure 16. Quenching of the sample thus is one cause of the inflection in the crystallite-size curves observed at high temperature.

The rapid crystallite growth, particularly at temperatures above 1100° C., seems to follow the exponential growth curve proposed by Fischer (8). Because of experimental limitations, however, Fischer's data were collected at temperatures below 875° C. and on quenched samples. His maximum rate of crystallite growth is about 100 Å./hr., whereas values calculated from Figure 17, with a heating rate of 6° C./min., can be more than 1000 Å./hr.

The reaction of the calcines with sulfur dioxide was investigated at 750°, 1050°, and 1200° C. under two different experimental conditions: calcination for 16 hours and subsequent sulfation, and simultaneous calcination and sulfation. The calcination-sulfation tests were a logical extension of the calcination study and provided data for comparison with other fixed-bed tests. The simultaneous calcination-sulfation reactions have been studied in fixed-bed tests and the combination of shock calcination with sulfation was thought to be the most realistic laboratory simulation of dry limestone injection that could be obtained without specialized equipment. The temperatures of the tests were selected to produce soft-, medium-, and hard-burned limes that would have different reactivities with sulfur dioxide.

The calcines for the consecutive tests were prepared by shock calcination and further heating for 16 hours. The hot calcines then were subjected for 15 minutes to a mixture of air and 4% SO_2. The samples calcined at 1050° C. were exposed to the sulfur dioxide for

5 and 30 minutes also to measure the rate of change of the crystallite size of the reaction product and to prepare samples at different stages of sulfation for study in the electron microscope. The crystallites of the calcium sulfate grew larger with rising temperature, and those on the limestone calcines were consistently larger than those on Iceland spar, as shown in Table IV.

The samples simultaneously calcined and sulfated at 750° C. for 15 minutes were incompletely calcined; neither lime nor calcium sulfate was detectable by x-ray in the treated Iceland spar, but both were present in the treated limestone.

The sulfated samples were examined in the electron microscope to gather fundamental data on the reaction and to obtain a qualitative comparison of the results of consecutive and simultaneous treatments. The sulfur dioxide reacts initially with lime to form individual crystals of $CaSO_4$ that form interlocking aggregates. On further sulfation these crystallites cover the entire surface of the particles, and the growth of adjacent crystals results in a general smoothing of the surface as the crystals unite into larger aggregates. At higher temperatures, these larger aggregates continue to grow and form a tight, smooth surface. Even with similar thicknesses of sulfated layers, the permeability of the surface changes considerably as the surface texture develops. Once the surface coating forms, diffusion processes are influenced by the texture of the sulfate layer.

TABLE IV

Properties of Sulfation Products

Sulfation conditions		Crystallite	Ratio of areas of		
Temp., °C.	Time, min.	size of $CaSO_4$, Å.	$CaCO_3$	CaO	$CaSO_4$
Sulfation of limestone calcines					
750	15	1725	0	1.00	2.20
1050	5	2950	0	1.00	0.35
1050	15	2325	0	1.00	0.42
1050	30	2450	0	1.00	0.68
1200	15	3075	0	1.00	0.13
Sulfation of Iceland spar calcines					
750	15	1350	0	1.00	0.48
1050	5	1600	0	1.00	0.05
1050	15	2050	0	1.00	0.03
1050	30	1950	0	1.00	0.35
1200	15	2275	0	1.00	0.07
Simultaneous calcination and sulfation of limestone					
750	15	2400	1.00	0.02	0.07
1050	15	2550	1.00	0.03	0.65
1200	15	3150	0	1.00	1.73
Simultaneous calcination and sulfation of Iceland spar					
750	15	-	1.00	0	0
1050	15	2825	1.00	0.24	0.19
1200	15	1950	0	1.00	0.33

A second general consideration was the mechanism of the sulfation reaction. Two principal models have been proposed: continuous-reaction and unreacted-core. In the continuous-reaction model, the sulfation reaction is thought to occur throughout the internal structure of the lime particles, and not just on the external surface. In the unreacted-core model, the sulfur dioxide reacts initially with the external or geometric surface of the lime particles and forms a coating. This initial phase is followed by a reaction between sulfur dioxide that has diffused through the outer surface layer of calcium sulfate to the lime in the unreacted core. Examination showed that the sulfation takes place by advance of the sulfate front, and no diffusion reaction is apparent along the shrinkage cracks. The unreacted-core or shell model thus appears to be correct, at least as it applies to these stones.

The surface of a particle of calcitic limestone simultaneously calcined and sulfated at 750° C. for 15 minutes is completely covered with the calcium sulfate, and the individual crystals are discrete. Crystals of calcium sulfate formed by consecutive calcination-sulfation reactions are smaller than those formed by simultaneous reaction, an observation in agreement with the x-ray crystallite-size data on the samples.

In contrast to the well-sulfated surface of the limestone calcine, the surface of Iceland spar simultaneously calcined and sulfated at 750° C. showed only slight sulfation. X-ray examination did not detect any lime or sulfate in the sample, although evidence of slight reaction was seen in the electron microscope. The surface of a particle of calcined and subsequently sulfated Iceland spar showed a good sulfation reaction, although it was less than that of the limestone. The comparatively small size of the crystals of the observed sulfate is in agreement with the x-ray crystallite-size data.

At 750° C., the limestone reacts better with sulfur dioxide than does Iceland spar under either consecutive or simultaneous conditions. The limestone behaved about the same under the two conditions, but the Iceland spar sulfated better when it had been calcined because the dissociation was complete after 16 hours at 750° C., whereas there was no detectable calcination in the 15-minute exposure under the simultaneous reaction conditions.

The limestone that had been calcined and sulfated simultaneously for 15 minutes at 1050° C. had surfaces on which the reaction had proceeded to the extent that the surface had become quite smooth and was composed of large aggregates of crystallites. The calcined material also sulfated quite well in 15 minutes at 1050° C., but its textural development indicated less sulfation of the oxide than in the simultaneous reactions. Thus, 30 minutes was required for the limestone calcine to sulfate to the same degree that was obtained in 15 minutes in the simultaneous treatment.

The surface of Iceland spar simultaneously calcined and sulfated for 15 minutes at 1050° C. indicated a greater degree of reaction than that at 750° C. The surface was completely covered by the sulfate, and intergrowth of crystals had smoothed the surface. An Iceland spar sample calcined at 1050° C. and then sulfated for 5 minutes had undergone a good surface reaction, and showed the unusual development of a few large single crystals of $CaSO_4$.

The data indicate that at 1050° C. the Iceland spar is beginning to sulfate quite well but still is less reactive than the limestone. These results are in agreement with the x-ray crystallite-size data which show that the crystallites of the calcium sulfate on the Iceland spar calcines are smaller than those on limestone calcines. Samples prepared at 1200° C. were generally too featureless to warrant presentation, although the general conclusions are applicable in that temperature region with one important exception. Thermal etching of the sulfation product at 1200° C. indicated simultaneous formation and decomposition of the calcium sulfate.

A comparison of the reactivities of the two calcites with sulfur dioxide can be made from the areas of the x-ray maxima. The ratios of areas for sulfated samples presented in Table IV show that limestone calcines react with sulfur dioxide better than the Iceland spar calcines under the conditions tested. Calcined materials showed a general decrease in reactivity with sulfur dioxide as the temperature was raised. When simultaneously calcined and sulfated, both materials reacted better at the higher temperatures because of the increased degree of calcination during the short 15-minute exposure. The Iceland spar sample calcined at 1050° C. showed a relatively large amount of unreacted calcium oxide compared to the limestone sample prepared under the same conditions. The Iceland spar oxide must have been inactive because of extensive recrystallization of the lime, or because its poor pore-size distribution caused it to be unavailable for reaction, or because of both of these interrelated factors. The 1200° C. samples were completely calcined in the 15-minute calcination-sulfation experiments.

All the isothermal shock-calcination data show that the properties of the calcined products of the limestone are distinctly different from those of the Iceland spar, even when prepared under the same conditions. The only significant difference in the starting materials was the crystallite size of the uncalcined stones. The mean crystallite size of the Iceland spar was 7125 Å. and that of the limestone 3875 Å., and the higher thermal stability of the Iceland spar undoubtedly reflects its larger crystallite size. The low-temperature (below 950° C.) calcinations completely dissociated the spar, but only very slowly, and produced a lime with small pores and small crystallites. The unfavorable pore-size distribution would require that reactions of lime with sulfur dioxide take place as the gas diffused into the small pores or through the sulfate layer formed during the early stages of sulfation.

The limestone calcines prepared at temperatures below 950° C. had larger crystallites than the spar calcines, but tended to have larger pore volumes (generally about twice as large) and a more favorable distribution of pore sizes. Potter (21) and others have shown that pores larger than 0.3 micron correlate well with the capacity to absorb sulfur dioxide in fixed beds. It appears that smaller pores require diffusion times too long to be of practical significance in actual injection tests.

During calcination at temperatures below 1000° C., the pores grow by coalescing of small pores into larger pores, which causes the large pores to grow at the expense of small pores as can be seen by the porosimetry data (Figures 14 and 15) and reach a maximum at about 1000° C.

Between 1000° and 1100° C., both materials show a decrease in crystallite size and a minimum in total pore volume. The coincidence of these changes in physical properties is interpreted as the end of sintering of the oxide as described by Hedin (13) and the beginning of recrystallization reactions. The small crystallites formed initially during calcination have grown by encompassing oxide forming at sites within a limited domain. The size of the region increases with rising temperature and gives rise to larger crystallites. This type of growth reaches a maximum at about 950° C. and a second type of growth begins that is characterized initially by the development of smooth areas containing large oxide crystals that show evidence of growth spirals and oxide crystal morphology. As the temperature continues to rise, geometrically outlined pores and massive oxide single crystals develop, as evidenced by the exponential growth of crystallite size at temperatures above 1100° C. noted in continuously heated samples.

Fischer (7) observed that his limestone calcines showed a minimum porosity at 1200° C., an increased porosity at 1320° C., and then a decrease in porosity. In this study, the limestone showed a minimum porosity at 1000° C. and the spar a minimum porosity at 1100° C. The pores in these samples are distributed so that big pores have become quantitatively the most significant, and the small pores are those interstitial or geometric pores that form as the calcium oxide crystals grow. In the electron microscope study, the emphasis is upon these small pores, so that the decrease in mean pore size observed in the limestone calcined at temperatures above 1000° C. is consistent with the interpretation of the calcination process presented previously. A final decrease in porosity occurs as Fischer (7) reported, re-emphasizing the insignificant contributions of the small pores to the total pore volume in calcines that are largely recrystallized.

The Iceland spar calcines show trends different from those of the limestone calcines, and their interpretation is less apparent. The principal difference between the high-temperature recrystallizations of Iceland spar and of limestone appears between 1050° and 1100° C. where the relative crystallite size of the oxide produced from the limestone increases 10%, which is only slightly greater than the mensuration error, whereas the crystallite size of the Iceland spar oxide increases more than 60%. Over the same temperature range the mean pore size of the Iceland spar calcine increases to 1882 Å. but that of the limestone calcine decreases from 2182 Å. at 1000° C. to 1958 Å. at 1100° C. These data indicate that Iceland spar calcined for 16 hours at 1100° C. is almost completely recrystallized but that the limestone is not. This interpretation is supported by the physical appearance of the surfaces of the samples as well as by a minimum in the total pore volume. The limestone showed some straight-edged geometric pores characteristic of samples undergoing recrystallization, but only minor growth spirals and little development of oxide crystal morphology. In contrast to the limestone, the Iceland spar surface showed good growth spirals and marked development of crystal morphology, in addition to numerous geometric pores.

The limestone crystallite size is maximum in the 1200° C. calcine. The limestone recrystallizes over a wider range of temperature (1000° to 1200° C.) and forms smaller crystallites than does the Iceland spar. No physical evidence has been observed that can explain this difference, but it must be related to the nucleation of the oxide during recrystallization and to the texture of the calcine.

The final decrease in crystallite size of the 16-hour calcines can result from too rapid cooling of the samples. In an attempt to confirm this observation, samples were cooled very slowly in the tube furnace and x-ray furnace from 1400° C. to near room temperature. All these samples showed a very reproducible decrease in crystallite size as indicated by Figures 16 and 17. No satisfactory explanation for this observation has been proposed, but the effect is real.

The sulfation reaction of lime with sulfur dioxide has been described in terms of continuous-reaction and of unreacted-core models. Borgwardt (3) has presented data for the continuous-reaction model that indicates that the sulfation reaction takes place throughout the interior of the particle and not just on the outer surface. The data of Hatfield and Kim (12) support the unreacted-core or shell-formation model as the mechanism of the sulfation reaction. The electron microscope studies show that in a fixed-bed test the reaction proceeds by the unreacted-core mechanism. Examination of a number of particles shows that the shell is seldom thicker than 70 microns, even after exposure for several hours, and the crystallites of the sulfate at the outer surface are generally larger than those at the reaction front. Calcines so treated with sulfur dioxide have such an impervious surface coating that they can be stored for months at room temperature with no detectable hydration or recarbonation of the lime in the unreacted core.

The limestone calcines were more reactive with sulfur dioxide than the Iceland spar calcines under all the experimental conditions. The difference in reactivity may reflect differences in calcination behavior, in the pore volumes and size distributions of the calcines, and in the temperatures at which recrystallization is complete. The data in Table IV show that at 750° C. the calcined limestone was more than 4 times as reactive as the Iceland spar calcine. At 1050° C., the reactivity of the Iceland spar calcine was one-tenth that at 750° C., whereas that of the limestone calcine was one-fifth that at 750° C. This larger decrease in reactivity of the Iceland spar calcine probably indicates a higher degree of recrystallization. At 1200° C., both calcines lost reactivity.

The difference between the two materials is especially marked in the simultaneously calcined and sulfated samples. After 15 minutes at 1050° C. in an atmosphere containing 4% SO_2, the ratio of areas $CaSO_4:CaCO_3:CaO$ is 0.19:1.00:0.24 for the Iceland spar and 0.65:1.00:0.03 for the limestone. The lime produced from the Iceland spar does not react with sulfur dioxide as well as the lime produced from the limestone, as can be seen by comparing the relative areas of $CaSO_4$ and CaO in the three-component samples. This may reflect diffusion problems resulting from the pore-size distribution in the samples, or from the recrystallization of the lime which decreases its reactivity.

Finally, it should be noted that, although both stones were screened to minus 20- plus 24-mesh at the beginning of the experiment, no attempt was made to control the particle size of the limes. The Iceland spar showed exceptional physical physical stability on heating, and there was practically no decrepitation of the material on shock calcining at any temperature. The limestone dusted badly during calcination at all temperatures. The surface area contributed by the decrepitation of the limestone probably was a factor in its higher reactivity with sulfur dioxide and may indeed be a desirable property of stones selected for injection, although this effect may disappear when the stone is very finely ground.

The physical and chemical properties of a calcine are influenced markedly by the crystallite size of the parent limestone. The high thermal stability of Iceland spar reflects its relatively large crystallite size, and its calcines react slowly with sulfur dioxide.

In addition to the decomposition of the calcium carbonate, calcination effects a recrystallization of the resultant calcium oxide which is accelerated by rising temperature and which decreases the reactivity of the calcine with sulfur dioxide.

Sulfation of lime takes place in two stages: reaction of sulfur dioxide and oxygen with the exposed surface of lime, followed by diffusion of the gaseous reactants through the resultant shell of calcium sulfate to the core of unreacted lime. Pores in the calcine smaller than about 0.1 micron do not admit sulfur dioxide rapidly enough to have significant effect on the sulfation reaction at short retention times.

Calcines react best with sulfur dioxide at temperatures below 1050° C., but simultaneous calcination and sulfation, which is required when powdered limestone is injected into power plant furnaces, is best carried out at temperatures of 1050° C. and above.

Electron Microscope Studies of Reaction Surfaces

Although many studies of the reaction of SO_2 with calcined calcium carbonates are made with natural limestones, these materials are not suitable for precise laboratory experiments because wide variations in their chemical and physical properties influence their behavior. To minimize these variations in properties and their influence on experimental conditions, a number of tests were made on the calcination and reaction of single crystals of Iceland spar.

Several crystals of the spar, about 12 mesh (1600 microns) in size, were calcined at 900° C. in the TGA apparatus until they reached a constant weight. The calcined crystals were then exposed to SO_2 for about 40 minutes and examined with the electron microscope.

The crystals were cleaved to expose the unreacted oxide cores and the reaction zone between the calcium sulfate and calcium oxide and the cleaved surfaces were replicated by the two-step polystyrene or faxfilm tape technique. In spite of its coarse crystallinity, the oxide rapidly hydrated on exposure to the atmosphere, so that replicas had to be made immediately after cleaving. The plastic replicas were platinum shadowed and carbon coated in the evaporator. The plastic portions of the replicas were removed by washing with a suitable solvent, and the shadowed carbon replicas were then examined with the electron microscope.

An area of calcium oxide in the unreacted core of the specimen is shown in Figure 18. These large calcite crystals did not react extensively with the SO_2, and the unreacted oxide comprised about 80% of the specimen. The surface features shown in Figure 18 are typical of the unreacted areas. The texture is generally massive, as might be expected along the cleavage plane of such a single crystal pseudomorph. The fine dark lines on the surface represent shrinkage cracks, fractures, and coalescing pores that were caused by the calcination. These features follow regular geometric patterns and probably are controlled in part by the structure of the calcium oxide pseudomorph after calcite. The coarse textural features on the surface indicate local irregularities or grain boundaries of crystals that are not in structural continuity with the crystals that comprise most of the surface.

The reaction zone between the $CaSO_4$ and CaO in the crystals is shown in Figure 19. The particle labeled A near the top of Figure 19 is the same particle labeled A near the bottom of Figure 18. These two figures show that in a distance of about 25 microns there is change from unreacted calcium oxide to a well-defined calcium sulfate zone. The line B-C in Figure 19 shows the approximate position of the calcium sulfate-calcium oxide reaction front.

These electron microscope studies thus confirm mercury porosimeter measurements which show that 90% of the surface area of the particles is accounted for by pores smaller than 0.035 micron. Measurements on Figure 18 show that the widths of the shrinkage cracks and

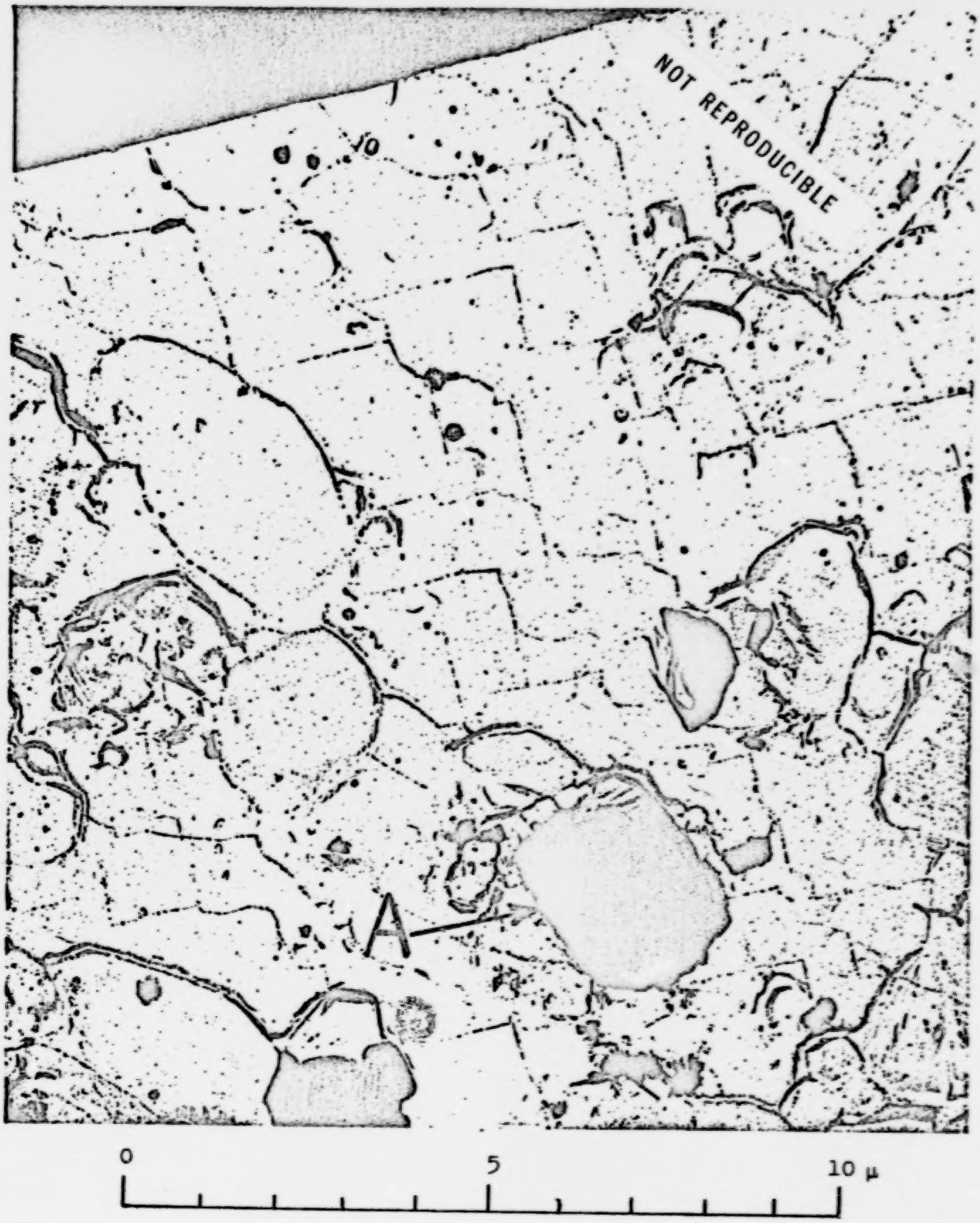

Figure 18

Surface Fractures on the Cleaved Surface of a Calcined Single Crystal of Calcite. 12,000X

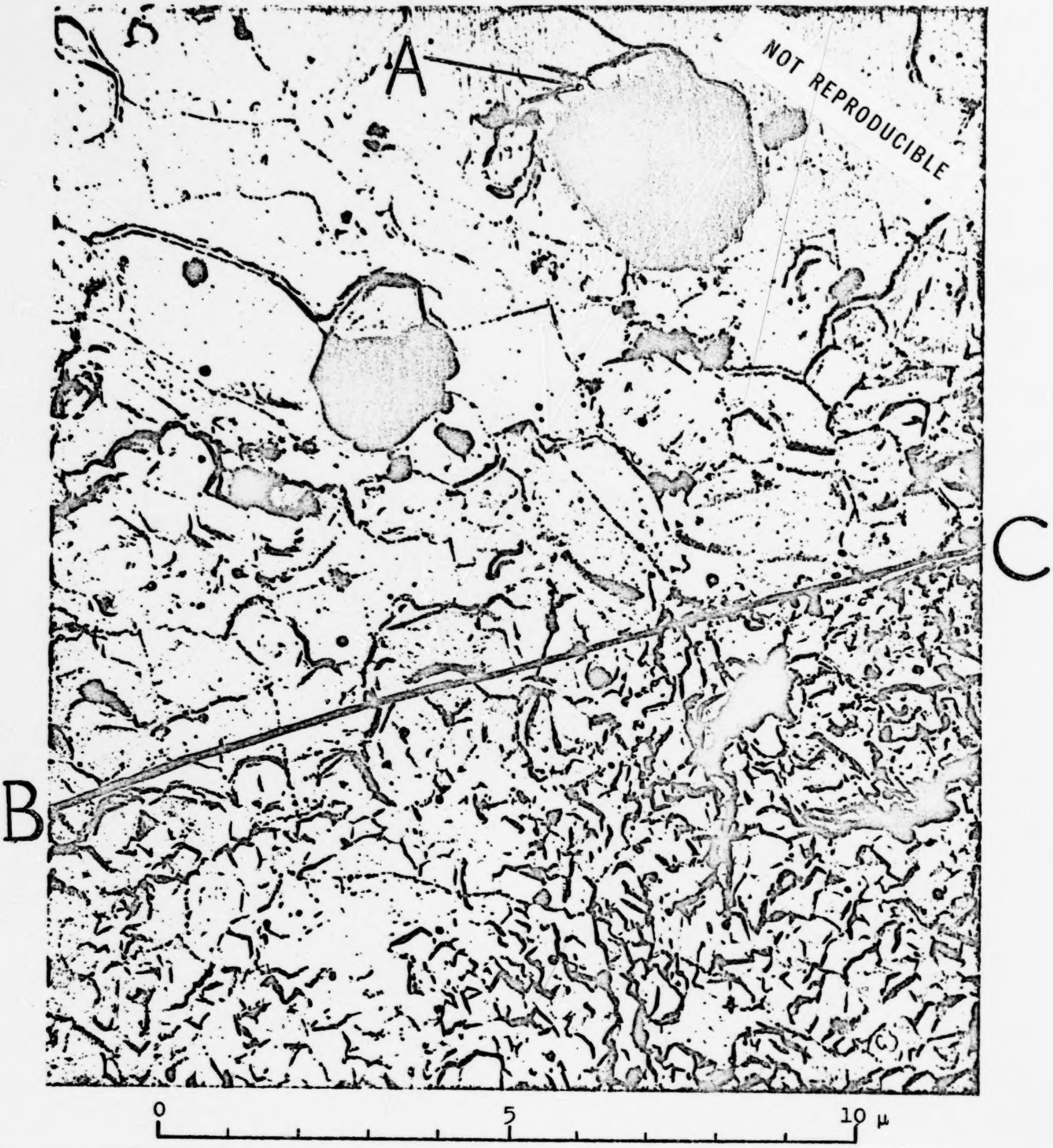

NOT REPRODUCIBLE

Figure 19

Reaction Zone of Calcined Single Crystal of Calcite

after Exposure to Sulfur Dioxide. 12,000X

[The line BC divides the region of unreacted CaO (upper) from that of product $CaSO_4$]

coalescing pores are no wider than 0.030 micron, and many are much smaller. The agreement of the measurements for the surface-area and size of contributing pores made by the two methods thus is not likely to be coincidental.

The electron micrographs clearly show that the reaction of the SO_2 with the lime does not follow these small fractures. Some of the fractures shown in Figure 19 can be followed well into the sulfate reaction zone. The geometric surface area of the particular grain may be much more important in promoting potentially active sites for SO_2 reaction than the fine (less than 0.1 micron) pores. If the retention time in the reaction zone is short, the geometric surface area is even more important than the total surface area. The micrographs also seem to indicate that the sulfate reaction takes place along a reasonably well-defined front so that diffusion models based on such a concept would be realistic for long reaction times.

A study of a series of photographs, of which the two presented here are a part, shows that the reaction zone is about 70 microns wide in this sample. The calculated volume of the reaction zone was compared with that of the unreacted oxide. It was assumed that the particles were spherical and that the bulk densities of the two zones were the same as the densities of the pure material (i.e., no allowance was made for voids or packing). The results of the calculations show the weight ratio $CaSO_4$:CaO to be about 1:4, or that about 20% of the weight is calcium sulfate.

These studies showed also that there is a general decrease in the crystallite size of the calcium sulfate as the reaction zone is approached. The average size of the calcium sulfate crystals at the outer edge of the sulfate reaction zone is about 1 micron, whereas the average size of the crystallites in the reaction zone, as seen in Figure 19, is 0.5 micron or less.

Properties of Calcite and Dolomite Calcines

In a comparison of the properties of calcines of a calcite and a dolomite as affected by the conditions of calcination and the initial particle size of the stone, the effects of the variables listed in the tabulation were studied in a factorial manner.

	Levels	
	1	2
Calcination		
Time, minutes	1	4
Temperature, °C.	1100	1225
Limestone		
Particle size, microns	384	136
Type	Calcite	Dolomite

The calcite, a very pure, coarse-grained limestone, designated Sample No. 89 Coarse, was the same stone that had been used in the textural comparison with Iceland spar and in the dead-burning tests. It contained only 0.4% accessory minerals (quartz and illite clay). Its mean crystallite size was 3875 Å., and its lattice constant, a, was 4.987 Å., which showed that there had been no significant substitution in its crystal lattice.

The dolomite, designated the James River Dolomite, BCR No. 2069, was supplied by a bidder for supplying limestone for the Shawnee full-scale injection tests. It contained 1.9% accessory minerals, largely quartz and feldspar, and was the purest dolomite available for the tests. Its mean crystallite size was 2075 Å., and its lattice constant, a, was 4.805 Å.

The stones were hand ground and dry screened, and the fractions then were dispersed and wet screened. The wet-screen fractions were washed with acetone and again dry screened. The final products were free of aggregates and fairly uniform in size. The minus 34- plus 42-mesh and minus 100- plus 115-mesh fractions were used in the tests; the average particle size was calculated as the arithmetic average of the two screens that just passed and just retained each fraction.

The calcinations were made in a 4.5-cm. i.d. vertical tube furnace. About 0.5 gram (essentially a monoparticle layer) of the stone fraction was placed in the bottom of a 3.5- x 3.5-cm. cylindrical holder made of platinum and covered with a perforated lid. A 1400-cc./minute stream of a mixture of 15% CO_2 and 85% N_2 was used to flush the furnace tube; the flow was sufficient to change the furnace atmosphere about 2.5 times per minute. The preheated furnace was raised abruptly around the sample, held for the desired time, and then lowered. The temperature was measured with a thermocouple with the bead just below the sample holder. A total of 5 to 8 heatings was made under each set of conditions, and the products were composited to obtain sufficient calcines for measurements of their properties. The properties of the calcines that were measured are listed in Table V.

TABLE V

Properties of Calcines Under Different Calcination Conditions

	Calcination conditions		Properties							
			SO_3 absorbed,[a]	Pore vol.,[b] cc./gram		Density,[b] gram/cc.		Calcination,	Crystallite size, Å.	
Time, min.	Temp., °C.	Particle size, μ	mg./100 mg.	A	B	A	B	%	CaO	MgO
				Calcite (89-C)						
1	1100	384	36	0.561	0.160	1.04	1.82	96.3	1800	-
4	1100	384	23	0.546	0.150	1.12	2.04	97.5	2300	-
1	1225	384	13	0.453	0.093	1.29	2.45	98.6	1900	-
4	1225	384	11	0.437	0.087	1.35	2.57	99.7	5200	-
1	1100	136	31	0.637	0.132	0.95	1.88	95.9	1300	-
4	1100	136	17	0.557	0.126	1.12	2.24	98.0	2700	-
1	1225	136	11	0.453	0.097	1.29	2.51	99.1	4800	-
4	1225	136	11	0.440	0.082	1.34	2.63	99.3	3800	-
				Dolomite (BCR-2069)						
1	1100	384	63	0.263	0.131	1.32	1.60	97.6	1450	500
4	1100	384	64	0.263	0.170	1.42	1.64	98.8	1750	750
1	1225	384	48	0.283	0.203	1.64	1.88	98.4	1900	1400
4	1225	384	38	0.276	0.204	1.78	2.04	99.3	2400	2550
1	1100	136	57	0.841	0.131	0.74	1.57	98.4	1750	500
4	1100	136	57	0.701	0.192	0.86	1.59	98.5	1950	650
1	1225	136	41	0.881	0.284	0.99	1.87	98.4	2200	1350
4	1225	136	36	0.722	0.226	0.97	1.93	98.9	2650	1750

---

[a] Weight gain in 30 minutes at 930° C. in an atmosphere of 4% SO_2, 4% O_2, and 92% N_2.

[b] A - Excluding pores between 98 and 0.035 μ in diameter; B - excluding pores between 17.5 μ and and 0.035 μ in diameter.

Statistical analysis was made of the data in which all four factors were tested--time and temperature of calcination, and particle size and type of stone. Analyses were made for each measured property and for its logarithm, as shown in Table VI. The residual variance in each property was considered to be the 3- and 4-factor interactions; these variances were recalculated in terms of residual error and are shown in Table VI in units of the property. Thus, the residual error is 4.8 mg. SO_3/100 mg. calcine for the analysis of the effects of the factors on SO_3 absorption; it is 22.5% of the absorption when the logarithm is considered. The residual error should approximate the experimental error of replicates provided none of the 3- or 4-factor interactions are significant.

Absorption of SO_3: The absorption of sulfur oxides was measured as the gain in weight of the calcine in 30 minutes at 930° C. in an atmosphere of 4% SO_2, 4% O_2, and 92% N_2. The capacity to absorb SO_3 was decreased by increasing the calcination time from 1 to 4 minutes, by increasing the calcination temperature from 1100° to 1225° C., and by grinding the stones to 136-micron (100-mesh) particles rather than to 384-micron (40-mesh) particles when the stones were calcined for these times at these temperatures. The dolomite was a much more effective absorbent for SO_3 than was the calcite under these conditions of calcination. These overall effects of the independent variables (called "main effects" in statistical language) were significant with respect to the residual error, regardless of consideration of the numerical change in the weight during absorption or of the percentage change in weight (corresponding, respectively, to the analysis of y or log y, where y is the weight gain).

TABLE VI

Analysis of Effects of Factors and Their Interactions on the Properties of Calcines

	SO_3 absorbed		Pore volume (<98μ)		Pore volume (<17.5μ)		Density (<98μ)		Density (<17.5μ)		Calcination		CaO crystallite size	
	y	log y	y	log y	y	log y	y	log y	y	log y	y	log y	y	log y
t, min.	**	**	*	**	-	-	*	**	*	*	**	**	-	(*)
T, °C.	**	**	*	**	-	-	**	**	**	**	**	**	*	*
PS,[a] μ	**	*	**	**	-	-	**	**	-	-	-	-	-	-
Type[a]	**	**	-	**	**	**	-	(*)	**	**	(*)	(*)	(*)	(*)
t x T	-	-	-	-	(*)	(*)	-	-	-	-	-	-	-	-
t x PS	-	-	*	*	-	-	-	-	-	-	-	-	-	-
t x type	*	*	-	-	-	(*)	-	-	-	(*)	-	-	-	-
T x PS	(*)	-	-	-	-	-	-	-	-	-	-	-	-	-
T x type	*	**	**	**	**	**	-	-	*	(*)	**	**	-	-
PS x type	-	-	**	**	(*)	(*)	**	**	-	(*)	-	-	-	-
Residual error	4.8	22.5%	0.032	3.9%	0.022	10.8%	0.061	3.8%	0.069	3.7%	0.43	0.46%	920	35%

---

[a] PS = particle size; type = calcite vs. dolomite.

Significance at indicated confidence level: ** 99%; *95%; (*) 90%; - not significant.

The type of stone, calcite or dolomite, interacted significantly with both the time of calcination and the temperature of calcination in affecting both the numerical and percentage change of absorption. These simple 2-factor interactions can be demonstrated by the following tabulation.

	Absorption of SO_3, mg./100 mg., under indicated conditions of calcination			
	Time, min.		Temp., °C.	
	1	4	1100	1225
Calcite (C)	23.0	15.5	27.0	11.5
Dolomite (D)	52.0	49.0	60.0	41.0
Ratio D:C	2.30	3.15	2.24	3.54

In the tabulation the SO_3 absorption is averaged for all particle sizes and temperatures when considering the interaction between type of stone and time of calcination. Similarly, in considering the interaction between type of stone and temperature of calcination, the averages for all particle sizes and times are calculated. For example, for the four calcite heatings for 1 minute it is calculated from the data in Table V: $23 = (36 + 13 + 31 + 11)/4$. The ratios of the absorption by dolomite to that by calcite indicate the interactions. The dolomite absorbed more than three times as much SO_3 as the calcite for all calcination times of 4 minutes, whereas it was only 2.3 times as effective for all calcination times of 1 minute. Similarly, the dolomite was 3.5 and 2.2 times as effective as the calcite at 1225° and 1100° C., respectively.

These conclusions are based upon a standard error of 22.5% in SO_3 absorption or a numerical error of 4.8 mg. SO_3/100 mg. calcine. This relatively high error suggests that one or more of the high-level interactions used in computing the error may also be significant.

A better estimate of the error for SO_3 absorption was obtained by running partial duplicates on the eight calcite samples. Complete duplicates were not made because this would entail duplication of the screening and firing; the firing was done in small monolayer batches and composited as described earlier. Duplicate absorption measurements were therefore made on the composited calcines. Each absorption of SO_3 was made in the TGA apparatus and the recorded weight increase was checked by weighing before and after absorption on an analytical balance and by chemical analysis of the product after absorption was complete. The recorded absorption was taken as the average of the three methods of determination. Table VII shows the analysis of variance from which the error of the partial duplicates is estimated as 1.2 mg. SO_3/100 mg. calcine or 5.9% of the average absorption by the calcite samples. The error of true duplicates would be expected to be only slightly greater than these values.

The data in Table VII show that there was a significant difference among the absorptions of the eight samples, that there was a difference among methods of determining the weight increase, and that the duplicates agreed better for some samples than for others. The TGA recorded weight increase was higher than that determined by the analytical balance or by chemical analysis; this was due to a drift in

TABLE VII

Analysis of Variance for Partial Duplicates of Eight Absorption Samples Using the Average of Three Methods of Analyses

Source of variation	Corrected sums of squares	Degrees of freedom	Mean square	F-ratio
Samples (S)	3727.75	7	532.54	123 **
Methods (M)	42.94	2	21.47	4.95**
Duplicates (D)	0.12	1	0.12	0.03
S x M	57.52	14	4.11	0.95
S x D	111.31	7	15.90	3.66*
M x D	0.83	2	0.42	0.10
Residual	60.77	14	4.34[a]	-
Total	4001.24	47		

Significance at indicated confidence level: ** 99%; * 95%.

[a] Error = $\sqrt{4.34/3}$ = 1.2 mg. SO_3/100 mg. calcine.

the calibration during the absorption run and is routinely corrected for in precise TGA work. However, the interaction between the duplicates and samples suggests that the error might be proportional to the measurement. This was verified by considering the data for the three methods of analysis for the eight dolomite samples. The residual error was 2.2 mg. SO_3/100 mg. calcine or 7.5% of the average absorption by the dolomite samples. The error analyses indicate that a percentage error is more appropriate for the absorption of SO_3 and that the analysis in Table VII of the logarithm of the absorptions is preferred for this property of the calcines.

The residual error of 22.5% in Table VI for the logarithm of the absorption of SO_3 is considerably larger than the error (5.9% to 7.5%) estimated for the runs. This suggests that there are one or more high-level interactions that are significant for the absorption of SO_3. The sums of squares for the 3- and 4-factor interactions are

Interaction[a]	Sums of squares
t x T x PS	0.00227
t x T x type	0.01875
t x PS x type	0.00006
T x PS x type	0.00093
t x T x PS x type	0.00047

[a] t = time, T = temperature, PS = particle size.

The heterogeneity of these variances is evident from the fact that the sum of squares for the interaction of time, temperature, and type is nearly an order of magnitude greater than the next greatest sum of squares. When this interaction is eliminated from the residuals, the error is calculated to be 7.3% of the measurement, which is in good agreement with the estimated error from the partial duplicates.

The interaction of time of calcination, temperature of calcination, and type of limestone can be demonstrated by the following tabulation which averages the results for the two particle sizes used.

Time, min.	Calcite 1100° C.	Calcite 1225° C.	Dolomite 1100° C.	Dolomite 1225° C.
1	33.5	12.0	60.0	44.5
4	20.0	11.0	60.5	37.0

The effect of changing the time of calcination from 1 minute to 4 minutes is insignificant for the calcite calcined at 1225° C. or for the dolomite calcined at 1100° C.; however, 40% and 20% decreases, respectively, in the SO_3 absorption are obtained by increasing the calcination time for calcite at 1100° C. and for dolomite at 1225° C. An insignificant 3-factor interaction would have shown more nearly the same effects for the two materials at the same temperature.

The interaction of time of calcination, temperature of calcination, and type of limestone on the capacity of the calcine to absorb SO_3 is shown in Figure 20. The isopleths of SO_3 absorption were constructed from an equation that contained only the significant effects shown in Table VI plus the three-factor interaction, time x temperature x type.

In coded form the equation is

$$\log y = 1.4641 - 0.04254x_1 - 0.13055x_2 - 0.02841x_3 + 0.22934x_4 + 0.02356x_1x_4 + 0.04466x_2x_4 - 0.03423x_1x_2x_4 \quad (20)$$

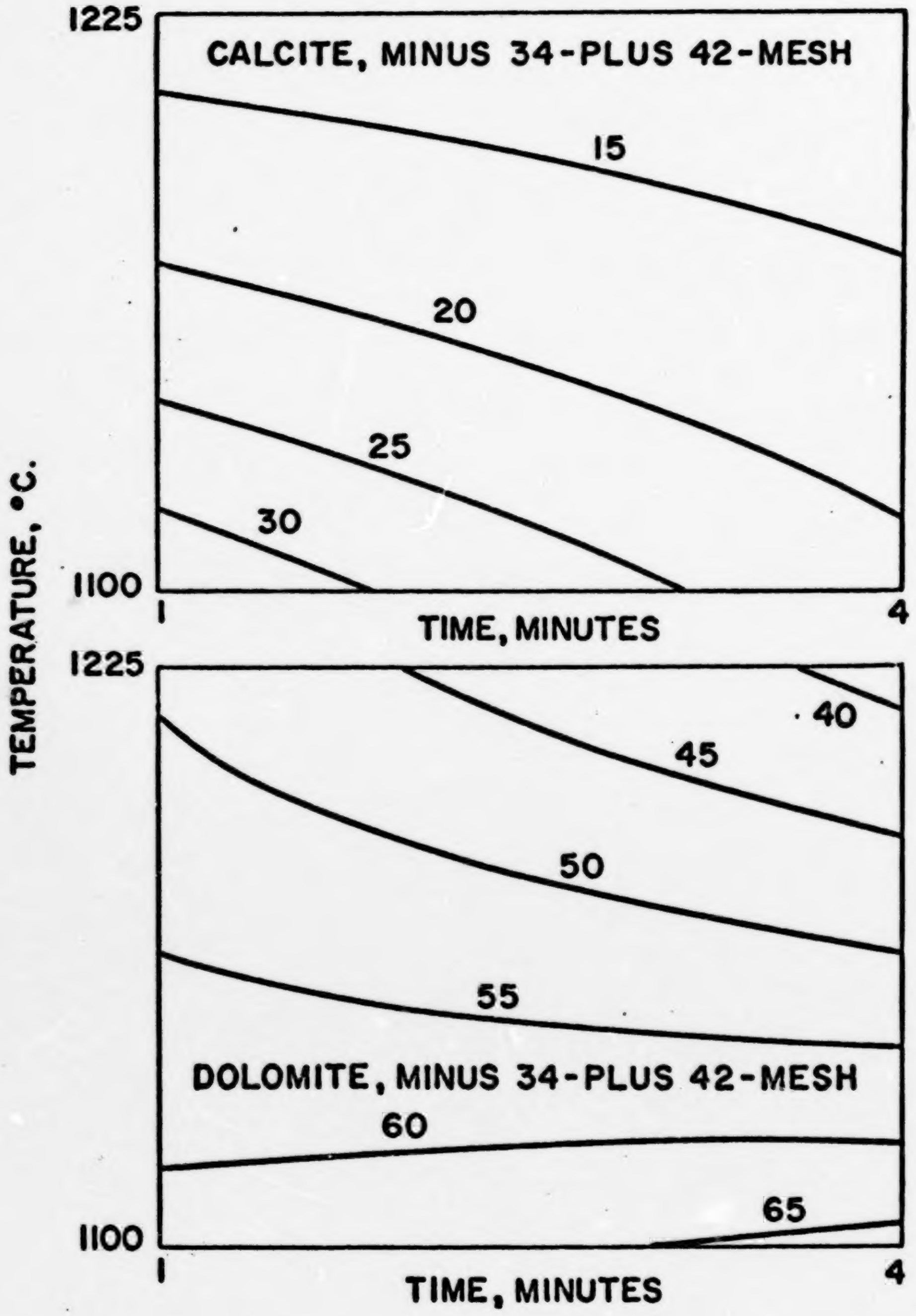

Figure 20. Isopleths of SO_3 Absorption As Functions of the Time and Temperature of Calcination. [Numbers on curves indicate weight gain (as SO_3)/100 mg. calcine]

where x_1 refers to the time of calcination, x_2 to temperature of calcination, x_3 to particle size of the limestone, and x_4 to the type of limestone. The coded variables, x_i, have the values of -1 and +1, respectively, for the low and the high levels of the real variables shown in Table V. The variables x_1, x_2, and x_3 are quantitative or continuous variables, since numbers can be assigned to the levels; variable x_4, however, is a qualitative or discrete variable and refers to a type of material for which the assignment of numbers to intermediate levels is questionable. The coefficients of equation 1 were calculated from the data in Table V by analysis of the logarithms of the SO_3 absorptions.

The contours of absorption of SO_3 by the calcite shown in Figure 20 are flatter with time when the temperature is high (1225° C.) than when the temperature is low (1100° C.); for the dolomite, the contours are flatter at the lower temperature. This results in a response surface for the calcite absorption that is steeper at short calcination times than at long calcination times; for the dolomite, the response surface is steeper at 4 minutes calcination time than at 1 minute calcination time. This suggests that at 1225° C. the calcite has already lost its reactivity toward SO_2 after 1 minute of calcination whereas the dolomite still has capacity to react at this temperature. The optimum conditions for the calcite absorption would therefore be at some calcination time shorter than 1 minute, whereas the temperature of calcination would be more critical than the time of calcination in obtaining the optimum conditions for the reactivity of the dolomite.

(In Figure 20, no units have been shown for intermediate times and temperatures because it cannot be established from these tests whether the scales should be linear, logarithmic, exponential, or of some other form.)

Other Properties of the Calcines: The total pore volume (of pores between 98 and 0.035 micron), the two density measurements, and the degree of calcination have residual errors either in y or log y that approximate the errors of measurement of these properties. The residual errors for the crystallite size of CaO are 920 Å. in y and 35% in log y, and for the logarithm of the pore volume of pores between 17.5 and 0.035 micron the error is about 11%. These are considered larger than the measuring errors and they therefore suggest that there are significant 3- or 4-factor interactions of both of the variables studied that affect these properties. These interactions are identified, in coded form, as

$x_1x_2x_4$ for the pore volume (17.5 to 0.035 micron)

both $x_1x_2x_3$ and $x_1x_2x_3x_4$ for the crystallite size of the CaO.

The 3-factor interactions can be illustrated in the same manner as was done above for the interaction of $x_1x_2x_4$ in the absorption of SO_3. The 4-factor interaction, $x_1x_2x_3x_4$, is more difficult to understand in physical significance, but it can be readily demonstrated in mathematical terms by considering the two 2-factor interactions, x_1x_2 and x_3x_4, and constructing the following tabulation.

Crystallite Size of CaO for Different Combinations of x_1x_2 and x_3x_4 Interactions

x_1x_2	x_3x_4 -	x_3x_4 +
-	2540 Å.	2080 Å.
+	2030 Å.	2570 Å.

The low value (-) for each 2-factor interaction is taken as a combination in which one of the factors is at the low level and the other is at the high level; the high value (+) for the interactions indicate that both factors are at the high level or both are at the low level. The 4-factor interaction for the CaO crystallite size is then demonstrated by the decrease that occurs as one 2-factor interaction is changed from its low value to its high value while the other 2-factor interaction is maintained at its low value, and by the increase that occurs at the high value of the second interaction; in the absence of a 4-factor interaction these effects would be about the same.

A very prominent interaction in the total pore volume, and the density obtained therefrom, is that of the particle size of the limestone and the type of limestone. This is evident from the 5th column of Table V where the smaller particle size of the dolomite gives rise to a much larger total pore volume over the coarser grind than that for the calcite. This may explain why the total pore volume is not as good an index for reactivity as is the pore volume which includes only those pores 17.5 to 0.035 micron in diameter; the effect of particle size for different types of stones is largely eliminated by selection of the proper pore volume.

The pore volume which includes only pores of 17.5 to 0.035 micron, column 6 in Table V, has a significant interaction between the type of stone and the temperature of calcination. Changing the temperature of calcination from 1100° to 1225° C. caused a decrease in this pore volume for the calcite and an increase for the dolomite. This temperature change caused a decrease in the absorption of SO_3 for both types of stone, although the decrease was not as pronounced, percentagewise, for the dolomite as for the calcite.

The degree of calcination, column 9 of Table V, ranged from about 96 to 100% under the conditions of the tests. The dolomite was slightly more nearly completely calcined at 1100° C. than was the calcite, but it is doubtful that differences in the degree of calcination can be related to the reactivity with SO_3. The particle size of the stone was not significant for the degree of calcination under these conditions.

The absorption of SO_3 by a calcine is influenced greatly by the conditions of calcination as well as by the type of stone and the degree of grinding the stone prior to calcination. The significant interactions of these factors on several properties of the calcine have been identified. There is not a complete correlation of the effects of the factors for SO_3 absorption with any single measurable property; it is quite likely that the absorption of SO_3 depends on several of the other properties of the calcine.

The presence of high-level interactions of factors for many of the properties of calcines raises serious questions as to the applicability of second-order designs to study of the system. In the ranges of the variables studied, third-order designs appear to be required for many of the properties, and the crystallite growth of CaO may require even higher-order design. It should be noted, however, that the order of the design required to represent a property adequately will be decreased as the ranges of the factors are decreased. This may permit the use of second-order designs for injection conditions where the experimental conditions vary less widely, particularly for the time of calcination. It is probable, however, that this information can be obtained only under actual injection test conditions at a power plant.

COMPARISON OF LIMESTONES

Introduction

The injection of limestone into a power plant combustion chamber results in dispersion of the particles of the stone in the gas, calcination, and reaction of the calcine with the SO_2 in the gas. The system is polythermal in that the temperature of the injected material rises from ambient to nearly that of the flame, and then cools at an unknown and perhaps variable rate. The calcination reaction is endothermic and serves to lower the temperature attained by the particles on injection; the sulfation reaction is exothermic and, if sufficiently rapid, serves to raise the temperature of the particles. The short retention times of both calcination and sulfation, the high temperatures attained, and the high velocity of the gas stream and its entrained solids make it difficult to reproduce the conditions in the laboratory and measure the reactions with the precision desired.

Laboratory simulations of the injection system include compromises of one kind or another. Fixed-bed tests with calcined stone do not include the calcination reaction; dispersion of the particles in the gas stream is not attained in fixed beds of either raw stone or calcine, and the rate of mass transfer is much slower than is attained in practice. Most laboratory tests have been capacity tests rather than rate tests, and the correlation of capacity with rate has not been demonstrated sufficiently to establish much confidence in capacity tests alone. Results of isothermal tests of capacity vary markedly with the temperature and with the stone (2). The dispersed-phase reactor of Battelle (6) approaches the injection system physically, but the problems of sampling, freezing all reactions, and sensitivity to chemical analytical errors preclude the precise determination of mechanisms, rates, and efficacy of the process that is desired.

This section of the report describes tests of selected stones in an attempt to relate their calcination and sulfation properties--both capacities and rates--to the chemical and mineralogical properties of the stones. Like other laboratory tests, these suffer from compromises that prevent determination of the absolute correlations desired. Several rate and capacity measurements were made, but it cannot be determined at present which, if any, of them apply closely to the injection system.

It was hoped that activation energies and frequency factors of the sulfation reaction could be obtained from the polythermal TGA studies, and that the resulting kinetic parameters could be used in the equations derived in Appendix C. The weight of the sample in the TGA apparatus is the combined result of the amount of calcination that has occurred, the uptake of SO_2, the amount of oxidation to sulfate, the amount of decomposition of the sulfite as the temperature is raised, and perhaps the substitution of SO_2 for CO_2 without calcination. It became obvious that a determination of weight as a function of time and temperature would hardly suffice to define the kinetic parameters of sulfation, even though many of the kinetic parameters of the other reaction were known. The TGA was not sufficiently sensitive to detect a change in weight when SO_2 was in the atmosphere until the temperature was 50° to 100°C. above that at which decomposition began when SO_2 was absent. This implies either a retardation of the calcination reaction by SO_2 or a substitution reaction of SO_2 for CO_2 in which no appreciable weight change occurred. In either case, the kinetics of calcination in nitrogen cannot be used to predict calcination losses when SO_2 is present. The multiplicity of simultaneous reactions, as described above, precludes the accurate determination by TGA of the kinetic parameters for sulfation. The sulfation of the various stones, however, has pointed out distinctive characteristics that may be correlated with their chemical and mineralogical properties.

Selection of Limestones

A group of 70 to 80 stones was supplied by the Air Pollution Control Office (APCO), and each stone was studied petrographically to identify the rhombic carbonates and the accessory minerals, and to determine the range of grain sizes in each stone. From this group 35 stones were selected for calcination and sulfation tests, and a detailed mineralogical characterization was made of each stone.

The compositions of the 35 limestones are shown in Table VIII; 18 stones were primarily calcites, 13 were dolomites, 2 were mixtures of calcites and dolomites, and 2 were mixtures of magnesite and dolomite. The chemical compositions were determined spectroscopically by Bituminous Coal Research, Inc.; the ignition losses agreed with those we obtained

TABLE VIII

Chemical and Mineralogical Properties of Limestones

BCR No.	Composition, wt. %[a] Ign. loss	CaO	MgO	Fe_2O_3	Na_2O	K_2O	MnO_2	Gangue[b]	Grain size, coded[c]	Unit-cell length, a, Å.	Crystallite size, µ
					Calcites						
1336	43.2	53.4	1.5	0.2	0.0057	0.0284	0.0085	1.6	3.0	4.978	0.149
1343	42.5	54.1	0.5	0.4	0.0115	0.0575	0.0345	0.7	1.0	4.989	0.167
1350	43.6	54.7	0.5	0.2	0.0056	0.0282	0.0451	2.6	2.0	4.986	0.177
1355	33.1	41.5	1.2	1.6	0.2542	0.4349	0.0268	24.6	1.0	4.982	0.096
1359	43.6	54.7	0.7	0.1	0.0056	0.0282	0.0141	0.9	1.0	4.985	0.124
1363	36.1	42.2	0.9	1.6	0.1406	0.6518	0.1278	18.0	1.0	4.989	0.124
1368	40.1	49.1	1.3	0.9	0.0898	0.2636	0.9165	8.8	2.6	4.978	0.097
1369	43.4	54.3	0.8	0.1	0.0396	0.0736	0.0085	0.8	1.0	4.987	0.127
1377	27.3	28.4	2.8	5.1	0.2326	3.9985	0.0872	43.8	1.0	4.975	0.162
1379	41.3	48.7	2.2	0.4	0.1526	0.2818	0.0411	6.6	3.0	4.980	0.097
1677	26.5	31.2	1.1	0.7	0.0735	0.2058	0.0110	45.0	1.0	4.987	0.177
1679	42.7	52.1	1.4	0.3	0.0917	0.0802	0.0086	3.6	1.0	4.975	0.068
1681	37.7	44.9	2.2	0.6	0.0623	0.2056	0.0093	13.8	1.0	4.985	0.115
1685	43.9	48.2	4.6	0.4	0.0505	0.0280	0.0617	3.0	2.8	4.986	0.145
1687	43.2	53.4	1.2	0.1	0.0284	0.0568	0.0284	1.5	2.6	4.986	0.177
1691	38.6	47.3	1.7	0.6	0.0860	0.3438	0.0430	12.4	1.0	4.984	0.107
1692	42.9	54.8	0.3	0.1	0.0286	0.0286	0.0086	0.6	3.0	4.985	0.153
1693	42.7	53.3	0.6	0.2	0.0573	0.1031	0.0086	2.8	1.0	4.985	0.130
					Dolomites						
1337	47.2	29.0	22.7	0.2	0.0053	0.0264	0.0079	1.0	2.0	4.811	0.119
1340	46.2	30.7	19.9	1.4	0.0054	0.0269	0.2690	2.0	1.5	4.808	0.141
1341	46.7	29.8	22.4	0.3	0.0053	0.0266	0.0080	0.7	3.0	4.806	0.211
1367	43.9	32.5	15.8	5.2	0.0224	0.0280	0.5610	7.0	1.0	4.816	0.085
1380	46.7	30.4	21.9	0.3	0.0266	0.0266	0.0080	0.6	2.5	4.805	0.189
1678	30.8	19.7	14.5	1.3	0.0830	0.9826	0.0415	35.0	1.5	4.808	0.141
1680	42.4	28.2	19.3	0.9	0.0346	0.2534	0.0691	9.2	1.0	4.806	0.171
1686	46.9	29.7	22.0	0.2	0.0159	0.0266	0.0080	1.0	3.0	4.806	0.189
1688	47.1	29.1	22.2	0.5	0.0159	0.0265	0.0159	0.5	1.5	4.807	0.182
1690	34.0	22.4	15.5	1.1	0.0396	1.1286	0.0792	24.2	3.0	4.809	0.098
1695	42.2	28.9	23.1	0.6	0.0289	0.0289	0.0087	4.8	3.0	4.808	0.189
1701	42.5	34.5	13.5	4.3	0.0920	0.1553	0.4542	8.6	1.3	4.822	0.090
1702	44.6	33.2	18.0	0.8	0.0277	0.2715	0.0083	4.6	1.3	4.810	0.070
					Mixtures						
1360	44.5	45.0	7.2	0.7	0.0277	0.0277	0.0888	3.4	2.5	4.910	0.135
1694	38.0	37.2	12.4	0.6	0.0310	0.0310	0.0093	12.6	3.0	4.886	0.159
					Magnesites						
1375	46.4	15.8	32.2	0.9	0.0322	0.1340	0.0080	10.0	2.5	4.720	0.147
1376	48.8	7.1	41.0	0.8	0.0154	0.0256	0.0154	28.0	2.5	4.720	0.220

---

[a] Calculated from composition of calcine.

[b] Accessory minerals.

[c] 1 = fine, < 63 µ; 2 = medium, 63-250 µ; 3 = coarse, > 250 µ.

in our calcination tests. The CaO, MgO, Fe_2O_3, Na_2O, K_2O, and MnO_2 contents were determined on the calcines: they were recalculated to reflect the compositions of the original stones. The amounts of accessory minerals, column 9 of Table VIII, were determined by decomposing 3 to 5 grams of each limestone in 400 ml. of 1% acetic acid and maintaining the pH at 4 by addition of acetic acid until all the rhombic carbonates were dissolved; this required about 24 hours for the calcites, 1 to 2 weeks for the dolomites, and several weeks for the stones that contained considerable magnesite ($MgCO_3$). The accessory minerals were recovered unaltered, and their amounts are listed in Table IX.

The last three columns of Table VIII show the microscopic grain texture; the x-ray unit cell length, a, of the major carbonate phase; and the x-ray crystallite size within the grains. The grain texture, column 10, was determined petrographically and coded to agree with the scale used by Harvey (10); for the purpose of this tabulation the rather broad groups of fine, medium, and coarse grain sizes are labeled 1, 2, and 3, respectively, with an occasional variation from integers as the predominant grain size approached the arbitrary values of 63 or 250 microns that separated the groups. The grains were irregular in shape, and there was a large range of grain sizes in each limestone; the predominant grain size in each stone is therefore given a semi-quantitative rating for correlation with its calcination and sulfation parameters.

TABLE IX

Accessory Mineral Content of Limestones

	Accessory minerals, wt, %									
BCR No.	Total	Quartz	Illite	Montmorillonite	Chert	Tremolite	Limonite	Feldspar	Muscovite	Glass frit
					Calcites					
1336	1.6	0.0	0.0	0.0	0.0	1.0	0.0	0.0	0.0	0.0
1343	0.7	0.3	0.1	0.0	0.2	0.0	0.1	0.0	0.0	0.0
1350	2.6	1.6	0.9	0.0	0.0	0.0	0.1	0.0	0.0	0.0
1355	24.6	16.0	8.6	0.0	0.0	0.0	0.0	0.0	0.0	0.0
1359	0.9	0.4	0.0	0.0	0.0	0.0	0.0	0.0	0.1	0.4
1363	18.0	6.0	6.0	0.0	0.0	0.0	0.0	0.0	6.0	0.0
1368	8.8	4.2	4.2	0.0	0.0	0.0	0.4	0.0	0.0	0.0
1369	0.8	0.4	0.4	0.0	0.0	0.0	0.0	0.0	0.0	0.0
1377	43.8	13.1	13.1	0.0	0.0	0.0	4.5	0.0	13.1	0.0
1379	6.6	4.6	0.0	0.0	0.0	0.0	0.0	1.0	0.0	0.0
1677	45.0	14.0	0.0	14.0	0.0	0.0	3.0	0.0	0.0	14.0
1679	3.6	1.7	1.7	0.0	0.0	0.0	0.2	0.0	0.0	0.0
1681	13.8	4.6	4.6	0.0	4.6	0.0	0.0	0.0	0.0	0.0
1685	3.0	1.0	1.0	0.0	0.9	0.0	0.1	0.0	0.0	0.0
1687	1.5	0.5	0.5	0.0	0.4	0.0	0.0	0.0	0.0	0.1
1691	12.4	3.8	8.0	0.0	0.0	0.0	0.6	0.0	0.0	0.0
1692	0.6	0.3	0.2	0.0	0.0	0.0	0.1	0.0	0.0	0.0
1693	2.8	1.0	1.8	0.0	0.0	0.0	0.0	0.0	0.0	0.0
					Dolomites					
1337	1.0	0.7	0.0	0.2	0.0	0.0	0.1	0.0	0.0	0.0
1340	2.0	2.0	0.0	0.0	0.0	0.0	0.0	0.0	0.0	0.0
1341	0.7	0.0	0.0	0.0	0.0	0.5	0.0	0.1	0.0	0.0
1367	7.0	0.3	0.0	0.0	0.0	0.0	6.7	0.0	0.0	0.0
1380	0.6	0.1	0.1	0.0	0.0	0.0	0.0	0.1	0.0	0.3
1678	35.0	15.7	15.7	0.0	0.0	0.0	1.8	1.8	0.0	0.0
1680	9.2	3.1	0.0	0.0	0.0	0.0	0.0	3.1	0.0	3.0
1686	1.0	0.3	0.3	0.0	0.3	0.0	0.0	0.0	0.0	0.0
1688	0.5	0.2	0.2	0.0	0.0	0.0	0.0	0.0	0.0	0.1
1690	24.2	20.6	3.6	0.0	0.0	0.0	0.0	0.0	0.0	0.0
1695	4.8	1.4	0.5	0.0	0.0	1.4	0.0	0.0	1.4	0.0
1701	8.6	3.0	0.0	0.0	0.0	0.0	5.6	0.0	0.0	0.0
1702	4.6	2.3	2.3	0.0	0.0	0.0	0.0	0.0	0.0	0.0
					Mixtures					
1360	3.4	0.0	0.4	0.0	1.3	0.0	1.3	0.0	0.0	0.4
1694	12.6	4.0	0.0	0.0	0.0	4.0	0.0	0.0	0.6	0.0
					Magnesites					
1375	10.0	1.0	0.0	0.0	0.0	0.0	0.0	0.0	0.0	0.0
1376	28.0	0.7	0.0	0.0	0.0	0.0	0.0	0.0	0.0	0.0

The unit-cell length, a, column 11 of Table VIII, was determined by measuring the d-spacings corresponding to various Miller indices (hkℓ) in the x-ray diffraction pattern and using the method of least squares (18) to obtain the unit-cell dimensions or lattice constants. Goldsmith and Graf (9) showed that both the a and c dimensions of the unit cell were functions of the degree of substitution of magnesium for calcium in both calcite and dolomite and of calcium for magnesium in dolomite. The larger ratio of the radius of Ca to that of O (0.67) compared with that of Mg to O (0.47) results in a decrease in the cell dimension when magnesium substitutes for calcium, and an increase when calcium substitutes for magnesium. Thus, the length of the lattice constant, a, is an indication of the kind and degree of substitution in the rhombic carbonates; the pure constituents have ideal values of 4.990 Å. for calcite, 4.808 Å. for dolomite, and 4.633 Å. for magnesite.

The x-ray crystallite size, column 12 of Table VIII, represents the mean size of the crystallites within the grains of the major carbonate minerals--calcite, dolomite, or magnesite--in each stone. This property was measured by the x-ray line-broadening technique described by Rau (22) using the value of the pure diffraction breadth due to crystallites as defined by Azaroff (1). The $(10\bar{1}4)$ reflection was used to calculate the mean crystallite size for the stones because it is the strongest diffraction maximum for the rhombohedral carbonates and is particularly useful when the samples contain mixtures of carbonate species. The crystallite sizes are reported in microns rather than the customary Angstrom units (1 Å. = $10^{-4}\mu$). Both the crystallite size and the lattice dimension of a limestone are properties of the composition of the carbonate fraction of the stone, particularly the distribution of calcium and magnesium atoms in the unit cell.

The accessory minerals of each stone, column 9 of Table VIII, were further identified as to amount and type of impurity by petrographic methods. The results are presented in Table IX for ten of the more common impurities found in the stones, including an unidentified fritted glass. Pyrite, mica, and some unidentified phases were found in a few stones but in very small amounts. The total residue from the acetic acid treatment ranged from 0.5 to 45% of the stone. The 10 components listed in Table IX account for essentially all the impurities for all the stones except the magnesites (BCR 1375 and 1376); for these two stones the bulk phase of the acetic acid residue, after 3 months' treatment, was undissolved magnesite.

Calcination

The calcination tests were made in the TGA with 50 mg. of the minus 24- plus 28-mesh fraction of each stone. The sample was spread as a single layer in the sample dish and covered with glass wool and a perforated lid to prevent sample loss and allow escape of gases. The equipment was flushed with nitrogen gas at the rate of 500 ml. per minute, and the heating rate was approximately 5° C. per minute. Typical smoothed curves of weight versus temperature are shown in Figures 21 and 22.

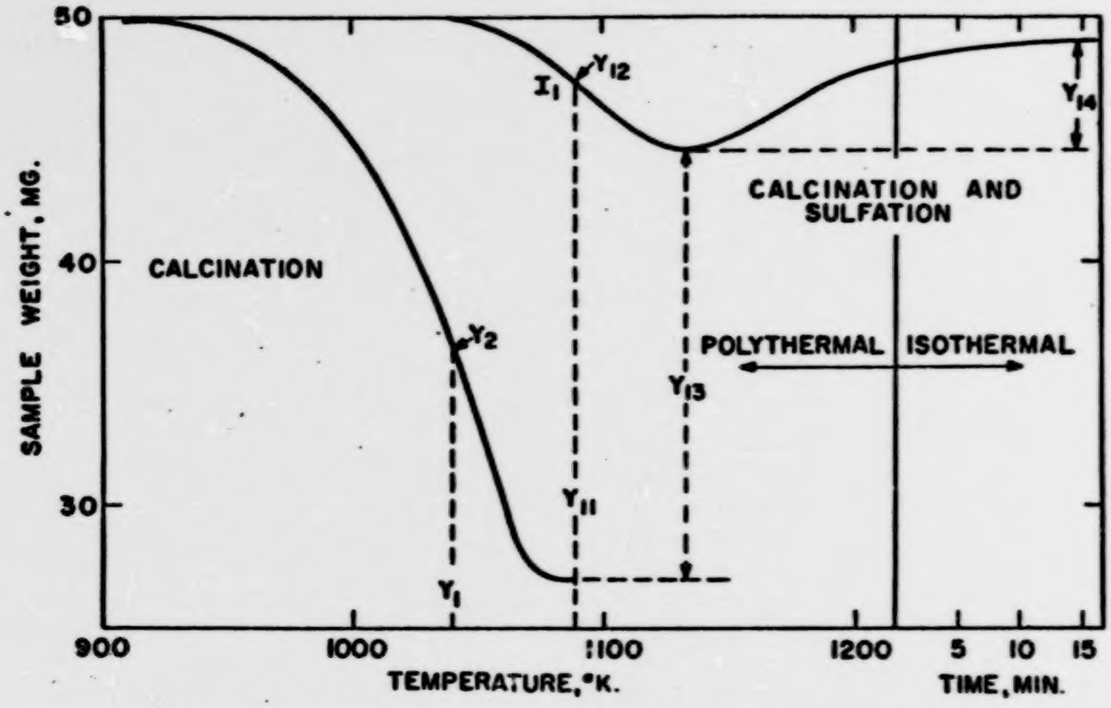

Figure 21. Calcination and Sulfation of a Calcite, BCR 1679.

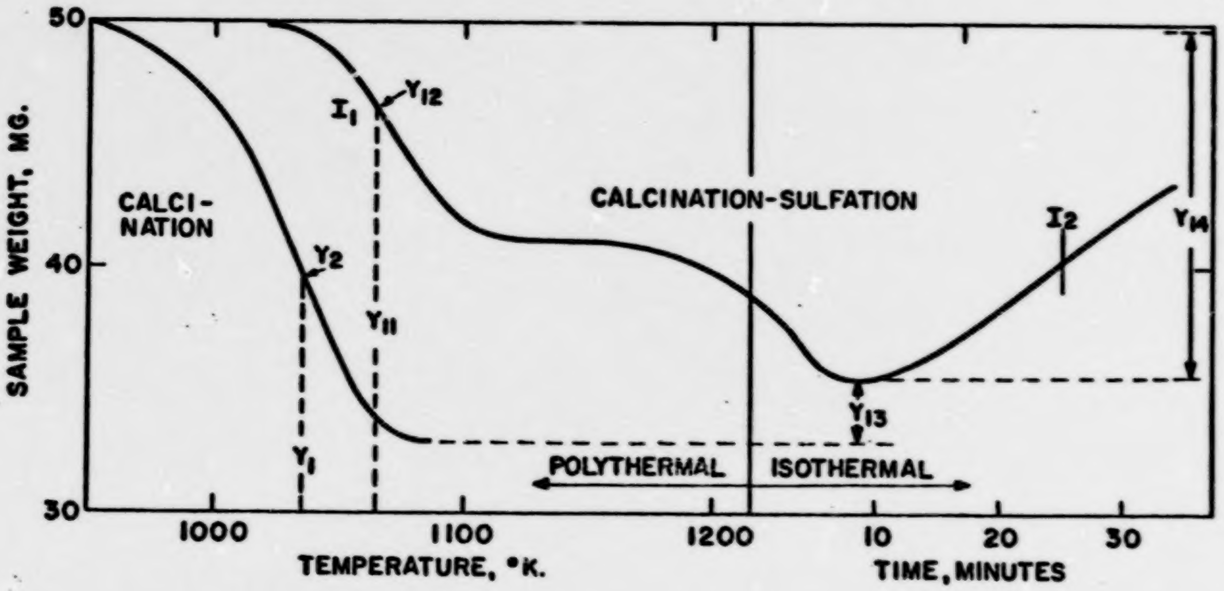

Figure 22. Calcination and Sulfation of a Dolomite, BCR 1690.

The parameters for calcination are given in columns 2 through 5 of Table X. The inflection temperature is the point at which the curve changes from concave downward to concave upward, and also is the temperature at which the rate of calcination, column 3, is greatest for the particular sample size, particle size, and heating rate. The activation energy and pre-exponential term of the Arrhenius equation, columns 4 and 5, were determined by least squares as described in Appendix B; the relation between these parameters is shown in Figure 1.

Sulfation

Isothermal: Capacity measurements of the absorption of sulfur oxides by 50 mg. of precalcined stone were made in the TGA at 930° C. Each stone was soft-calcined at 900° C. for 30 minutes in a nitrogen atmosphere, and the minus 24- plus 28-mesh fraction of the calcine was subjected for 30 minutes to a flow of 500 ml./min. of an atmosphere of 4% SO_2, 4% O_2, and 92% N_2. Curves similar to those of Figure 2 were drawn to obtain the first-stage and total weight gains. Columns 6 through 9 of Table X show the important characteristics of each stone with respect to isothermal sulfation at 930° C.; these include the total capacity, the maximum rate of weight gain, the first-stage capacity, and the time to complete the first stage under these conditions.

Polythermal Calcination-Sulfation

The polythermal calcination-sulfation tests were made on 50 mg. of stone at a heating rate of about 5° C. per minute in a flow of 500 ml./min. of an atmosphere of 4% SO_2, 4% O_2, and 92% N_2. The

TABLE X

Calcination and Isothermal Sulfation of Limestones

	Polythermal calcination				Isothermal sulfation[a]			
							First stage	
BCR No.	Inflection point T_I, °K.	$-(dw/dt)_I$, mg./°K.	E, kcal./mole	log k_o	Total wt. gain, mg.	$(dw/dt)_m$, mg./min.	wt. gain, mg.	Time, min.
				Calcites				
1336	1079	0.249	51.5	9.55	14.64	5.29	14.10	3.1
1343	1068	0.378	68.2	13.15	25.76	11.14	22.90	3.2
1350	1058	0.388	68.0	13.29	28.35	10.27	25.50	4.0
1355	1036	0.240	52.1	10.11	20.86	7.57	16.50	3.7
1359	1057	0.231	51.8	9.76	13.78	3.99	12.10	3.6
1363	1067	0.320	52.0	9.71	24.63	10.75	20.20	3.5
1368	1056	0.269	41.4	7.60	24.44	7.93	19.00	3.3
1369	1087	0.299	30.2	5.00	16.41	7.58	13.80	4.0
1377	1076	0.217	73.7	14.06	16.21	5.21	11.00	4.5
1379	1078	0.297	69.0	13.28	16.30	7.96	14.60	4.1
1677	1031	0.206	33.6	6.14	12.72	6.17	9.60	5.3
1679	1048	0.351	57.0	11.10	39.99	16.47	35.00	3.1
1681	1065	0.366	51.7	9.67	27.91	10.80	21.30	3.2
1685	1032	0.280	48.4	9.32	25.59	13.17	22.50	2.8
1687	1029	0.244	47.9	9.21	26.97	11.19	23.50	3.3
1691	1073	0.255	65.5	12.59	33.13	13.67	25.60	3.4
1692	1073	0.374	72.3	15.01	23.79	9.11	17.50	3.4
1693	1057	0.358	61.9	10.04	26.41	16.82	23.50	2.7
				Dolomites				
1337	1069	0.250	55.1	10.36	18.36	9.22	16.20	3.4
1340	1060	0.398	70.7	13.85	15.60	8.71	13.60	3.3
1341	1060	0.390	55.0	10.42	10.90	6.12	9.80	3.2
1367	1040	0.330	38.5	7.19	21.81	15.31	18.00	2.9
1380	1025	0.320	51.2	10.13	32.47	9.00	29.20	3.9
1678	1048	0.204	63.2	12.25	20.88	10.71	14.90	2.4
1680	1046	0.356	67.1	13.33	31.37	13.00	27.80	4.2
1686	1034	0.389	55.7	10.98	34.62	13.98	28.50	3.1
1688	1045	0.332	75.3	15.02	38.90	15.05	32.20	4.5
1690	1040	0.265	47.6	9.10	19.70	10.27	17.50	2.9
1695	1065	0.353	56.5	10.72	12.48	6.34	10.00	3.6
1701	1025	0.289	51.0	10.02	34.13	14.07	26.80	3.0
1702	1044	0.357	53.7	10.28	26.03	9.43	22.00	4.1
				Mixtures				
1360	1049	0.381	66.1	12.96	38.50	14.14	24.60	2.9
1694	1049	0.365	28.3	4.76	12.45	8.62	8.60	1.7
				Magnesites				
1375	910	0.214	25.5	5.22	13.70	5.81	10.00	3.7
1376	922	0.327	50.9	11.21	10.22	1.87	5.60	4.8

---

[a] For 30 minutes at 930° C.; based on 50 mg. initial calcine.

heating rate was approximately the same as that for the polythermal calcination tests, and the atmosphere was the same as for the isothermal sulfation tests. Typical smoothed curves for the change in weight with rising temperature are shown in Figures 21 and 22 for stones BCR 1679, a calcite; and BCR 1690, a dolomite. The temperature rise stopped at 940° C. (1213° K.), the upper temperature limit of the TGA equipment; the reactions were isothermal at 930° C. beyond this point and the units on the abscissa of Figures 21 and 22 then are indicated by time in minutes.

The behavior of a stone (BCR 1679) that had sulfated markedly during calcination is shown in Figure 21, and that of a stone (BCR 1690) in which little reaction had occurred during calcination is shown in Figure 22; this effect is indicated by the height of the minimum of the calcination-sulfation curve above the final calcination curve (y_{13}). A test for carbonate at the completion of each run showed that decarbonation had been completed. Two inflection points, I1 and I2, are indicated by arrows on the calcination-sulfation curves; these are the points of most rapid weight loss and weight gain, respectively. The inflection points are calculated by the computer in applying the spline-curve fit to the data; the same is true of the minimum in the curve. The minimum and the second inflection I2 frequently occurred while the system was isothermal at 940° C., as in Figure 22.

The important characteristics of all the stones in the polythermal calcination-sulfation tests are given in Table XI. The three temperatures are T_O, the temperature at which weight loss was first detected; T_{I1}, the inflection temperature at which the rate of weight loss was greatest; and T_{min}, the temperature at which the weight was a minimum (the rates of sulfation and calcination were equal). (If T_{min} was not attained below 940° C., its value was obtained by extrapolation.) The slope, $(dw/dT)_I$, is the maximum rate of weight loss; this occurred at the inflection temperature T_{I1}. Columns 6, 7, and 8 of Table XI show the weight gains per 50 mg. of calcine resulting from sulfation that occurred before calcination was finished and after calcination was finished, and the total of these two weight gains, respectively. This is illustrated in Figures 21 and 22 by y_{13}, y_{14}, and $y_{13} + y_{14}$. The last three columns of Table XI show the times in minutes that elapsed from the onset of loss of weight to the completion of calcination, the time after calcination was completed to constant weight, and the heating rate in each run.

Correlations

Tables VIII and IX contain the chemical and mineralogical properties of the 35 stones, and Tables X and XI show the calcination and sulfation characteristics of the stones. In the correlations, x variables are assigned to the chemical and mineralogical properties

TABLE XI

Polythermal Calcination and Sulfation of Limestones

	Temperature, °C., of				Wt. gain, mg./50 mg. initial calcine			Time, minutes		Heating rate, dT/dt, °K./min.
BCR No.	Initial wt. loss, T_0	Inflection point,[a] T_{I_1}	Min. wt., T_{min}	$(dw/dT)_I$[b]	During calcination	After calcination	Total	During calcination	After calcination	
					Calcites					
1336	1139	1184	1239	0.373	9.86	3.35	13.20	22.0	98.0	4.53
1343	1102	1203	1266	0.176	6.96	17.39	24.35	35.1	83.9	4.68
1350	1109	1185	1301	0.123	15.78	2.84	18.62	39.6	70.4	4.84
1355	1066	1191	1218	0.189	9.87	12.41	22.27	31.8	68.2	4.77
1359	1150	1198	1231	0.325	14.54	12.94	27.48	16.4	93.5	4.91
1363	1118	1203	1243	0.195	13.77	12.83	26.60	22.9	77.1	5.47
1368	1138	1209	1242	0.308	12.52	15.03	27.55	20.4	79.6	5.07
1369	1102	1204	1261	0.147	17.84	9.54	27.39	34.4	75.6	4.63
1377	1074	1197	1219	0.221	3.71	13.62	17.33	30.3	49.7	4.79
1379	1150	1200	1250	0.270	12.78	4.43	17.21	19.3	80.7	5.18
1677	1108	1183	1227	0.068	12.24	3.54	15.78	26.5	63.5	4.50
1679	1028	1077	1133	0.085	27.75	11.69	39.44	24.5	95.5	4.30
1681	1150	1212	1251	0.352	3.53	32.42	35.96	20.8	59.2	4.83
1685	1030	1079	1151	0.146	23.53	12.48	36.01	25.2	74.8	4.80
1687	1118	1149	1258	0.159	17.78	7.75	25.53	30.1	79.9	4.65
1691	1124	1210	1233	0.186	16.94	17.92	34.85	22.9	57.1	4.78
1692	1122	1151	1185	0.395	15.59	7.71	23.29	13.7	96.2	4.58
1693	1157	1208	1251	0.221	17.10	17.45	34.55	18.1	91.9	5.18
					Dolomites					
1337	1137	1191	1282	0.163	23.11	11.93	35.04	29.1	70.9	5.00
1340	968	1040	1107	0.325	12.27	0.74	13.01	29.2	70.8	4.77
1341	1002	1079	1214	0.267	15.38	0.38	15.76	39.6	20.4	5.35
1367	977	1022	1212	0.120	23.17	10.52	33.69	49.1	60.8	4.78
1380	961	1009	1285	0.218	14.82	8.82	23.64	66.5	63.5	4.87
1678	1043	1069	1223	0.217	4.62	13.58	18.21	36.5	53.5	4.94
1680	951	1067	1308	0.151	16.15	5.21	21.35	68.9	31.1	5.18
1686	1019	1066	1295	0.258	17.33	9.98	27.31	51.8	48.2	5.32
1688	938	1029	1314	0.213	6.62	15.69	22.31	68.9	61.1	5.45
1690	1001	1068	1257	0.171	2.42	20.91	23.33	47.1	52.9	5.44
1695	977	1056	1378	0.130	15.57	2.42	17.99	78.4	41.6	5.12
1701	987	1046	1282	0.088	25.22	10.96	36.17	55.3	44.7	5.33
1702	956	1055	1258	0.159	16.61	18.95	35.56	57.7	47.3	5.24
					Mixtures					
1360	1081	1178	1226	0.100	25.95	10.09	36.04	29.4	45.6	4.92
1694	1020	1047	1296	0.182	8.39	4.68	13.06	38.2	50.1	4.60
					Magnesites					
1375	907	954	1091	0.266	17.91	5.97	23.88	37.4	92.6	4.93
1376	943	975	1053	0.749	7.03	14.26	21.29	22.0	108.0	5.00

---

[a] Temperature at which rate of weight loss was maximum.

[b] Maximum rate of weight loss, at T_{I_1}.

of each stone, and y variables are assigned to the calcination and sulfation characteristics. The assignments are listed below.

Chemical and Mineralogical Properties

Composition, wt. %, of initial limestone

x_1	Ignition loss	x_{11}	Accessory minerals
x_2	CaO	x_{12}	Quartz
x_3	MgO	x_{13}	Illite
x_4	Fe_2O_3	x_{14}	Montmorillonite
x_5	Na_2O	x_{15}	Chert
x_6	K_2O	x_{16}	Tremolite
x_7	MnO_2	x_{17}	Limonite
		x_{18}	Feldspar
		x_{19}	Muscovite
		x_{20}	Glass frit (unidentified)

Physical Properties

x_8	Grain size, coded
x_9	Lattice constant, a, Å.
x_{10}	Crystallite size, microns

Calcination and Sulfation Characteristics

Polythermal Calcination

y_1	Inflection temperature, °K.
y_2	Maximum rate of weight loss, mg./(50 mg. stone)(°K.)
y_3	Arrhenius activation energy, E
y_4	Arrhenius frequency factor, $\log k_o$

Calcination and Sulfation Characteristics (cont'd)

Isothermal Sulfation at 930° C.

y_5	Total weight gain, mg./50 mg. calcine
y_6	Maximum rate of weight gain, mg./(50 mg. calcine)(min.)
y_7	Weight gain during first stage, mg./50 mg. calcine
y_8	Time for completion of first stage, min.

Polythermal Calcination-Sulfation

y_9	Temperature at which weight loss began, °K.
y_{10}	Temperature of first inflection point I1, °K.
y_{11}	Temperature at which weight was minimum, °K.
y_{12}	Maximum rate of loss of weight, mg./(50 mg. stone)(°K.)
y_{13}	Weight gain during calcination, mg./50 mg. calcine
y_{14}	Weight gain after calcination, mg./50 mg. calcine
y_{15}	Total weight gain, mg./50 mg. calcine
y_{16}	Time to completion of calcination, min.
y_{17}	Time after completion of calcination, min.
y_{18}	Heating rate, °K./min.

In addition to the x variables of chemical and mineralogical composition and the y variables of calcination and sulfation parameters, there were derived from combinations of these variables a group of parameters related to the capacity of the stone for sulfation and the rate of sulfation. These values, presented in Table XII, include the weight gain per 50 mg. of stone while calcination is taking place, the weight gain up to the inflection point I2 where the gain is most rapid, and the total gain in weight of sulfation. It is assumed that calcination was completed at the point at which the weight was a minimum, although it probably was completed slightly later. The fact that the inflection point I2 was reached close to the point of minimum weight in many of the runs indicates that calcination was completed at about this point. It

TABLE XII

Capacity of Limestones for SO_2 and Rate of Sulfation

	Capacity mg./50 mg. initial stone			Rate, mg./min. with 50 mg. initial stone		
BCR No.	To $T_{min.}$,[a] w_1	To I2,[b] w_2	Total, w_3	Av. to $T_{min.}$,[a] r_1	Max. after calcination, r_2	Combination,[c] r_3
			Calcites			
1336	5.6	5.9	7.5	0.255	0.059	0.253
1343	4.0	5.5	14.0	0.114	0.248	0.286
1350	8.7	8.9	10.3	0.220	0.058	0.213
1355	6.6	7.9	14.9	0.208	0.048	0.210
1359	8.2	10.1	15.5	0.500	0.071	0.464
1363	8.8	14.2	17.0	0.384	0.034	0.336
1368	7.5	10.5	16.5	0.368	0.654	0.823
1369	9.1	9.8	14.5	0.265	0.214	0.379
1377	2.7	3.1	12.6	0.089	0.408	0.408
1379	7.5	11.9	10.1	0.389	0.128	0.413
1677	9.0	10.3	11.6	0.340	0.134	0.386
1679	15.9	18.8	22.6	0.649	0.242	0.786
1681	2.2	10.2	22.4	0.106	0.758	0.690
1685	13.2	14.3	20.2	0.524	0.257	0.678
1687	8.6	10.1	13.0	0.286	0.172	0.364
1691	10.4	14.6	21.4	0.454	0.521	0.791
1692	8.9	12.3	13.3	0.650	0.063	0.602
1693	9.8	12.8	19.8	0.541	0.410	0.761
			Dolomites			
1337	7.6	9.4	13.9	0.261	0.209	0.367
1340	6.6	6.6	7.0	0.226	0.013	0.216
1341	9.9	10.0	10.1	0.250	0.014	0.218
1367	13.0	14.2	18.9	0.265	0.219	0.399
1380	7.9	13.9	12.6	0.119	0.107	0.176
1678	3.2	6.1	12.6	0.088	0.213	0.246
1680	9.3	13.2	12.3	0.135	0.125	0.199
1686	9.2	14.9	14.5	0.178	0.284	0.356
1688	3.5	7.9	11.8	0.051	0.168	0.167
1690	1.6	7.3	15.4	0.034	0.368	0.320
1695	9.0	11.4	10.4	0.115	0.064	0.130
1701	14.5	17.3	20.8	0.262	0.180	0.345
1702	9.2	19.3	19.7	0.159	0.301	0.366
			Mixtures			
1360	11.1	12.7	16.7	0.378	0.237	0.501
1694	5.2	8.7	8.1	0.136	0.084	0.170
			Magnesites			
1375	9.6	15.7	12.8	0.257	0.061	0.291
1376	3.6	2.6	10.9	0.164	0.078	0.229

---

[a] Temperature at which weight is minimum.

[b] Inflection point at which rate of weight gain is maximum.

[c] $r_3 = (r_1 + r_2)10^3/T$ min.

is possible that calcination was completed before the minimum weight was reached, and that the minimum weight resulted from the decomposition of $CaSO_3$; this possibility is unlikely, however, because many of the minima occurred in the isothermal region where the rate of oxidation of sulfite to sulfate should be either constant or proportional to the amount of sulfite present.

The last three columns of Table XII are rates of gain in weight resulting from sulfation. Column 5, r_1, is the average rate of weight gain, mg. per 50 mg. of stone per minute, during calcination; it is the quotient of the weight gain at the minimum point of the curve, w_1, divided by the time required for completion of calcination, y_{16}, from Table XI. Column 6, r_2, is the slope at the inflection point I2 and is obtained from the computer printout of the spline-curve fit; it is the maximum rate of weight gain in mg. per 50 mg. of stone per minute after calcination was complete. The last column of Table XII, r_3, is a combination of the two rates with a consideration of the temperature, T_{min} °K. (y_{11}), at which the weight was minimum; the rate r_3 is arbitrarily defined as

$$r_3 = (r_1 + r_2)10^3/T_{min} \tag{21}$$

This expression gives equal weight to the average rate of sulfation during the calcination period and the maximum rate of sulfation after calcination is complete; it also gives higher values of r_3 for stones that calcined completely at lower temperatures in the polythermal tests.

The reason behind this arbitrary use of T_{min} in equation 21 is that stones that require higher temperatures than other stones for complete calcination should have higher activation energies for reaction and consequently be less reactive at any lower temperature; the reciprocal of the absolute temperature was chosen to express this factor, and 10^3 was introduced to keep the magnitude of the rates at about the same order as those of r_1 and r_2.

The correlations of the chemical and mineralogical properties, x variables, of the limestones with each other are shown in Table XIII, and the correlations of the calcination and sulfation parameters, y variables, with each other are shown in Table XIV. These tables are triangular because the lower left half of the matrix is identical with the upper right half, that is, the correlation of x_i with x_j is identical with that of x_j with x_i. The numbers in the tables are the correlation coefficients of each pair of variables.

The correlation coefficients range from -1 to +1 and measure the association between each pair of variables. For example, the correlation of each variable with itself is unity as seen from the values on the diagonals of the matrices. The closer a correlation coefficient approaches -1 or +1 the more nearly perfect is the association between the two variables.

A positive value of the correlation coefficient indicates that as one variable increases the other variable also increases; a negative value indicates that one of the variables of the pair decreases when

TABLE XIII

Intercorrelation of Chemical and Mineralogical Properties

	x_1	x_2	x_3	x_4	x_5	x_6	x_7	x_8	x_9	x_{10}	x_{11}	x_{12}	x_{13}	x_{14}	x_{15}	x_{16}	x_{17}	x_{18}	x_{19}	x_{20}
x_1	1.00	0.22	0.38	-0.35	-0.67	-0.65	0.02	0.29	-0.31	0.12	-0.96	-0.87	-0.70	-0.48	-0.04	-0.05	-0.31	-0.12	-0.49	-0.45
x_2	-	1.00	-0.81	-0.37	-0.03	-0.31	-0.03	-0.04	0.83	-0.18	-0.43	-0.43	-0.25	-0.15	0.13	-0.07	-0.29	-0.30	-0.18	-0.18
x_3	-	-	1.00	0.09	-0.39	-0.12	-0.00	0.26	-0.97	0.27	-0.18	-0.11	-0.20	-0.15	-0.16	0.15	0.03	0.21	-0.15	-0.11
x_4	-	-	-	1.00	0.44	0.57	0.51	-0.35	-0.19	-0.29	0.44	0.30	0.35	-0.04	-0.09	-0.10	0.89	-0.01	0.54	-0.05
x_5	-	-	-	-	1.00	0.62	0.10	-0.31	0.37	-0.35	0.64	0.60	0.66	0.05	-0.03	-0.15	0.25	0.05	0.56	0.02
x_6	-	-	-	-	-	1.00	0.01	-0.20	0.09	-0.02	0.69	0.58	0.70	-0.03	-0.07	-0.11	0.37	0.07	0.88	-0.03
x_7	-	-	-	-	-	-	1.00	-0.04	-0.08	-0.37	0.01	-0.01	0.02	-0.08	-0.10	-0.13	0.47	-0.06	-0.01	-0.09
x_8	-	-	-	-	-	-	-	1.00	-0.20	0.35	-0.30	-0.16	-0.32	-0.18	-0.08	0.38	-0.32	-0.11	-0.21	-0.21
x_9	-	-	-	-	-	-	-	-	1.00	-0.16	0.11	0.02	0.13	0.16	0.19	-0.11	-0.15	-0.27	0.18	0.11
x_{10}	-	-	-	-	-	-	-	-	-	1.00	-0.06	-0.20	-0.20	0.18	-0.07	0.22	-0.21	0.10	0.10	0.22
x_{11}	-	-	-	-	-	-	-	-	-	-	1.00	0.88	0.70	0.52	0.00	-0.02	0.42	0.17	0.52	0.51
x_{12}	-	-	-	-	-	-	-	-	-	-	-	1.00	0.67	0.33	-0.05	-0.07	0.19	0.17	0.30	0.31
x_{13}	-	-	-	-	-	-	-	-	-	-	-	-	1.00	-0.10	0.05	-0.16	0.19	0.18	0.52	-0.13
x_{14}	-	-	-	-	-	-	-	-	-	-	-	-	-	1.00	-0.05	-0.05	0.24	-0.05	-0.05	0.98
x_{15}	-	-	-	-	-	-	-	-	-	-	-	-	-	-	1.00	-0.08	-0.09	-0.08	-0.07	-0.06
x_{16}	-	-	-	-	-	-	-	-	-	-	-	-	-	-	-	1.00	-0.13	-0.08	-0.00	-0.06
x_{17}	-	-	-	-	-	-	-	-	-	-	-	-	-	-	-	-	1.00	-0.04	0.32	0.21
x_{18}	-	-	-	-	-	-	-	-	-	-	-	-	-	-	-	-	-	1.00	-0.08	0.12
x_{19}	-	-	-	-	-	-	-	-	-	-	-	-	-	-	-	-	-	-	1.00	-0.06
x_{20}	-	-	-	-	-	-	-	-	-	-	-	-	-	-	-	-	-	-	-	1.00

TABLE XIV

Intercorrelation of Calcination and Sulfation Parameters

	y_1	y_2	y_3	y_4	y_5	y_6	y_7	y_8	y_9	y_{10}	y_{11}	y_{12}	y_{13}	y_{14}	y_{15}	y_{16}	y_{17}	y_{18}
y_1	1.00	0.06	0.27	0.21	-0.37	-0.36	-0.38	0.08	0.52	0.58	-0.03	0.43	-0.22	-0.01	-0.19	-0.41	0.28	-0.14
y_2	-	1.00	0.25	0.25	0.29	0.35	0.30	-0.21	-0.32	-0.30	0.08	0.06	0.20	-0.12	0.07	0.26	-0.18	0.16
y_3	-	-	1.00	0.99	0.34	0.19	0.32	0.20	-0.03	0.06	-0.07	0.24	-0.12	0.02	-0.08	0.03	0.00	0.21
y_4	-	-	-	1.00	0.37	0.18	0.34	0.22	-0.10	-0.01	-0.08	0.23	-0.10	-0.01	-0.09	0.07	-0.03	0.19
y_5	-	-	-	-	1.00	0.80	0.96	-0.03	-0.20	-0.16	0.05	-0.27	0.37	0.37	0.61	0.21	-0.01	0.13
y_6	-	-	-	-	-	1.00	0.79	-0.32	-0.23	-0.27	-0.05	-0.39	0.44	0.33	0.63	0.15	-0.02	0.16
y_7	-	-	-	-	-	-	1.00	0.01	-0.22	-0.21	0.06	-0.25	0.37	0.32	0.57	0.25	0.07	0.14
y_8	-	-	-	-	-	-	-	1.00	-0.00	0.20	0.16	-0.11	-0.12	-0.13	-0.20	0.18	-0.03	0.04
y_9	-	-	-	-	-	-	-	-	1.00	0.93	-0.12	0.32	-0.07	0.19	0.10	-0.83	0.61	-0.31
y_{10}	-	-	-	-	-	-	-	-	-	1.00	-0.06	0.22	-0.13	0.23	0.08	-0.73	0.47	-0.23
y_{11}	-	-	-	-	-	-	-	-	-	-	1.00	-0.21	-0.17	0.00	-0.14	0.62	-0.36	0.43
y_{12}	-	-	-	-	-	-	-	-	-	-	-	1.00	-0.45	0.09	-0.30	-0.39	0.32	0.01
y_{13}	-	-	-	-	-	-	-	-	-	-	-	-	1.00	-0.27	0.60	0.01	0.06	-0.10
y_{14}	-	-	-	-	-	-	-	-	-	-	-	-	-	1.00	0.61	-0.15	0.08	0.17
y_{15}	-	-	-	-	-	-	-	-	-	-	-	-	-	-	1.00	-0.12	0.12	0.06
y_{16}	-	-	-	-	-	-	-	-	-	-	-	-	-	-	-	1.00	-0.64	0.43
y_{17}	-	-	-	-	-	-	-	-	-	-	-	-	-	-	-	-	1.00	-0.47
y_{18}	-	-	-	-	-	-	-	-	-	-	-	-	-	-	-	-	-	1.00

the other increases. For example, the correlation between the ignition loss, x_1, and the amount of accessory mineral in the limestone, x_{11}, is -0.96; as the amount of impurities increases in the limestone the ignition loss decreases because of the lower carbonate content. This correlation is not perfect (-1) because some of the impurities may lose weight on ignition, and because of different ratios Ca:Mg in the stones. The correlation between the contents of montmorillonite, x_{14}, and the fritted glass, x_{20}, was 0.98; these impurities occurred together in all the stones in the test group.

Significance at the 0.01 (99%) confidence level was used in all comparisons; $R_{01} = 0.45$. The significant correlations in Table XIII are: x_1x_5, x_1x_6, x_1x_{11}, x_1x_{12}, x_1x_{13}, x_2x_3, x_2x_9, x_3x_9, x_4x_6, x_4x_{17}, x_4x_{19}, x_5x_6, x_5x_{11}, x_5x_{12}, x_5x_{13}, x_5x_{19}, x_6x_{11}, x_6x_{12}, x_6x_{13}, x_6x_{19}, $x_{11}x_{12}$, $x_{11}x_{13}$, $x_{11}x_{14}$, $x_{11}x_{19}$, $x_{12}x_{13}$, $x_{13}x_{19}$, and $x_{14}x_{20}$. Most of these correlations are obvious from knowledge of the properties of the limestones and of the effect of one property upon another; other correlations are less obvious and may be characteristic only of the group of limestones tested.

The significant correlations among the calcination and sulfation characteristics, Table XIV, are: y_1y_9, y_1y_{10}, y_3y_4, y_5y_6, y_5y_7, y_5y_{15}, y_6y_7, y_6y_{15}, y_7y_{15}, y_9y_{10}, y_9y_{16}, $y_{11}y_{16}$, $y_{13}y_{15}$, $y_{14}y_{15}$, and $y_{16}y_{17}$.

Among the calcination parameters, the association of the activation energy, y_3, with the frequency factor, y_4, was 0.99 as was seen in Figure 1; the only other significant correlations of a calcination parameter were those of the inflection temperature, y_1, with y_9 and y_{10}, the temperatures of first weight loss and of the first inflection point I1 in the polythermal calcination-sulfation tests.

The isothermal sulfation characteristics, y_5, y_6, and y_7, all correlated significantly among themselves; each of these values also correlated at a value of about 0.6 with the corresponding value in the polythermal calcination-sulfation test, y_{15}.

Among the polythermal calcination-sulfation tests, the time to complete the calcination of the stone, y_{16}, was related inversely to the temperature of first weight loss, y_9, the first inflection temperature, y_{10}, and the time after calcination to cessation of reaction, y_{17}; it was directly associated with the temperature at which calcination was complete, y_{11}. The total weight gain, y_{15}, was correlated at about 0.6 with both the weight gain during calcination, y_{13}, and the weight gain after calcination, y_{14}, as one would expect, since $y_{15} = y_{13} + y_{14}$; the differences among stones in absorbing SO_2 during calcination accounts for the lack of perfect correlation.

The correlation coefficients between each y variable and each x variable are shown in Table XV, those between each derived capacity, w, and rate, r, property and each x variable are shown in Table XVI, and those between each derived property and each y variable are shown in Table XVII.

TABLE XV

Correlation of Calcination and Sulfation Parameters with Chemical and Mineralogical Properties of Limestones

	y_1	y_2	y_3	y_4	y_5	y_6	y_7	y_8	y_9	y_{10}	y_{11}	y_{12}	y_{13}	y_{14}	y_{15}	y_{16}	y_{17}	y_{18}
x_1	-0.01	0.58	0.15	0.16	0.31	0.29	0.40	-0.17	-0.23	-0.30	0.10	0.12	0.53	-0.20	0.27	0.24	0.08	0.17
x_2	0.36	0.08	-0.02	-0.05	0.11	0.03	0.14	-0.08	0.68	0.62	-0.21	0.20	0.25	0.06	0.25	-0.63	0.74	-0.45
x_3	-0.32	0.29	0.07	0.11	0.02	0.09	0.05	-0.06	-0.78	-0.78	0.33	-0.11	0.05	-0.20	-0.12	0.77	-0.66	0.50
x_4	-0.15	-0.21	-0.02	-0.01	-0.04	0.09	-0.11	0.02	-0.28	-0.20	-0.12	-0.22	0.00	0.08	0.06	0.17	-0.29	0.09
x_5	0.06	-0.45	0.08	0.06	-0.05	-0.12	-0.11	0.22	0.19	0.34	-0.19	-0.07	-0.22	0.18	-0.03	-0.25	0.02	-0.01
x_6	0.19	-0.41	0.24	0.21	-0.18	-0.25	-0.24	0.22	0.03	0.16	-0.09	0.02	-0.45	0.20	-0.20	-0.07	-0.19	0.05
x_7	-0.14	-0.07	-0.22	-0.21	0.06	0.11	0.02	-0.14	-0.06	-0.07	-0.13	0.02	0.15	0.04	0.16	-0.02	-0.00	0.13
x_8	-0.05	0.16	-0.07	-0.02	-0.18	-0.22	-0.18	-0.31	-0.06	-0.23	0.16	0.26	0.01	-0.39	-0.32	0.08	-0.09	0.13
x_9	0.37	-0.24	-0.06	-0.10	-0.06	-0.14	-0.07	0.12	0.80	0.81	-0.29	0.14	-0.04	0.16	0.10	-0.76	0.66	-0.51
x_{10}	-0.04	0.20	0.17	0.18	-0.14	-0.23	-0.12	0.18	-0.15	-0.15	0.34	0.10	-0.22	-0.47	-0.57	0.31	-0.27	0.03
x_{11}	-0.10	-0.58	-0.11	-0.11	-0.28	-0.25	-0.37	0.24	0.06	0.15	-0.10	-0.18	-0.49	0.15	-0.28	-0.11	-0.24	-0.07
x_{12}	-0.16	-0.55	-0.10	-0.09	-0.26	-0.23	-0.32	0.11	0.00	0.08	-0.09	-0.13	-0.56	0.23	-0.27	-0.07	-0.19	0.07
x_{13}	0.12	-0.49	0.19	0.17	-0.03	-0.08	-0.13	-0.04	0.13	0.21	-0.16	0.06	-0.45	0.39	-0.05	-0.18	-0.13	0.01
x_{14}	-0.24	-0.31	-0.32	-0.31	-0.24	-0.22	-0.26	0.49	0.12	0.14	-0.06	-0.29	-0.06	-0.20	-0.21	-0.10	-0.02	-0.25
x_{15}	0.03	0.20	-0.03	-0.03	0.20	0.13	0.12	-0.14	0.23	0.21	-0.04	0.22	-0.15	0.56	0.34	-0.19	-0.08	-0.08
x_{16}	0.06	0.17	-0.38	-0.39	-0.39	-0.23	-0.41	-0.44	-0.14	-0.23	0.29	0.01	-0.17	-0.31	-0.40	0.13	-0.18	-0.17
x_{17}	-0.24	-0.27	-0.14	-0.12	-0.00	0.15	-0.09	0.05	-0.18	-0.17	-0.10	-0.35	0.18	-0.01	0.14	0.11	-0.24	-0.06
x_{18}	-0.03	-0.05	0.25	0.27	0.06	0.09	0.08	0.09	-0.21	-0.17	0.13	-0.04	-0.11	-0.15	-0.22	0.25	-0.30	0.17
x_{19}	0.29	-0.23	0.21	0.18	-0.18	-0.26	-0.24	0.25	0.07	0.21	-0.03	0.01	-0.28	0.06	-0.18	-0.08	-0.11	0.06
x_{20}	-0.26	-0.28	-0.28	-0.26	-0.19	-0.18	-0.20	0.53	0.06	0.10	-0.01	-0.30	-0.04	-0.23	-0.23	-0.03	-0.08	-0.22

TABLE XVI

Correlation of Capacities and Rates of Reaction With Chemical and Mineralogical Properties of Limestones

	w_1	w_2	w_3	r_1	r_2	r_3
x_1	0.39	0.36	-0.01	0.16	-0.21	-0.05
x_2	0.26	0.10	0.22	0.64	0.08	0.51
x_3	-0.04	0.10	-0.26	-0.54	-0.22	-0.54
x_4	0.07	-0.03	0.18	-0.22	0.10	-0.08
x_5	-0.10	-0.09	0.19	0.05	0.16	0.16
x_6	-0.41	-0.40	-0.03	-0.28	0.25	-0.00
x_7	0.20	0.11	0.19	0.06	0.31	0.25
x_8	-0.06	-0.07	-0.44	-0.03	-0.20	-0.16
x_9	0.04	-0.11	0.20	0.55	0.21	0.54
x_{10}	-0.23	-0.38	-0.63	-0.31	-0.37	-0.49
x_{11}	-0.37	-0.34	-0.02	-0.26	0.18	-0.05
x_{12}	-0.47	-0.37	-0.03	-0.31	0.15	-0.11
x_{13}	-0.39	-0.30	0.17	-0.19	0.35	0.13
x_{14}	0.05	-0.04	-0.13	0.07	-0.08	-0.01
x_{15}	-0.21	0.01	0.37	-0.10	0.55	0.32
x_{16}	-0.15	-0.16	-0.40	-0.20	-0.23	-0.31
x_{17}	0.24	0.07	0.22	-0.07	0.09	0.01
x_{18}	-0.08	-0.01	-0.18	-0.20	-0.11	-0.22
x_{19}	-0.25	-0.28	-0.06	-0.15	0.08	-0.04
x_{20}	0.06	-0.01	-0.14	0.04	-0.11	-0.05

TABLE XVII

Correlation of Capacities and Rates of Reaction With Calcination and Sulfation Parameters of Limestones

	w_1	w_2	w_3	r_1	r_2	r_3
y_1	-0.27	-0.35	-0.20	0.13	0.08	0.14
y_2	0.19	0.29	-0.03	-0.01	-0.11	-0.08
y_3	-0.17	-0.15	-0.11	0.01	-0.05	-0.02
y_4	-0.15	-0.12	-0.13	-0.01	-0.10	-0.06
y_5	0.33	0.52	0.55	0.13	0.30	0.31
y_6	0.41	0.51	0.58	0.20	0.28	0.34
y_7	0.34	0.53	0.50	0.12	0.23	0.26
y_8	-0.07	-0.05	-0.18	-0.11	-0.11	-0.16
y_9	-0.12	-0.22	0.11	0.47	0.27	0.50
y_{10}	-0.17	-0.28	0.12	0.34	0.30	0.43
y_{11}	-0.23	-0.03	-0.21	-0.54	-0.02	-0.44
y_{12}	-0.45	-0.33	-0.26	0.08	0.10	0.12
y_{13}	0.94	0.73	0.40	0.59	-0.16	0.30
y_{14}	-0.30	0.08	0.72	-0.09	0.79	0.49
y_{15}	0.52	0.67	0.92	0.41	0.52	0.66
y_{16}	0.00	0.17	-0.17	-0.65	-0.22	-0.62
y_{17}	0.05	-0.07	0.09	0.59	-0.02	0.41
y_{18}	-0.11	0.16	0.06	-0.31	0.04	-0.22

The x-y correlations show that the ignition loss, x_1, of a limestone is correlated positively with the maximum calcination rate, y_2, and the weight gain during calcination, y_{13}.

The CaO content of the stone, x_2, is correlated positively with the temperature of first weight loss, y_9, with the temperature of the inflection point I1, y_{10}, and with the time after calcination is complete to cessation of sulfation, y_{17}; x_2 is correlated negatively with the time to complete calcination, y_{16}. The magnesium content, x_3, has the opposite effect and is correlated negatively with y_9, y_{10}, and y_{17}, but correlated positively with y_{16}. This means that the calcites start to lose weight at higher temperatures than the dolomites, but are completely calcined sooner. The Na_2O content, x_5, was correlated negatively with the maximum rate of calcination, y_2.

The lattice constant a, y_9, was correlated positively with the inflection temperature at I1, y_{10}, and with the reaction time after calcination was completed, y_{17}, but was correlated negatively with y_{16}, the time during calcination. The crystallite size, x_{10}, varied inversely with the total polythermal weight increase, y_{15}, whereas increasing the quartz content, x_{12}, adversely affected the weight gain during calcination, y_{13}.

Increase in the accessory mineral content, x_{11}, decreased the maximum rate of calcination, y_2, whereas the weight gain after calcination, y_{14}, was proportional to the chert content, x_{15}.

The derived capacity and rate properties were correlated significantly with a few x variables, Table XVI, but there were several significant relations of the y variables with these properties, Table XVII. Both w_1 and w_2, the capacities to the end of calcination and to the inflection point I2, were not related significantly to any chemical or mineralogical property; w_3, the total polythermal capacity was related inversely to the crystallite size within the carbonate grains, x_{10}.

The average rate of SO_2 pickup during calcination, r_1, was correlated positively with the CaO content, x_2, and with the unit-cell constant, x_9; it was related inversely to the MgO content, x_3. These correlations imply a higher initial rate of reaction with SO_2 for calcites than for dolomites. This is illustrated in Table XVIII in which the values of the average rate, r_1, are arranged from lowest to highest for 33 stones (omitting the magnesites), and the properties of the slowly reacting stones (upper 16) were compared with those of the faster reactors (lower 17). The slowly reacting stones included 10 of the 13 dolomites, 5 of the 18 calcites, and 1 of the 2 mixtures. There was a significant difference between the average unit-cell length, x_9, of the slowly reacting stones and that of the better performers.

TABLE XVIII

Correlation of Initial Reaction Rate with Chemical Properties and Texture of Limestones

(Initial rate, r_1, is the average rate of weight loss up to the point of minimum weight)

		Weight ratios					
BCR No.	Initial rate, r_1, mg./min.	CO_2:CaO, x_1/x_2	Rhombic-carbonates to CaO, $(100-x_{11})/x_2$	Fe_2O_3, %, x_4	Grain size, coded, x_8	Unit-cell length, a, Å, x_9	Crystal-lite size, μ, x_{10}
			Slow-reacting stones				
1690	0.034	1.518	3.384	1.1	3.0	4.809	0.098
1688	0.051	1.619	3.419	0.5	1.5	4.807	0.182
1678	0.088	1.563	3.299	1.3	1.5	4.808	0.141
1377	0.089	0.961	1.979	5.1	1.0	4.975	0.162
1681	0.106	0.840	1.920	0.6	1.0	4.985	0.115
1343	0.114	0.786	1.835	0.4	1.0	4.989	0.167
1695	0.115	1.460	3.294	0.6	3.0	4.808	0.189
1380	0.119	1.536	3.270	0.3	2.5	4.805	0.189
1680	0.135	1.504	3.220	0.9	1.0	4.806	0.171
1694	0.136	1.022	2.349	0.6	3.0	4.886	0.159
1702	0.159	1.343	2.873	0.8	1.3	4.810	0.070
1686	0.178	1.579	3.333	0.2	3.0	4.806	0.189
1355	0.208	0.798	1.817	1.6	1.0	4.982	0.096
1350	0.220	0.797	1.781	0.2	2.0	4.986	0.177
1340	0.226	1.505	3.192	1.4	1.5	4.808	0.141
1341	0.250	1.567	3.332	0.3	3.0	4.806	0.211
Average	0.139	1.275	2.769	1.0	1.9	4.867	0.154
Std. dev.	0.016	0.084	0.170	0.3	0.2	0.021	0.010
			Fast-reacting stones				
1336	0.255	0.809	1.843	0.2	3.0	4.978	0.149
1337	0.261	1.628	3.414	0.2	2.0	4.811	0.119
1701	0.262	1.232	2.649	4.3	1.3	4.822	0.090
1369	0.265	0.799	1.827	0.1	1.0	4.987	0.127
1367	0.265	1.351	2.862	5.2	1.0	4.816	0.085
1687	0.286	0.809	1.845	0.1	2.6	4.986	0.177
1677	0.340	0.849	1.763	0.7	1.0	4.987	0.177
1368	0.368	0.817	1.857	0.9	2.6	4.978	0.097
1360	0.378	0.989	2.147	0.7	2.5	4.910	0.135
1363	0.384	0.855	1.943	1.6	1.0	4.989	0.124
1379	0.389	0.848	1.918	0.4	3.0	4.980	0.097
1691	0.454	0.816	1.852	0.6	1.0	4.984	0.107
1359	0.500	0.797	1.812	0.1	1.0	4.985	0.124
1685	0.524	0.911	2.012	0.4	2.8	4.986	0.145
1693	0.541	0.801	1.824	0.2	1.0	4.985	0.130
1679	0.649	0.820	1.850	0.3	1.0	4.975	0.068
1692	0.650	0.783	1.814	0.1	3.0	4.985	0.153
Average	0.398	0.936	2.072	0.9	1.8	4.950	0.124
Std. dev.	0.032	0.058	0.112	0.4	0.2	0.016	0.007

A similar difference was noted for the ratios x_1/x_2 and $(100 - x_{11})/x_2$, all of which agree with the dolomite-calcite distribution. The relationships between x_1, x_2, x_3, and x_{11} can be determined by considering each limestone to consist only of $CaCO_3$, $MgCO_3$, and accessory mineral, and the ignition loss to be due to CO_2 alone. These considerations lead to the equations

$$x_1 + x_2 + x_3 + x_{11} = 100 \tag{22}$$

$$x_1 = 0.7847x_2 + 1.0914x_3 \tag{23}$$

$$x_{11} = 100 - 1.7847x_2 - 2.0914x_3 \tag{24}$$

from which is derived

$$\frac{100 - x_{11}}{x_2} = 1 + \frac{x_1}{x_2} + \frac{x_3}{x_2} \tag{25}$$

so that any two of the ratios in equation 25 fixes the third ratio. In the multiple regression that follows, only two of the ratios are used to avoid redundance of major composition variables.

The stones that had the highest reaction rates, r_2, also had smaller average crystallite sizes, x_{10}, than those of the slower reactors. There were no significant differences, however, between the Fe_2O_3 contents, x_4, or the microscopic grain sizes, x_8, of the two groups of stones.

The maximum rate of absorption of SO_2 after calcination was complete, r_2, was correlated positively with the chert content of the stone, x_{15}, (Table XVI), but the combined rate expression, r_3, was correlated positively with both the CaO content, x_2, and the unit-cell length, x_9, and negatively with the ignition loss, x_1. A summary comparison of the 16 stones with the lowest values of r_3 and the 17 stones with highest values of r_3 is shown in Table XIX. Only 3 of the 13 dolomites were in the better performing group, and only 5 of the 18 calcites were in the poorer performing group. This is reflected in the average values of x_1/x_2 and x_9 for the two groups. The effect of the impurities is shown by the average values of $(100 - x_{11})/x_2$ for the two groups. The x-ray crystallite size, x_{10}, was smaller for the better performing group, but the Fe_2O_3 content, x_4, and the microscopic grain size, x_8, bore no relation to the rate of reaction, r_3.

The many correlations in Table XVII between the capacity and rate expressions and the y variables can be explained from the relations

$$w_1 = y_{13} \cdot (100-x_1)/100 \tag{26}$$

$$w_3 = y_{15} \cdot (100-x_1)/100 \tag{27}$$

$$r_1 = w_1/y_{16} \tag{28}$$

$$r_3 = (r_1 + r_2) \cdot 10^3/y_{11} \tag{29}$$

and the correlations discussed previously. The characteristics w_2 and r_2, the capacity and rate at the inflection point I2, were obtained from the computer printout and have no inherent correlations by derivation. The weight gain after calcination, w_2, was correlated significantly with y_5, y_6, and y_7 from the isothermal tests and with y_{13} and y_{15} from the polythermal calcination-sulfation tests. The only significant correlation of r_2 among the y variables was a weak proportionality with the total capacity, y_{15}, of the polythermal calcination-sulfation tests.

TABLE XIX

Correlation of Combination Reaction Rate[a] with Chemical Properties and Textures of Limestones

		Weight ratios					
BCR No.	Combination rate, r_3,[a] mg./min.	CO_2:CaO, x_1/x_2	Rhombic carbonates to CaO, $(100-x_{11})/x_2$	Fe_2O_3, %, x_4	Grain size, coded, x_8	Unit-cell length, a, Å, x_9	Crystallite size, μ, x_{10}
			Slow-reacting stones				
1695	0.130	1.460	3.294	0.6	3.0	4.808	0.189
1688	0.167	1.619	3.419	0.5	1.5	4.807	0.182
1694	0.170	1.022	2.349	0.6	3.0	4.886	0.159
1380	0.176	1.536	3.270	0.3	2.5	4.805	0.189
1680	0.199	1.504	3.220	0.9	1.0	4.806	0.171
1355	0.210	0.798	1.817	1.6	1.0	4.982	0.096
1350	0.213	0.797	1.781	0.2	2.0	4.986	0.177
1340	0.216	1.505	3.192	1.4	1.5	4.808	0.141
1341	0.218	1.567	3.332	0.3	3.0	4.806	0.211
1678	0.246	1.563	3.299	1.3	1.5	4.808	0.141
1336	0.253	0.809	1.843	0.2	3.0	4.978	0.149
1343	0.286	0.786	1.835	0.4	1.0	4.989	0.167
1690	0.320	1.518	3.384	1.1	3.0	4.809	0.098
1363	0.336	0.855	1.943	1.6	1.0	4.989	0.124
1701	0.345	1.232	2.649	4.3	1.3	4.822	0.090
1686	0.356	1.579	3.333	0.2	3.0	4.806	0.189
Average	0.240	1.259	2.747	1.0	2.0	4.868	0.155
Std. dev.	0.017	0.087	0.172	0.3	0.2	0.021	0.009
			Fast-reacting stones				
1687	0.364	0.809	1.845	0.1	2.6	4.986	0.177
1702	0.366	1.343	2.873	0.8	1.3	4.810	0.070
1337	0.367	1.628	3.414	0.2	2.0	4.811	0.119
1369	0.379	0.799	1.827	0.1	1.0	4.987	0.127
1677	0.386	0.849	1.763	0.7	1.0	4.987	0.177
1367	0.399	1.351	2.862	5.2	1.0	4.816	0.085
1377	0.408	0.961	1.979	5.1	1.0	4.975	0.162
1379	0.413	0.848	1.918	0.4	3.0	4.980	0.097
1359	0.464	0.797	1.812	0.1	1.0	4.985	0.124
1360	0.501	0.989	2.147	0.7	2.5	4.910	0.135
1692	0.602	0.783	1.814	0.1	3.0	4.985	0.153
1685	0.678	0.911	2.012	0.4	2.8	4.986	0.145
1681	0.690	0.840	1.920	0.6	1.0	4.985	0.115
1693	0.761	0.801	1.824	0.2	1.0	4.985	0.130
1679	0.786	0.820	1.850	0.3	1.0	4.975	0.068
1691	0.791	0.816	1.852	0.6	1.0	4.984	0.107
1368	0.823	0.817	1.857	0.9	2.6	4.978	0.097
Average	0.540	0.951	2.092	1.0	1.7	4.949	0.123
Std. dev.	0.043	0.060	0.116	0.4	0.2	0.016	0.008

---

[a] $r_3 = (r_1 + r_2)10^3/T_{min}$.

The y variable, y_{18}, which was included in the correlations to determine whether there was a bias for any particular property of the stone that was due to the heating rate, is a random variable with a mean of 4.93° ± 0.31° C./min. There was no correlation of this rate with any calcination or sulfation characteristic, which indicates that slight variations in the heating rates had no significant effect on the properties measured. There was a weak positive correlation, 0.50, with the magnesium content of the stone, x_3, and a similar weak negative correlation, -0.51, with the lattice constant, x_9; since x_3 and x_9 are highly correlated, -0.97, the correlations with y_{18} amount to a single event. It is to be expected statistically that there will be, on the average, one erroneous correlation out of 100 tests of correlation when the confidence level is set at 0.01 (or 99%). It is concluded that the variation in the heating rate had no effect on the measurements.

Multiple Correlations

The single correlations discussed above indicate that no single property of a limestone is sufficient to predict its capacity for, or rate of absorption of, SO_2. An effort was made to find the significant factors, or combination of factors, that by linear regression might be useful in predicting the effectiveness of a limestone for removal of SO_2 from the stack gas of a power plant. The method used to identify the significant factors in a group of 10 or less is shown in Appendix D. Two models were used

$$Q = \sum_{i=1}^{10} b_i z_i + b_o \qquad (30)$$

and

$$\log Q = \sum_{i=1}^{10} b_i z_i + b_o \qquad (31)$$

where Q is w_j or r_j from Table XII and the ten z factors are defined in terms of the x factors of Tables VIII and IX.

$z_1 = x_1/x_2$	ratio, ignition loss:CaO
$z_2 = (100 - x_{11})/x_2$	ratio, rhombic carbonates:CaO
$z_3 = x_4$	Fe_2O_3 content, %
$z_4 = x_8$	microscopic grain size, coded
$z_5 = x_9$	unit-cell length, a, Å.
$z_6 = x_{10}$	x-ray crystallite size, μ
$z_7 = \log x_5$	log % Na_2O
$z_8 = \log (x_5 + x_6 + x_7)$	log % (Na_2O + K_2O + MnO_2)
$z_9 = x_{11}-(x_{12} + x_{15} + x_{20})$ $= x_{13} + x_{14} + x_{16} +$ $x_{17} + x_{18} + x_{19}$	sum of illite, montmorillonite, tremolite, limonite, feldspar, and muscovite
$z_{10} = x_{17}/x_4$	fraction of uncombined Fe_2O_3[a]

---

[a] In some of the stones the value of z_{10} was greater than unity because of the rather inexact determination of x_{17}; for these stones the value of z_{10} was taken as 1.0 in the regression.

The coefficients of the significant factors for the linear (equation 30) and the logarithmic (equation 31) models are listed in Table XX for each of the capacity, w, and rate, r, characteristics. In each regression, the two magnesites, BCR 1375 and 1376, were omitted from consideration, so that the equations apply only to calcites, dolomites, and their mixtures.

Of the ten z factors considered in the multiple regressions, four to eight were eliminated as not contributing significantly to a particular characteristic. Six factors were significant in the regressions for the capacity measures w_1 and w_3, and five factors were significant for the combined rate expression r_3. The rate r_2 was poorly described by all 10 factors, and only 2 factors were significant in predicting this property. The unit-cell length, z_5, was a significant factor in each linear model and in most of the logarithmic models; increasing the unit-cell length, which is equivalent to selecting limestones that are purer calcites, caused most of the properties to increase (an exception is w_2). The clay mineral combination represented by factor z_9 affected adversely each property except r_2. The Na_2O content in its logarithmic form, z_7, was a significant factor in all capacity measures, and many of the z factors had different effects on the linear and logarithmic models.

A preliminary study of principal component analyses for some of the y variables in relation to the x variables is given in Appendix E, from which it is concluded that multivariate analysis of the present data has little promise of producing a useful relation for evaluating stones for the injection process.

TABLE XX

Coefficients of Significant Factors in Multiple Correlation Equations

$(Q = w_j \text{ or } r_j)$

	w_1	w_2	w_3	r_1	r_2	r_3
$Q = \sum_{i=1}^{10} b_i z_i + b_o$						(10)
b_1	-	34.46	-	-	-	0.6592
b_2	-	-24.89	-	-0.1259	-	-
b_3	1.163	-	-	-	-	-
b_4	-	-	-1.571	-	-	-
b_5	2.278	-70.42	5.685	0.1179	0.06258	-
b_6	-	-	-32.14	-	-	-2.405
b_7	3.973	5.576	3.603	-	-	-
b_8	-3.289	-	-	-	0.1343	-
b_9	-0.3489	-0.4735	-0.3280	-0.01191	-	-0.009091
b_{10}	3.757.	-	2.818	0.1651	-	0.1818
b_o	-	389.31	-	-	-	-17.897
S.D.[a]	2.637	2.803	3.001	0.119	0.164	0.139
R^b	0.701	0.737	0.769	0.735	0.415	0.776
$\log Q = \sum_{i=1}^{10} b_i z_i + b_o$						(11)
b_1	3.066	-	-	-	-	0.7816
b_2	-2.122	-0.3157	0.05114	-0.2681	-	-
b_4	-	-	-0.06688	-	-	-
b_5	-4.555	-2.845	0.2942	-	-	4.218
b_6	-	-	-	-	-3.026	-2.864
b_7	0.2394	0.2114	0.1834	-	0.2787	-
b_8	-0.1838	-	-	-	-	-
b_9	-0.01818	-0.01968	-0.01403	-0.02129	-	-0.009271
b_{10}	-	-	0.1200	0.2753	-	0.2122
b_o	25.274	16.149	-	-	-	-21.654
S.D.[a]	53	33	25	66	140	37
R^b	0.697	0.724	0.751	0.730	0.468	0.818

---

[a] Standard deviation.

[b] R = multiple correlation coefficient for equation containing only the significant z_i's.

Application to Stones Considered for Use in Shawnee Tests

Battelle Memorial Institute (6) used the dispersed-phase reactor to study five stones that are to be used in the injection tests at TVA's Shawnee steam plant and determined apparent reaction rates of each stone at five temperatures. These stones were characterized mineralogically and chemically to obtain the ten z factors that are needed in equations 30 and 31 for calculation from the coefficients in Table XX of the six capacity and rate characteristics defined in Table XII. The results are given in Table XXI.

The first row of reaction parameters for each stone listed in Table XXI was calculated by the linear model 30, the second row by the logarithmic model 31, and the third row is the arithmetic average of the two results. Taking the average of the two results decreased the prediction error by a factor of $\sqrt{2}$. There are, however, at least two glaring discrepancies in the predicted properties: the weight gain during calcination, w_1, for stone 2062 is predicted to be greater than that at the inflection point I2, w_2; and the value of w_2 for stone 2069 is predicted to be higher than the total capacity, w_3. These predictions are not in agreement with the shape of the calcination-sulfation curves, and result from prediction errors for the different properties as listed in Table XX.

The predictions of the reactivity parameters of Table XXI for the various stones were compared with the smoothed apparent reaction rates reported by Battelle (Table F-3 of reference 6). The rates were smoothed by deriving by least squares the equation of the linear relation between

TABLE XXI

Predicted Reactivity Parameters of Limestones to be Tested at Shawnee

BCR No.	Calcd. by eq. No.	Predicted parameters					
		w_1	w_2	w_3	r_1	r_2	r_3
2060	10	7.399	10.905	17.072	0.298	0.229	0.566
	11	6.930	10.188	15.176	0.250	0.224	0.550
	Av.	7.164	10.547	16.124	0.274	0.227	0.558
2061	10	7.004	7.326	14.709	0.352	0.127	0.572
	11	6.802	7.773	11.057	0.315	0.122	0.552
	Av.	6.903	7.549	12.883	0.334	0.124	0.562
2062	10	10.638	7.280	11.758	0.511	0.126	0.268
	11	6.849	7.672	15.539	0.579	0.030	0.238
	Av.	8.743	7.476	13.648	0.545	0.078	0.253
2064	10.	6.945	7.314	13.881	0.354	0.128	0.494
	11	6.648	7.954	11.072	0.318	0.101	0.446
	Av.	6.797	7.634	12.477	0.336	0.115	0.470
2069	10	6.870	13.161	11.055	0.160	0.229	0.037
	11	6.602	14.191	13.219	0.137	0.091	0.134
	Av.	6.736	13.676	12.137	0.149	0.160	0.085

the logarithm of the apparent rate and the reciprocal of the absolute temperature as illustrated in Figures F-1 through F-5 of reference 6, and recalculating the apparent rates at the temperatures reported. (The apparent rate at 1910° F. for stone 2060 was omitted in the regression.) The comparison of the predicted parameters from the chemical and mineralogical properties with the smoothed reaction rates at five temperatures is shown in Table XXII in terms of the correlation coefficients. Since there were five stones in the comparisons, each significance test is based on only three degrees of freedom.

As shown in Table XXII, there is a significant correlation between the total weight of SO_3 absorbed, w_3, in the polythermal calcination-sulfation test and the apparent reaction rates at 1603° and 1681° F. No other calculated parameter is correlated significantly with any of the isothermal reaction rates of Battelle, and the association of the values of w_3 with the apparent reaction rates decreases as the temperature at which they were measured increases. The relationships between the apparent reaction rates and two of the calculated parameters, w_3 and r_2, are shown in Figure 23. The correlation with w_3 of the rates at the two lowest temperatures is rather good, but the rates at higher temperatures have no consistent association with the predicted values of w_3. The calculated rate, r_2, which is the maximum rate of weight gain after calcination is complete, is slightly associated with the apparent reaction rates of Battelle, although the relation is not significant for any of the temperatures. The facts that r_2 is predicted by only two properties of the stone, and its prediction error (Table XX) is quite

TABLE XXII

Correlation with TVA Results of Reaction Parameters Calculated from Battelle Data

(Battelle data were smoothed by regression; TVA results are average values from Table III-XIV)

Reaction parameter	Correlation coefficient[a] at indicated temperature, °F. (°C.)				
	1603 (873)	1681 (915)	1807 (986)	1910 (1043)	2000 (1093)
w_1	0.29	0.13	-0.36	-0.42	-0.51
w_2	0.10	0.15	0.26	0.24	0.21
w_3	0.97	0.91	0.34	0.18	-0.08
r_1	0.10	-0.02	-0.36	-0.38	-0.41
r_2	0.63	0.69	0.55	0.45	0.28
r_3	0.32	0.33	0.18	0.12	0.04

---

[a] $R_{05} = 0.88$, $R_{01} = 0.96$, $R_{001} = 0.99$.

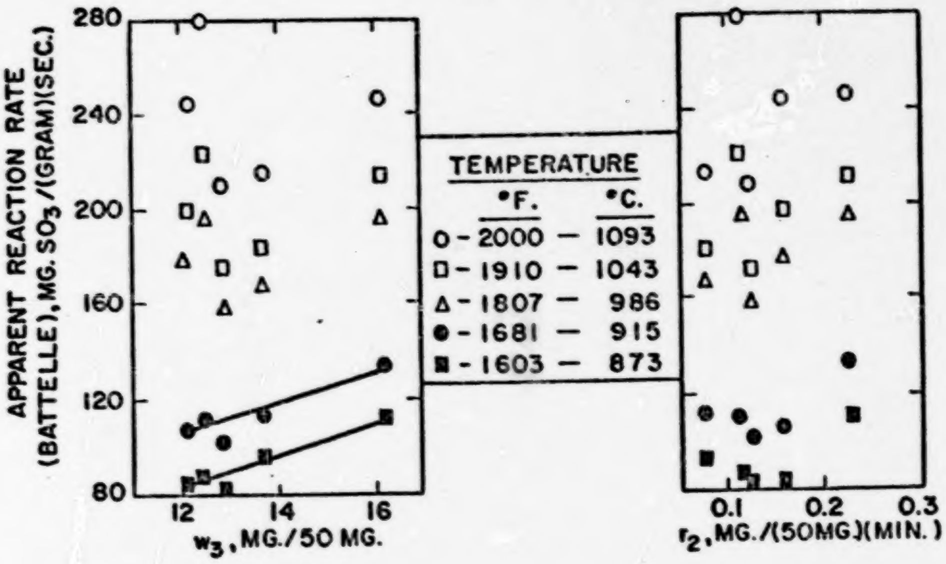

Figure 23. Comparison of Calculated Reaction Parameters With Battelle's Apparent Reaction Rates.

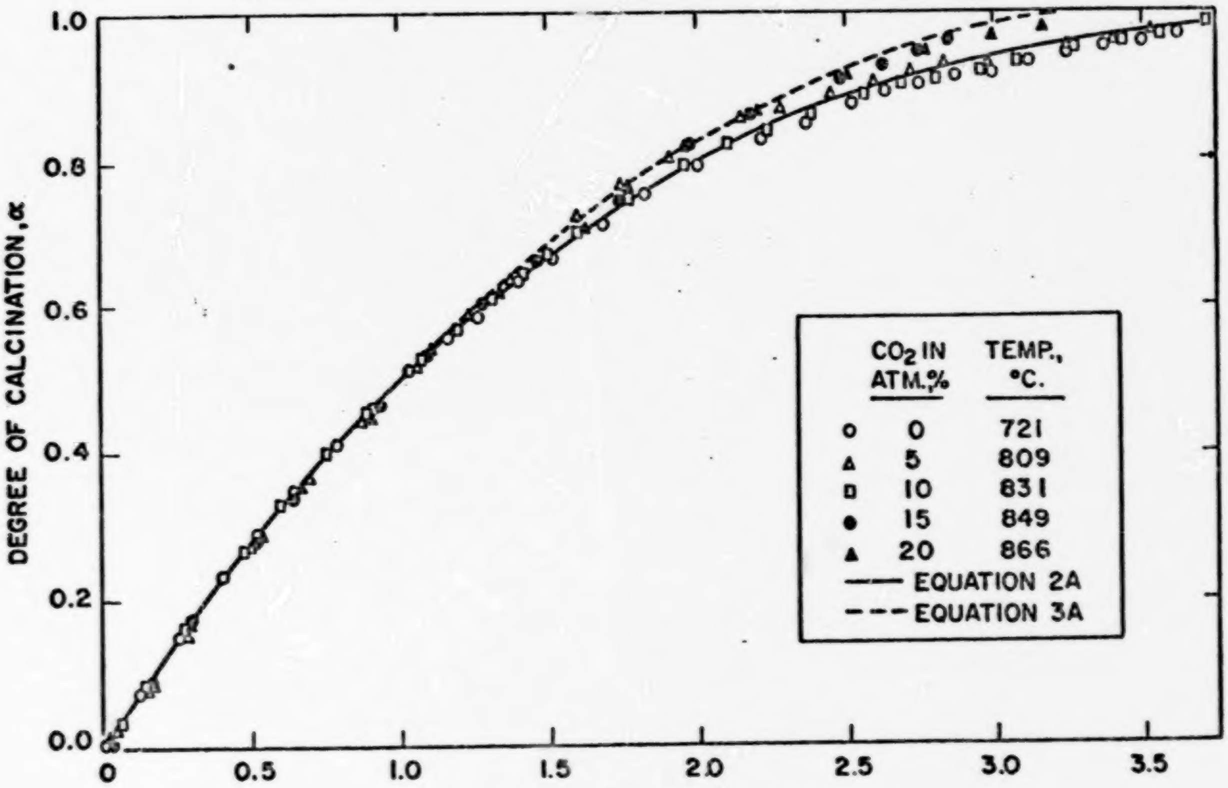

Figure 24. Relation Between Reduced Time and Degree of Calcination of Minus 24- Plus 28-Mesh Colbert Limestone.

large, would indicate that the slight association of r_2 with the reaction rates for these five stones probably is a fortuitous rather than a dependable relation; it is also possible that a better expression for r_2 may be found with different combinations of chemical and mineralogical properties of the stones.

It should be noted that the correlations of w_3 with the Battelle rates were significant only in the temperature range in which w_3 was measured for determining the regression coefficients. The calcination-absorption tests were polythermal only up to 940° C. (1724° F.), and the temperature was never higher than this because of equipment limitations. The rates that were measured at higher temperatures by Battelle--at 1807°, 1910°, and 2000° F.; 986°, 1043°, and 1093° C.--apparently are not associated with the same chemical and mineralogical properties that determine the rates of reaction at lower temperatures. Two possible explanations of failure to extrapolate the low temperature results to those at higher temperature are the increased fluxing of some of the impurities and the increase of the crystallite size of CaO as the temperature rises; both of these factors are minimized below 1750° F., and their effects on reactivity were not available to be related to the chemical and mineralogical composition.

The relative importance of the properties of limestones as reflected in their reactivity with sulfur oxides is discussed in Appendix F.

REFERENCES

1. Azaroff, L. V., "X-Ray Diffraction Methods," 56th Norelco X-Ray Analytical School, p. 3, Philips Electronics Instruments, Mt. Vernon, N. Y., 1967.

2. Bituminous Coal Research, Inc., Progress Report, "Research on Methods for Control of Sulfur Dioxide Emissions From Coal-Burning Power Boilers" (BCR Report L-273) March 7, 1968.

3. Borgwardt, R. H., "Kinetics of Reaction of SO_2 With Calcined Limestone," U. S. Public Health Service Symposium on Limestone-Sulfur Dioxide Reaction Kinetics and Mechanisms, NAPCA, Cincinnati, Ohio (1969). (Abstract)

4. Borgwardt, R. H., Environmental Science and Technology, 4 (1), 59 (1970).

5. Coutant, R. W., Barrett, R. E., Simon, R., and Lougher, E. H., "Investigation of the Kinetics of Reaction of a Limestone With SO_2 in Flue Gas." Paper presented at the Dry Limestone Injection Process Symposium, Gilbertsville, Ky., June 1970.

6. Coutant, R. W., Campbell, B., Barrett, R. E., and Lougher, E. H. "Summary Report on Investigation of the Reactivity of Limestone and Dolomite for Capturing SO_2 From Flue Gas." NAPCA Contract No. PH-86-67-115. June 27, 1969.

7. Fischer, H. C., J. Am. Ceram. Soc., 38 (7), 245-51 (1955).

8. Fischer, H. C., J. Am. Ceram. Soc., 38 (8), 284-8 (1955).

9. Goldsmith, J. R., and Graf, D. I., Am. Mineralogist, 43, 84-101 (1958).

10. Harvey, R. D., "The Mineralogy and Petrography of Carbonate Rocks Related to Sulfur Dioxide Reactivity." Presented at the 3rd Limestone Symposium, St. Petersburg, Florida. December 4-8, 1967.

11. Hastings, C., "Approximations for Digital Computers," p. 189, Sheet 65, Princeton Univ. Press, N. J. (1955).

12. Hatfield, J. D., and Kim, Y. K., "Limestone Calcination and Sulfation Investigations," U. S. Public Health Service Symposium on Limestone-Sulfur Dioxide Reaction Kinetics and Mechanisms, NAPCA, Cincinnati, Ohio (1969). (Abstract)

13. Hedin, R., "Investigation of the Lime-Burning Processes," Svenska Forskningsinst. Cement Betong Vid Kgl. Tek. Högskol. Stockholm, Handl., 32, Stockholm, Sweden, 123 pp. (1961).

14. Heek, K. H. van, and Jüntgen, H., "A Contribution Concerning Kinetics and Mechanism of Calcination and Reaction of Carbonates With SO_2 Under Non-Isothermal Conditions." Paper presented at the Limestone Symposium, St. Petersburg, Florida, Dec. 1967.

15. Heek, K. H. van, and Jüntgen, H., "Kinetics of the Reactions of Calcium Compounds With SO_2." Paper presented at the Dry Limestone Injection Process Symposium, Gilbertsville, Ky., June 1970.

16. Klaus, R. L., and Van Ness, H. C., *A.I.Ch.E. J.*, **13** (6), 1132-6 (1967).

17. Mayer, R. P., and Stowe, R. A., "Physical Characterization of Limestone and Lime," Azbe Award No. 4, National Lime Association, Washington, D. C., 26 pp. (1964).

18. McClellan, G. H., and Lehr, J. R., *Am. Mineralogist*, **54**, 1374-91 (1969).

19. Mezaki, R., and Kittrell, J. R., *Ind. Eng. Chem*., **59**, 63-9 (1967).

20. Palache, C., Berman, H., and Frondel, C., *Dana's System of Mineralogy*, **2**, 7th ed., John Wiley & Sons, New York, N. Y., p. 211 (1951).

21. Potter, A. E., "Sulfur Oxide Capacity of Limestones," *U. S. Public Health Service Symposium on Limestone-Sulfur Dioxide Reaction Kinetics and Mechanisms*, NAPCA, Cincinnati, Ohio (1969). (Abstract)

22. Rau, R. C., *Advan. X-Ray Anal*., **5**, 104-16 (1962).

23. Snedecor, G. W., *Statistical Methods*, p. 91, Iowa State College Press, Ames, Iowa, 1956.

APPENDIX A: MECHANISM OF CALCINATION REACTION

A phase-boundary-controlled reaction is represented (1) by the expression

$$d\alpha/dt = k(1 - \alpha)^{\ell} \qquad (1A)$$

where α = the fraction reacted

ℓ = the order of the reaction (i.e., the exponent of the unreacted portion, $1 - \alpha$, at time t)

k = the rate constant

When the reaction is controlled by the external surface of the reactant, the value of ℓ depends upon the shape of the particles. For spherical particles, the value of ℓ is 2/3, since the surface varies as the 2/3 power of the volume; when the reaction progresses faster in two dimensions than in the third dimension, however, as with cylinders or discs, the value of ℓ approaches 1/2.

The integrated form of equation 1A is

$$1 - (1 - \alpha)^{1/3} = 0.20630\ t/t_{0.5} \qquad (2A)$$

for $\ell = 2/3$, and

$$1 - (1 - \alpha)^{1/2} = 0.29289\ t/t_{0.5} \qquad (3A)$$

for $\ell = 1/2$. In equations 2A and 3A, α is the fraction of reaction at time t; $t_{0.5}$ is the time for 50% reaction; and the constants result from geometrical considerations of the particle shape and the advancing front of the reaction.

The degree of calcination, α, is plotted against the reduced time coordinate, $t/t_{0.5}$, in Figure 24 for all the isothermal calcination runs that have been made in this laboratory on minus 24- plus 28-mesh Colbert limestone for different partial pressures of CO_2. The theoretical curves, equations 2A and 3A, are shown for comparison with the experimental points.

It is concluded that the phase-boundary-controlled model represents the data adequately, and that for this particle size, minus 24- plus 28-mesh, equation 2A represents the data better than equation 3A. This implies that the reaction proceeds at the same rate in all three dimensions of the particle. It is possible that finer grinding of the limestone will produce flatter particles that may follow equation 3A more closely than equation 2A; the fact that the results at higher temperatures, where spalling is more pronounced, approached the theoretical curve 3A supports this assumption.

APPENDIX B: CALCULATION OF KINETIC PARAMETERS FOR CALCINATION

The kinetic equation for thermogravimetric studies of calcination is

$$d\alpha/dt = k(1 - \alpha)^{2/3} \tag{1B}$$

Substituting the heating rate equation, $dT = qdt$, and the Arrhenius equation, $k = k_o \exp(-E/RT)$, into equation 1B and integrating, there is obtained

$$(1 - \alpha)^{1/3} = 1 - (k_o/3q)\int_{T_o}^{T} \exp(-E/RT)dT \tag{2B}$$

where

α = fraction of limestone calcined at time t or at temperature T

q = heating rate, °K./min.

T_o, T = temperatures at which the fraction decomposed is 0 and α, respectively

k_o, E = Arrhenius parameters for specific rate constant, k

R = gas constant

The thermogravimetric measurements are the weights, w, of the undecomposed limestone at different times, t, or temperatures, T, and the relation to the fraction decomposed is

$$1 - \alpha = (w - w_f)/(w_o - w_f) \tag{3B}$$

where w_o and w_f are the original and final weights of the sample, respectively, (that is, when $\alpha = 0$ and $\alpha = 1$, respectively).

The data (w, T) were smoothed by a spline-curve computer program based upon the technique of Klaus and Van Ness (16), which assures no discontinuities in the first two derivatives, dw/dT and d^2w/dT^2. The smoothed data were used to evaluate the kinetic parameters, k_0 and E, of equation 2B by a nonlinear least-squaring technique. The integral in equation 2B was evaluated precisely by integrating once by parts

$$\int_{T_0}^{T} \exp(-E/RT)dT = [T \exp(-E/RT)]_{T_0}^{T} - (E/R)\int_{X_0}^{X} \frac{\exp(-X)}{X} dX \qquad (4B)$$

where $X = E/RT$

X_0 = value of X at T_0

and evaluating the residual integral by a Hastings approximation (11) with an error of less than 10^{-6}.

The least-squares surface was made more regular by redefining the pre-exponential parameter of the Arrhenius equation (19) by the relation

$$k = k_1 \exp(-E/RT_{0.5}) \qquad (5B)$$

to obtain

$$k = k_1 \exp[-(E/R)(1/T - 1/T_{0.5})] \qquad (6B)$$

where $T_{0.5}$ is the temperature, °K., at which the calcination is 50% complete ($\alpha = 0.5$). The reparameterization changed the poorly conditioned sum-of-squares surface into a well-conditioned surface. The contours of the surface were more circular or elliptical with a well-defined minimum rather than long and skewed with an ill-defined minimum, and convergence was improved markedly. The size of the confidence regions of the parameters was unchanged because there was no change in the rate equation itself.

APPENDIX C: KINETIC INTERPRETATION OF DIFFERENCES AMONG STONES

If we assume that, when limestone is injected into a combustion chamber to decrease the emission of SO_2, the important reactions are

$$CaCO_3 \xrightarrow{k_1} CaO + CO_2 \tag{1C}$$

$$CaO + SO_2 + 0.5O_2 \underset{k_3}{\overset{k_2}{\rightleftharpoons}} CaSO_4 \tag{2C}$$

$$CaO \xrightarrow{k_4} (\dot{CaO}) \tag{3C}$$

where each k_i can be represented in Arrhenius form by

$$k_i = k_{io} \exp(-E_i/RT) \tag{4C}$$

as derived in equation 17 for a particular stone, and that the injection is made at sufficiently high temperature (above 900° C.) so that calcination is not rate limiting, the rate equation for reaction 2 in excess oxygen is

$$dx/dt = k_2(a - x)(b\beta - x)(1 - \varepsilon) - k_3 x \tag{5C}$$

where a = the initial concentration of SO_2 in the gas

b = the concentration of lime after injection, of which β is the effective fraction that reacts in the first stage before a complete shell of product is formed

x = the amount of $CaSO_4$ formed at time t

ε = the degree of dead-burning that occurs under the injection conditions.

If the injection temperature is 1500° C. or below, the last term in equation 5C can be ignored, since the rate of decomposition of $CaSO_4$ will be less than 1% of its rate of formation. Assuming also that the particles cool from their highest temperature at a constant rate, ρ, and that the sulfation reaction stops when the temperature drops to 800° C. there is obtained on integration

$$\frac{1 - (\theta/S)}{1 - \theta} = \exp\left[-k_{20}a(S - 1)I/\rho\right] \tag{6C}$$

where S = the effective ratio $CaO:SO_2$ in the flue gas,

$S = (b\beta/a)(1-\epsilon)$

θ = the degree of desulfurization of the flue gas

$$I = \int_{T_1}^{T_2} \exp(-E_2/RT)dT \tag{7C}$$

T_1 = injection temperature, °K.

T_2 = temperature of cessation of sulfation, °K.

The value of the dead-burned fraction, ϵ, in the definition of S must also be evaluated from the Arrhenius parameters of reaction 3 by

$$1 - \epsilon = \exp\left[(k_{40}/\rho)\int_{T_1}^{T_2} \exp(-E_4/RT)dT\right] \tag{8C}$$

The important factors for desulfurization are therefore the effective ratio $CaO:SO_2$, S; the concentration of SO_2 in the flue gas, a; the injection temperature, T_1; the cooling rate, ρ; the kinetic parameters of the stone for sulfation; and dead-burning.

Assuming the dead-burning parameters of equation 17; an effective fraction, β, of lime to react to be 0.4; and a cooling rate of 220° C./sec.; the relationship between the injection temperature, the ratio $CaO:SO_2$, the SO_2 concentration, and the sulfation parameters is shown in Figure 25. In this figure the data are plotted to show the beneficial effects of a high frequency factor, k_{2o}, in the Arrhenius equation 4C, and of a low activation energy, E_2. The optimum injection temperature is predicted to decrease with the activation energy, E_2, for sulfation and with increasing SO_2 concentration in the flue gas; these relations might be modified with stones of different dead-burning characteristics and with different cooling rates. The effect of the SO_2 concentration is more pronounced when both Arrhenius parameters, k_{2o} and E_2, are either low or high; when one is low and the other high, the effect of concentration of SO_2 on its degree of removal is less pronounced. A large frequency factor, k_{2o}, makes the temperature range for good desulfurization less critical.

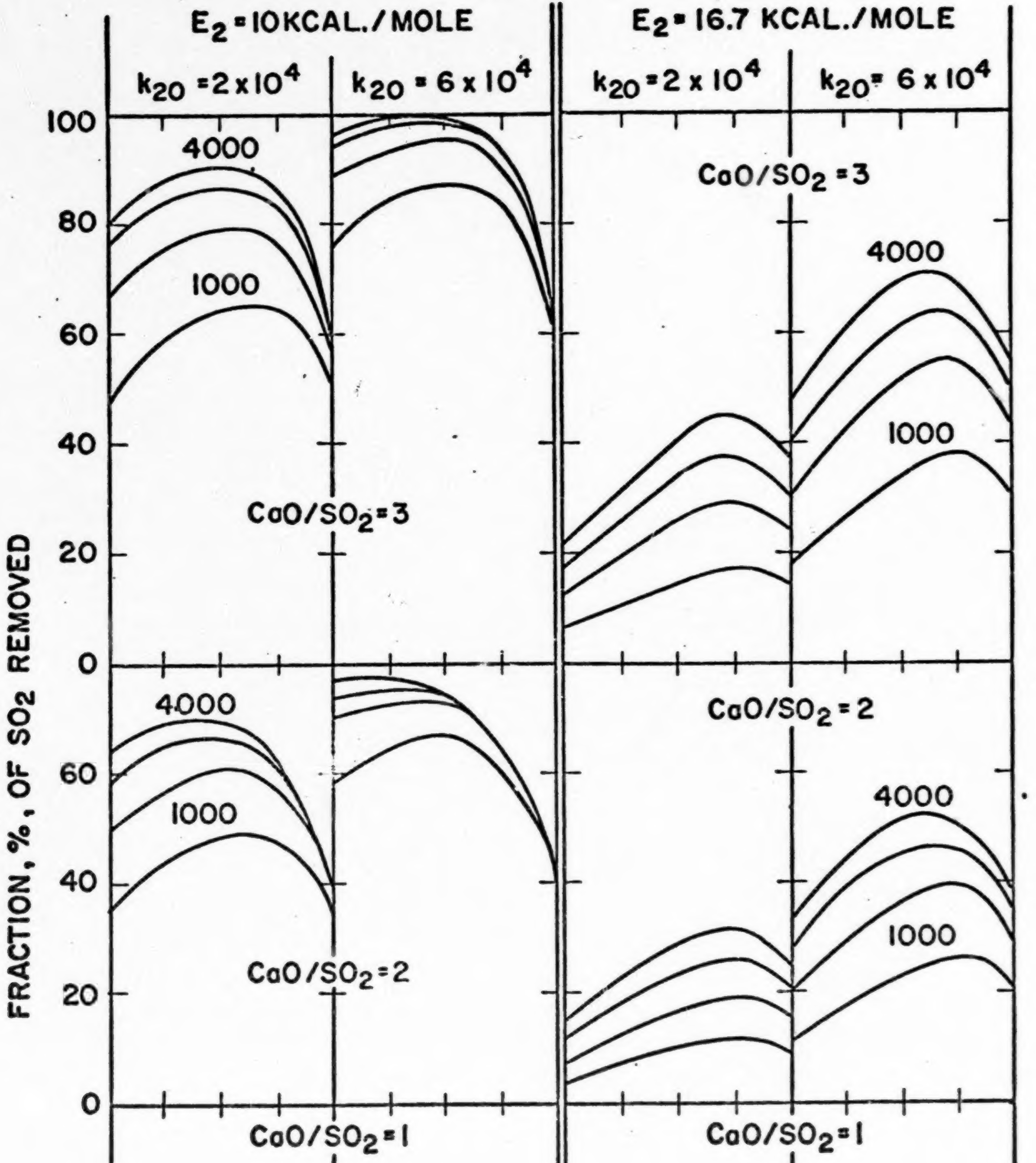

Figure 25. Effects of Amount of Injected Limestone and Kinetic Parameters on the Desulfurization of Stack Gas.

APPENDIX D: DETERMINATION BY REGRESSION ANALYSIS OF THE SIGNIFICANT FACTORS THAT AFFECT THE SO_2 ABSORPTION PROPERTIES OF LIMESTONE

Consider a dependent variable, y, that is a function of several, n, independent variables: x_1, x_2, $x_3 \ldots x_n$. It is desired to obtain the significant independent variables that, in conjunction with each other, affect the value of y, when a number of measurements are available that associate the value of y with a set of values of x's.

The method is based on the statistical t test for the significance of the coefficients of the x variables in a linear model. The process involves the successive elimination of one x factor at a time until each of the remaining factors or independent variables has attained a t value that is statistically significant, at some arbitrary confidence level, in the regression model.

Two regression models are used:

$$y = a_1x_1 + a_2x_2 + a_3x_3 + \ldots a_nx_n \qquad (1D)$$

$$y = b_1x_1 + b_2x_2 + b_3x_3 + \ldots b_nx_3 + b_o \qquad (2D)$$

where the a's and b's are the coefficients of the factors in the respective models. Model 2 contains a constant term, b_o, but model 1 contains only a linear combination of the independent variables.

The coefficients of a_i in equation 1D and b_i in equation 2D are determined by minimizing the sums of squares, $\Sigma(y_{obs} - y_{1c})^2$ and $\Sigma(y_{obs} - y_{2c})^2$, respectively; y_{obs} is the set of observed values of the dependent variable, y, and y_{1c} and y_{2c} are the corresponding sets calculated by equations 1D and 2D respectively. The corresponding t statistic,

$$t_{1i} = a_i/SEa_i,\ i = 1,\ n \qquad (3D)$$

$$t_{2i} = b_i/SEb_i,\ i = 1,\ n + 1 \qquad (4D)$$

for each coefficient is calculated by equations 3D and 4D, where the first subscript of t refers to the model number, the second subscript, i, refers to the corresponding coefficient in the model, and the terms SEa_i and SEb_i are the standard errors of the respective coefficients that are derived from the least-squares fit of the models and the lack of fit, or residual variance, with respect to the observed values of y.

The least significant factor of the n factors is eliminated by testing the value of t for the term b_o in model 2; if this particular t value is greater than the t statistic at the prescribed confidence level, the remaining t values of model 2 are ranked from lowest to highest in absolute magnitude, and the variable corresponding to the least t value is eliminated unless it, too, exceeds the t statistic at the same confidence level. If the term b_o in model 2 is not significant, the above procedure is used to eliminate the least significant factor in model 1. The remaining n - 1 factors are then treated by regression with the same 2 models, equations 1D and 2D, and the second least contributing factor is eliminated. This process is repeated until all the remaining factors contribute significantly to the regression. (It should be noted that the order of listing the factors in equations 1D and 2D is unimportant, because the same least-squares solution is obtained in any order for a given number of linear factors.)

When the number of factors has been reduced to a set of significant factors, the observed values of y are further treated by regression to include these factors and their interactions with each other. The model is (for significant factors x_1, x_2, and x_3):

$$y = b_1x_1 + b_2x_2 + b_3x_3 + b_{12}x_1x_2 + b_{13}x_1x_3 + b_{23}x_2x_3 \qquad (5D)$$

Again, the term b_o is added to a second model to correspond to equation 2D. The least significant of the terms in equation 5D is eliminated as before, and the process is repeated until only significant terms remain in the expression.

The above procedure of selecting the most important factors for a particular response, or dependent variable, is carried out on a computer that makes the choice of model, eliminates the proper term, tests the t statistics, regroups for the next regression, and finally sets up and solves for the significant interaction terms.

The confidence level for the t statistics used in the multiple correlations was 90%. The process of elimination was limited to a total of 10 independent variables, n = 10, because the solution of a matrix of larger size frequently resulted in unrealistic values of the constants. The loss of significant figures in the matrix inversion of the sums-of-squares equations when n was larger than 10 sometimes gave R values larger than 1, as well as erroneous standard errors for the coefficients. For this reason, when the solution of equations 1D and 2D gave five or more significant factors, the interaction equation, 5D, was omitted. With four or fewer significant factors, the elimination procedure on the interaction equation usually returned to the original solution by eliminating the interaction terms.

APPENDIX E: MULTIVARIATE ANALYSIS--A LOOK AT PRINCIPAL-COMPONENTS PREDICTION

Principal-component analysis is a mathematical technique for summarizing a set of related measurements as a set of derived variates, frequently fewer in number, which are definable as independent linear functions of the original measurements. For example, if y, a dependent variable, is a function of n independent variables, $x_1, x_2, x_3, \ldots x_n$, it is possible to express y as a function of m combinations of the n variables by the equation

$$y = B_1X_1 + B_2X_2 + B_3X_3 + \ldots B_mX_m \qquad (1E)$$

where $m \leq n$, and

$$X_i = \sum_{j=1}^{n} B_{ij}X_j,\ i = 1, m \qquad (2E)$$

The derived variates, represented by capital X's, are orthogonal to each other, and the first derived variates, X_1, will account for the largest possible proportion of the total variation in the original x variables, the second will account for the largest possible proportion of the remainder, and so on. The derived variates are known as principal components, and the corresponding variances as latent roots. When all the principal components are taken, equation 1E results in a regression equation, when transformed to the original x variables, identical with that obtained by linear regression. Since the derived variates, X_i, are independent and arranged in the order of decreasing accountability of the total x variance, it is frequently possible, by geometrical manipulation, to obtain linear functions of the original variables that are chemically meaningful or consistent with other observations.

A total of thirteen x variables from Tables VIII and IX was used to derive the principal components in an attempt to explain certain y variables in Tables X and XI. Some of the x variables were combinations or sums of impurity constituents of Table IX that were used to include as many of the measured properties as possible. Multiple precision was required in the computer calculations. The fractions of the total x variation that are explained with different numbers of roots (eigenvalues) of the characteristic equation are shown in Figure 26; all the x variation would be explained by taking all thirteen of the eigenvalues. The first root explains 35% of the x variation, the first two roots 63%, the first three roots 75%, and so on. It is quite likely that the first five or six roots of the characteristic equation are required to reproduce the x variation within the precision with which it is measured. The following tabulation shows the effect of decreasing the number of roots from thirteen to eleven and nine on the standard deviation, S, and the correlation coefficient, R, for the empirical prediction equations for certain combinations of y variables that were used in the multiple correlations.

		Number of roots kept (dropped)		
Function		13(0)	11(2)	9(4)
y_{13}	S	4.87	4.90	5.49
	R	0.813	0.811	0.755
y_5	S	8.27	9.01	9.02
	R	0.656	0.569	0.568
y_{13}/y_{15}	S	0.213	0.217	0.229
	R	0.662	0.646	0.593

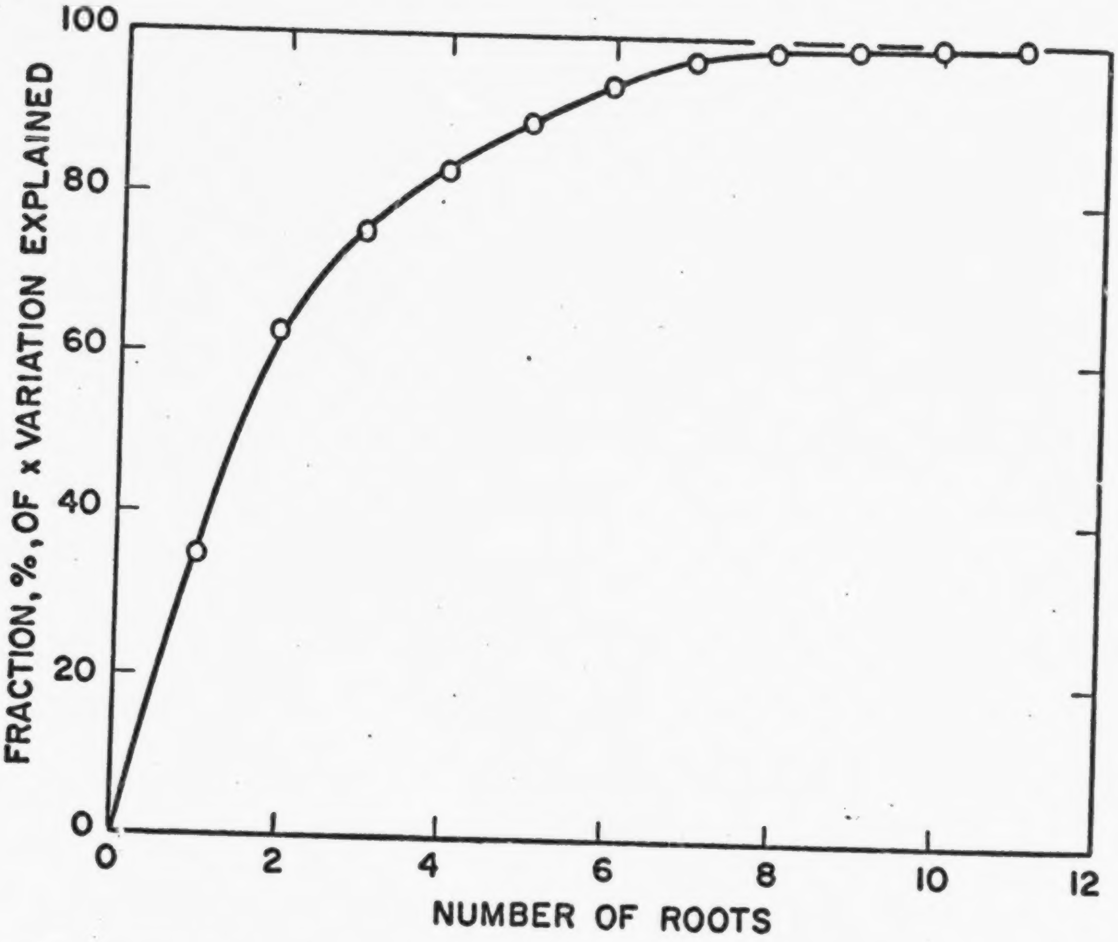

Figure 26. Number of Roots Required to Explain Variations Among 13 Measured Properties of Limestones.

The prediction of the polythermal uptake of SO_2 during calcination, y_{13}, was affected greatly by dropping the four smallest roots, but was not significantly affected by dropping the two smallest roots. The prediction of the total isothermal weight gain at 930° C., y_5, was affected more when the first two roots were dropped than when the third and fourth roots were dropped. The prediction of the fraction of SO_2 uptake during calcination, y_{13}/y_{15}, was affected increasingly as more roots were dropped.

It appears likely that the multivariate approach to elucidate the principal components of the chemical and mineralogical properties of limestones in relation to the SO_2 absorption will not produce a meaningful function that will have a practical value for the injection process based on the data of this report. The derived functions can be no better than the linear regression models, which in themselves leave much to be desired. Possible explanations include the imprecise measures of some of the x variables or even the inadvertent omission of one or more properties of the stones that may affect the sulfation characteristics markedly.

APPENDIX F: RELATIVE IMPORTANCE OF PROPERTIES OF LIMESTONES FOR REACTION WITH SULFUR OXIDES

The relative importance of the significant variables that affect the reactivity of limestones with SO_2 is shown in the attached table. The results are shown as the changes in the factors required to produce either an increase of 1 in the value of w_3 or a 10% increase in the value of w_3, depending on whether the linear or logarithmic equation is used to calculate the capacity w_3 using the coefficients of Table XX.

An increase of 0.81 in the ratio of rhombic carbonates to CaO in the stone (in the range 1.76 to 3.42) causes a 10% increase in the absorptive capacity of the stone; the same effect is obtained by either decreasing the microscopic grain size (code) by 0.62, increasing the lattice constant by 0.14 Å., increasing the Na_2O content by 68% of its value, decreasing the content of clay, feldspar, and limonite by 2.95% in absolute amount in the stone, or increasing the fraction or iron (if it has to be present) in limonite form by a value of 0.34.

Similarly, an increase of 1 in absolute capacity (next to last column in Table XXIII) requires either a decrease of 0.031 μ (310 Å) in the x-ray crystallite size, a decrease of 3.05% in the clay, feldspar, and limonite content, or an increase of 89.5% in the Na_2O content. All of these increases or decreases must be within the ranges listed.

TABLE XXIII

Changes in Limestone Properties Required to Produce

Measured Changes in Reactivity

	Property		Change in property to produce	
Designation	Description	Range	1 gram increase in weight gain per 50 grams of stone	A 10% increase in weight gain
z_2	% rhombic carbonates/% CaO	1.76-3.42	-	+0.81
z_4	Microscopic grain size, coded[a]	1-3	-0.64	-0.62
z_5	Lattice constant, *a*, Å.	4.805-4.989	+0.18	+0.14
z_6	X-ray crystallite size, μ	0.070-0.211	-0.031	-
z_7	Logarithm of Na_2O content	0.005-0.25	+89.5%[b]	+68.2%[b]
z_9	% clays, feldspar, and limonite	0.1-31	-3.05	-2.95
z_{10}	Fraction of Fe as limonite	0-1	+0.35	+0.34

---

[a] 1 = <63 μ; 2 = 63 - 250 μ; 3 = >250 μ.

[b] Percentage increase in sodium content.

The lattice constant, a, has a narrow range in all stones composed of dolomites and calcites, from 4.805 Å. for pure dolomite to 4.990 Å. for pure calcite. Its "independent" effect on SO_2 absorption is less than that of any of the other factors because of its short range; increasing the value of a from its lowest possible value to its highest possible value would increase the SO_2 absorption by only 1 gram per 50 grams of stone, about a 13% increase in absorptivity. The value of this factor, a, to the regression equations is that it takes the place of the constant, b_o, with which it is highly correlated, and improves the empirical relation by the slight amount of its effect.

Many of the factors are involved in a strict calcite-dolomite type of comparison. For example, a dolomite usually has a higher value of z_2 than does a calcite, and dolomites usually have smaller grain sizes, z_4, and smaller x-ray crystallite sizes, z_6, than calcites because of the more complex structure of dolomites as well as their "age". Dolomites, however, usually are associated with more impurities that are detrimental, z_9; iron is found in the crystal lattice, z_{10}, in dolomites more frequently than in calcites; and dolomites have smaller lattice constants a, z_5. It is the combination of these properties that affects absorptive capacity.

BLANK PAGE

X 25

G. H. McClellan[1] *and J. L. Eades*[2]

Authorized Reprint
from Special Technical Publication 472
Copyright
American Society for Testing and Materials
1916 Race Street, Philadelphia, Pa., 19103
1970

The Textural Evolution of Limestone Calcines*

REFERENCE: McClellan, G. H. and Eades, J. L., **"The Textural Evolution of Limestone Calcines,"** *The Reaction Parameters of Lime, ASTM STP 472*, American Society for Testing and Materials, 1970, pp. 209–227.

ABSTRACT: A pure limestone and Iceland spar were shock calcined at several constant temperatures in the range 750 to 1300 C in a study of the pore structure of the calcines. The calcines were examined with a scanning electron microscope to follow the development of the pore structure and to correlate changes in the pores and in the related surface area with the properties of the lime and the temperature of calcination.

Limestone calcines prepared at temperatures below 1000 C had larger pores and lower surface areas than Iceland spar calcines prepared at the same temperature. Raising the temperature of calcination caused a decrease in surface area and an increase in pore size of both materials. The decrease in surface area on calcination at 1000 C resulted from the growth of large pores at the expense of smaller pores, but the physical characteristics of the lime were largely unchanged. At temperatures above 1000 C the calcium oxide crystals sintered and grew in size as the pore size continued to increase and the surface area decreased.

The larger initial crystallite size of the Iceland spar resulted in an unfavorable pore size distribution in its calcined products prepared below 1000 C. The limestone calcines prepared at the same temperatures had larger pores and smaller surface areas. Literature reports confirm that there is an optimum temperature of calcination for each stone for producing the proper surface area, pore distribution, and lime condition for maximum solid-fluid reactivity.

KEY WORDS: calcite, limestone, roasting, calcium carbonate, calcium oxide, electric power plants, flue gases, sulfur dioxide, air pollution, injection, scanning electron microscope, density (mass/volume), porosity, poroismeters, evaluation, tests

The injection of dry limestone into power plant furnaces is the most economical means of decreasing sulfur dioxide concentrations in the effluent stack gas. The calcium oxide produced from the stone reacts with sulfur dioxide and oxygen to form calcium sulfate that can be removed by conventional dust-collecting systems. The results reported here are a part of a continuing laboratory study of the properties of calcines prepared by shock heating (calcinations carried out in an environment preheated to a selected temperature in contrast to calcining at rising temperatures). The materials examined were portions of the samples used by McClellan et al[3] in reactivity tests, and the physical properties of the calcines were correlated with their reactivities. The previous results showed that the nature of the original stone influences the properties of its calcines, including their reactivity with sulfur dioxide.

---

* Part of this work was performed under contract TV–29232A with the National Air Pollution Control Administration of the U.S. Public Health Service.

[1] Research chemist, Division of Chemical Development, Tennessee Valley Authority, Muscle Shoals, Ala. 35660.

[2] Research assistant professor, Department of Geology, University of Illinois, Urbana, Ill. 61801. Personal member ASTM.

Limestones and their calcines have been evaluated for industrial use largely on the basis of their chemical purity. Advances in industrial technology [*1*][4] have shown, however, that physical properties such as surface area, porosity, pore size distribution, and crystallite size are important factors in determining the rate and degree of the chemical reactions of the calcines.

In this study, two high-calcium limestones were shock calcined at temperatures between 750 and 1300 C. These two materials differ only in texture, so that the effects of composition can be ignored. The calcines of these stones were studied by scanning electron microscopy and by mercury porosimetry, and the results were used to interpret the changes in texture with rising temperature of calcination.

Experimental Procedure

The two limestones were a high-purity calcitic limestone (USDA Reference Sample 89) and Iceland spar (Ward's Scientific Company) in the form of clear crystals. Both stones were crushed and screened to produce a minus 20- plus 24-mesh fraction from which samples were hand picked to minimize the content of accessory minerals.

X-ray and petrographic examinations showed the samples to be free of accessory minerals. Their cell constants showed that both materials were pure calcites as defined by Goldsmith and Graf [*2*] and were without significant isomorphism.

A 3-g sample of each calcite was calcined in a platinum boat for 16 h at constant temperatures in the range 750 to 1300 C. The samples were placed abruptly in a preheated furnace to effect initial shock calcination; the long retention time was sufficient for complete calcination at each temperature.

---

[3] See p. 32.

[4] The italic numbers in brackets refer to the list of references appended to this paper.

Several particles of each calcine were stored under vacuum until they were examined in the scanning electron microscope. Immediately prior to the examination, each sample was coated in a vacuum evaporator with a 2:1 mixture of gold and palladium that was deposited from several directions to minimize charging of the rough, porous surfaces of the calcines during examination.

The pore volumes and pore size distributions were measured with a mercury porosimeter that had an upper pressure limit of 5,000 psia which limited penetration to pores 0.035 μm in diameter or larger. Apparent densities of the calcines were calculated from weights of the porosimeter penetrometer containing the sample and mercury. Densities calculated from measurements with only the pores larger than 17.5 μm in diameter filled with mercury are comparable to bulk densities determined by mercury displacement.

Results

Raising the temperature of calcination decreased the total pore volume and shifted the distribution toward larger pores in all calcines of sample 89 except that made at 1100 C (Fig. 1). This calcine showed a higher pore volume and a more even distribution of pores in the range 17.5 to 0.175 μm than the 1000 C calcine. Each Iceland spar calcine (Fig. 2) had less than half the total pore volume of the corresponding limestone calcine, and almost all the pores in the 750 and 850 C spar calcines were smaller

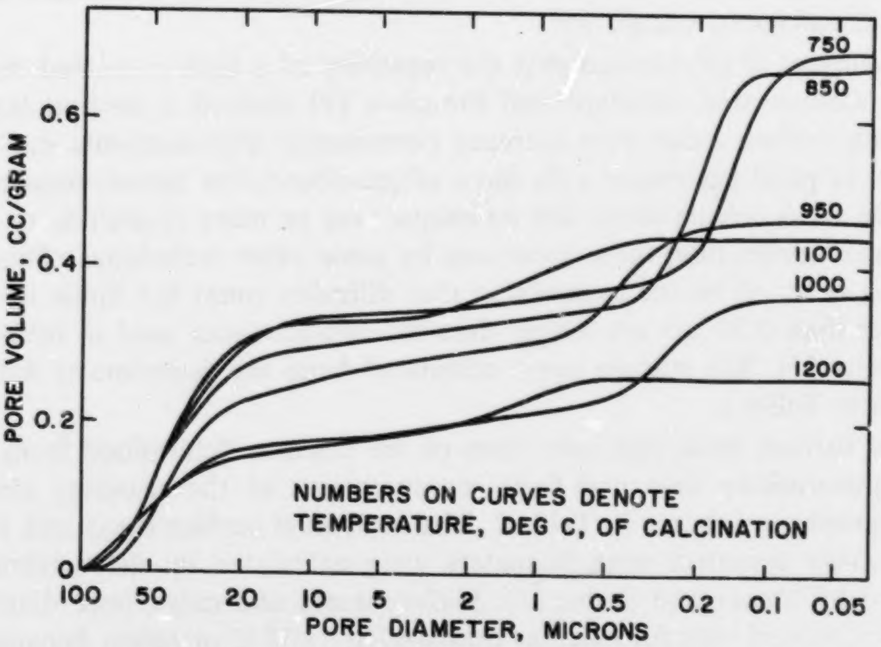

FIG. 1—*Pore volumes of 16-h limestone calcines.*

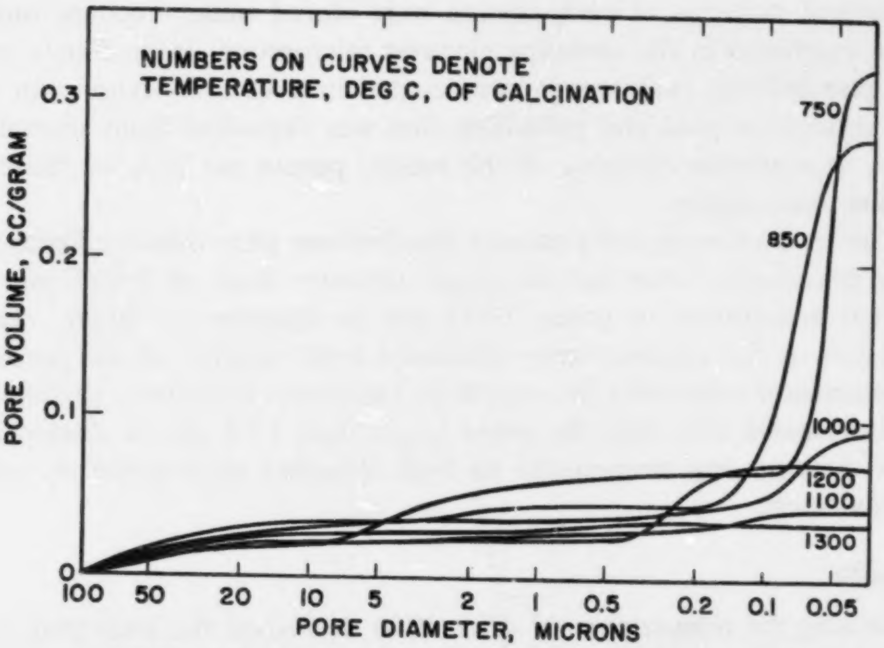

FIG. 2—*Pore volumes of 16-h Iceland spar calcines.*

than 0.2 μm. The total pore volume of the spar calcines decreased, and the pore distribution shifted toward larger pores with rising calcination temperature except for the 1200 C calcine. The total pore volume of this calcine was larger than that of the 1100 C spar calcine and may have resulted from the mechanism that caused the larger pore volume in the 1100 C calcine of sample 89.

Murray et al [*3*] showed that the reactivity of a lime is related directly to its surface area. Rootare and Prenzlow [*4*] derived a method for calculating surface areas from mercury porosimeter measurements that gives results in good agreement with those of gas-absorption measurements, and surface areas calculated by this technique may be more applicable to solid-fluid reactivities than those measured by some other techniques. This conclusion is based on the assumption that diffusion times for fluids in pores smaller than 0.30 μm are longer than the contact times used in measuring reactivity [*5*]. The surface areas calculated from the porosimeter data are shown in Table 1.

The surface areas and pore sizes of the calcines determined from mercury porosimetry data and from measurements of the scanning electron micrographs are shown in Table 2. The individual surface areas and equivalent mean spherical pore diameters were calculated by the method described by Mayer and Stowe [*1*]. Surface areas and mean pore diameters were calculated only for calcines prepared at 1100 C or below because the number of pores decreases rapidly at the higher temperatures as sintering becomes pronounced.

There is good agreement between the surface areas calculated from the porosimeter and from the electron microscopic data. The distribution of the surface area within a sample also is important. The data in Table 1 show that most of the surface area of samples calcined below 1000 C is associated with small pores, those smaller than 0.2 μm. If Potter's data [*5*] on the sulfur dioxide capacity of limestones are correct, diffusion into pores this small and smaller is too slow to be effective in short-time reactivity tests. The formation of films of calcium sulfate on the surface could block areas containing many of these pores, further decreasing their availability for reaction. The pores provide the fluids access to the surface area of the solids, and materials with mean pore diameters larger than 0.2 μm are more responsive in short-term reactivity tests because of the shorter times required for diffusion of sulfur dioxide into these larger pores. As shown in Table 2, calcines of sample 89 had mean pore diameters larger than those of Iceland spar calcines prepared at the same temperature, and the pore diameters of both materials increased with rising temperature of calcination.

Raising the temperature of calcination changes the nature of the solid lime as well as its pore size distribution. McClellan et al[3] showed that the crystallite size of the limes of both materials slowly increases with rising temperature of calcination below 950 C and decreases slightly at 1000 C. At temperatures above 1000 C, the rate of crystallite growth increases with rising temperature. These changes in the physical properties of the lime decrease the potential reactivity of the lime surface as crystal perfection increases and crystal growth influences the texture of the surface itself.

Scanning electron microscopy has previously been used to study the surface of limes prepared in commercial kilns.[5] The work reported here is the first laboratory study of shock-treated limestone calcines prepared under laboratory control at several different temperatures.

The main advantage of scanning electron microscopy over optical and transmission electron microscopy is its greater depth of focus, which is as much as 100 times that of the other techniques. This advantage, combined with the simple sample preparation, allows the investigator to examine the unaltered surface of materials and to obtain information that was previously unavailable, or only to be guessed at, on surface texture and pore size, shape, and distribution. In the study of limes, scanning electron microscopy presents clear evidence on surface areas and the properties of pores.

[5] See p. 3.

TABLE 1—*Surface areas of calcines calculated from porosimeter measurements.*

	Surface Area[a]		Surface Area[a]		Surface Area[a]	
Pore Size, µm	M^2/g	% of Total	M^2/g	% of Total	M^2/g	% of Total
LIMESTONE 89						
	750 C calcine		850 C calcine		950 C calcine	
17.5	0.12	0.3	0.08	0.04	0.07	1.5
5.0	0.17	0.5	0.12	0.6	0.11	2.4
1.75	0.22	0.6	0.16	0.8	0.19	4.0
1.0	0.36	1.0	0.26	1.3	0.28	5.9
0.5	0.54	1.5	0.43	2.1	1.15	24.5
0.4	0.71	2.0	0.84	4.1	1.87	39.8
0.2	3.72	10.3	8.62	42.4	3.76	80.0
0.1	26.26	72.9	20.17	99.3	4.70	100.0
0.05	35.68	99.0	20.31	100.0	4.70	100.0
0.035	36.03	100.0	20.31	100.0	4.70	1000.
	1000 C calcine		1100 C calcine		1200 C calcine	
17.5	0.04	0.6	0.06	5.2	0.03	5.9
5.0	0.08	1.1	0.09	7.3	0.05	9.7
1.75	0.15	2.2	0.17	13.7	0.09	16.1
1.0	0.32	4.7	0.37	29.2	0.31	57.6
0.5	0.67	9.9	0.82	65.4	0.50	92.3
0.4	0.96	14.1	0.92	73.2	0.54	100.0
0.2	4.88	71.8	1.06	84.5	0.54	100.0
0.1	6.79	100.0	1.12	89.6	0.54	100.0
0.05	6.79	100.0	1.25	100.0	0.54	100.0
0.035	6.79	100.0	1.25	100.0	0.54	100.0
ICELAND SPAR						
	750 C calcine		850 C calcine		1000 C calcine	
17.5	0.01	0.0	0.01	0.0	0.01	0.1
5.0	0.03	0.0	0.01	0.0	0.01	0.1
1.75	0.09	0.1	0.04	0.1	0.02	0.3
1.0	0.19	0.3	0.06	0.2	0.05	0.7
0.5	0.25	0.4	0.06	0.2	0.05	0.7
0.4	0.28	0.4	0.06	0.2	0.05	0.7
0.2	0.38	0.6	0.06	0.2	0.08	1.2
0.1	0.38	0.6	4.26	13.2	1.02	14.5
0.05	47.38	75.3	29.86	92.7	5.95	84.3
0.035	62.93	100.0	32.20	100.0	7.06	100.0

TABLE 1 (*continued*).

Pore Size, μm	Surface Area[a]		Surface Area[a]		Surface Area[a]	
	M²/g	% of Total	M²/g	% of Total	M²/g	% of Total
	1100 C calcine		1200 C calcine		1300 C calcine	
17.5..........	0.00	0.0	0.00	0.1	0.00	2.0
5.0..........	0.01	0.7	0.01	0.4	0.01	5.0
1.75..........	0.01	0.7	0.01	0.6	0.02	11.6
1.0..........	0.03	2.5	0.02	1.0	0.03	15.6
0.5..........	0.04	3.4	0.02	1.0	0.06	29.1
0.4..........	0.05	5.0	0.04	1.9	0.10	50.8
0.2..........	0.08	7.6	1.14	56.6	0.20	100.0
0.1..........	0.40	37.9	1.89	93.8	0.20	100.0
0.05..........	0.69	65.2	2.02	100.0	0.20	100.0
0.035..........	1.06	100.0	2.02	100.0	0.20	100.0

[a] Area contributed by pores of indicated and all larger sizes.

TABLE 2—*Correlation of porosimeter and scanning electron microscope measurements.*

Calcination Temperature, deg C	Porosimeter		Scanning Electron Microsocpe		
	Surface Area, M²/g	Pore Size, μm[a]	Surface Area, M²/g	Pore Size, μm	No. of Pores[b]
			LIMESTONE 89		
750..........	36.0	0.05	27.4	0.06	482
850..........	20.3	0.09	14.6	0.12	514
950..........	4.7	0.37	4.2	0.42	471
1 000..........	6.8	0.26	6.7	0.26	502
1 100..........	1.2	1.44	1.4	1.27	188
			ICELAND SPAR		
750..........	62.9	0.03	66.5	0.03	477
850..........	32.2	0.05	46.4	0.04	470
950..........	...	...	46.0	0.04	348
1 000..........	7.0	0.25	10.8	0.16	368
1 100..........	1.1	1.58	0.9	1.92	75

[a] Calculated from the relation $A = 6/D\rho$, where A = surface area, M²/g; D = mean diameter, μm, of pores assumed to be spherical; ρ = absolute density, g/cm³.

[b] Number of pores measured for calculation of pore size.

In calcines prepared at temperatures below 1000 C, the most diagnostic features are the pores and their growth by coalescing. A representative area of the 750 C limestone (sample 89) calcine is shown in Fig. 3 in which the evolving pore structure of the lime is superimposed on a residual rhombohedral cleavage fragment of the stone. There is a wide range of pore sizes, even in this soft-burned stone. The solid lime is generally featureless, and no significant points of contact have developed between the individual lime units within each particle. Electron micrographs of 750 C Iceland spar calcine show essentially the same evolution of pores, but the pores are smaller and there are more per unit area.

The 850 C calcines (Fig. 4) show continuing coalescing of the pores, although residual rhombohedral features of the original stone persist. This figure shows that the larger pores grow at the expense of the smaller ones, as observed in the porosimeter data. There is no evidence of individual calcium oxide units within the larger particles.

The 950 C calcines (Fig. 5) show additional coalescing of pores superimposed on detectable cleavage features of the original stone. The pores

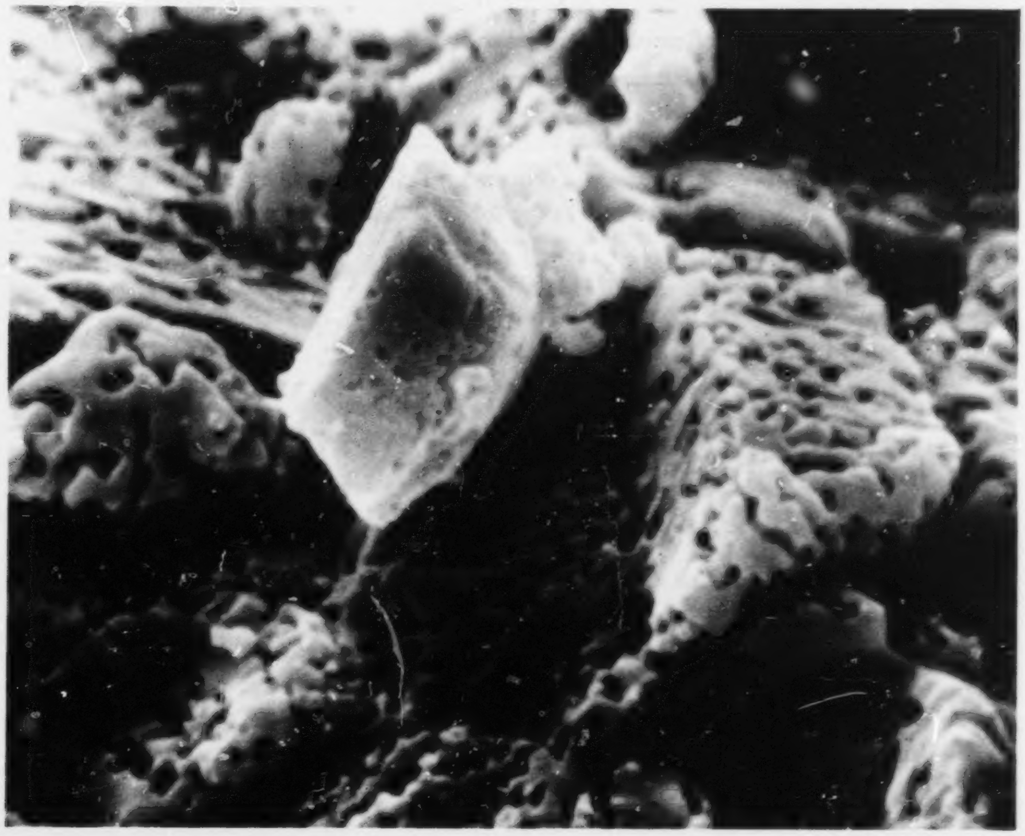

FIG. 3—*Limestone calcined at 750 C showing pore evolution superimposed on cleavage fragments (×6300).*

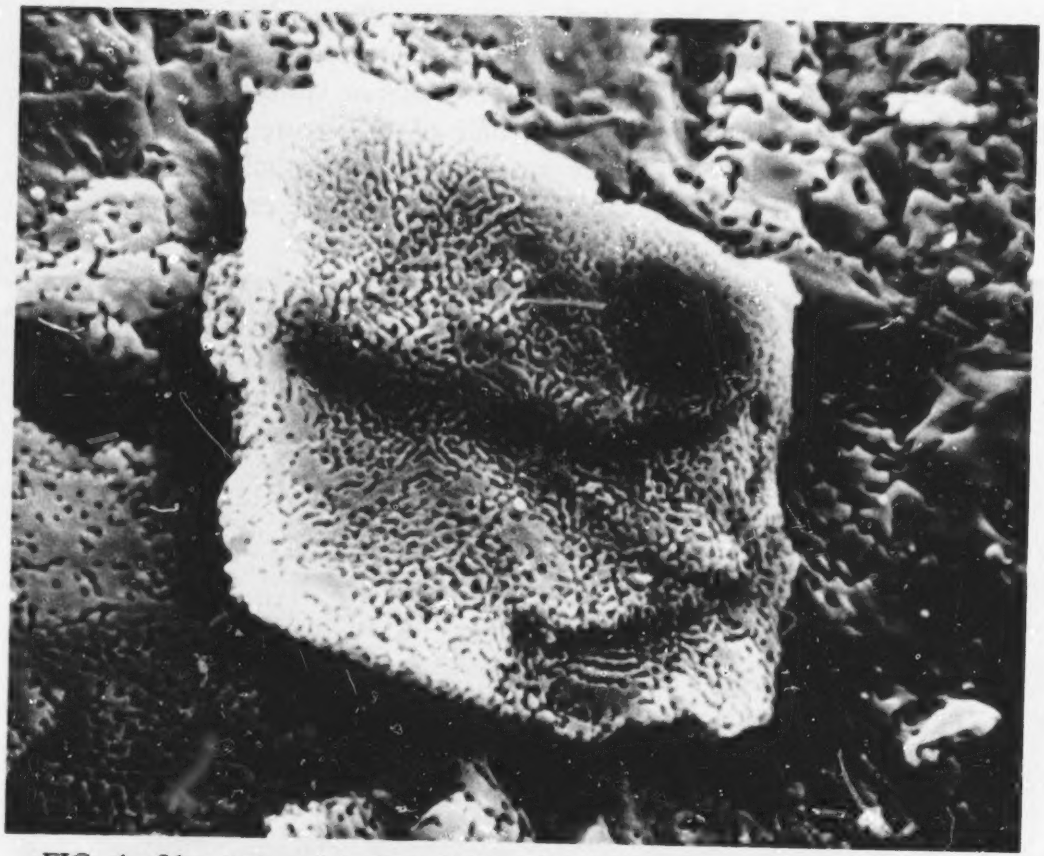

FIG. 4—*Limestone calcined at 850 C showing coalescing of pores* (×2640).

seem to be oriented randomly, and there was no detectable crystallographic control of pore evolution in any of the calcines studied. Discrete subunits of calcium oxide, which appear for the first time in calcines prepared at 950 C, can be seen throughout Fig. 5.

The 1000 C calcines show final pore growth by coalescing, and the calcine of sample 89 (Fig. 6) is representative of this stage. Pores 0.5 μm or larger are abundant, and the subunits of lime appear relatively unchanged from those in the 950 C calcines. The open textural appearance and an essentially unchanged lime appear to indicate optimum surface availability for solid-fluid reaction.

The Iceland spar 1000 C calcine (Fig. 7) shows only a few pores as large as 0.05 μm, and most of the pores are much smaller. The distinguishable lime subunits seem smaller (about 0.1 μm) than the lime in the limestone calcine (about 0.5 μm) and seem to have proportionally larger points of contact.

Calcines prepared at 1100 C or above show sintering and shrinking of the oxide that is not seen in the lower-temperature calcines. The limestone calcine, shown in Fig. 8, has a more compact texture with extensive contacts developed between the lime units, and a pronounced decrease in porosity over that shown in Fig. 6. Growth loops or spirals are present on the individual lime units in the right half of the figure, indicating that crystal growth and development of single-crystal morphology has begun, even though residual rock cleavage features are still present.

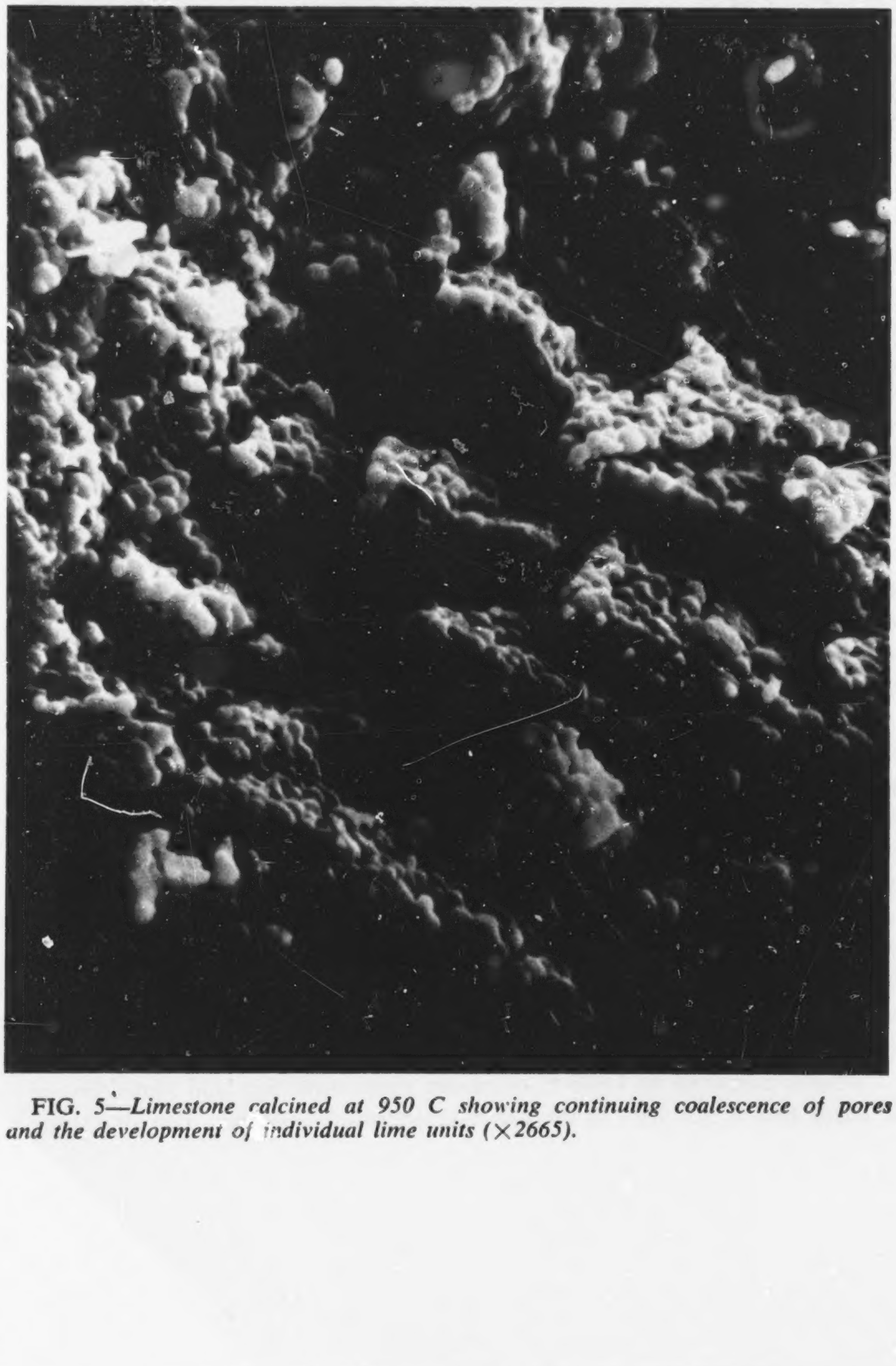

FIG. 5—*Limestone calcined at 950 C showing continuing coalescence of pores and the development of individual lime units (×2665).*

The 1100 C Iceland spar calcine in Fig. 9 also shows the increased compactness of the lime and the resultant decrease in porosity. Although growth spirals are not well developed, many of the lime units are developing flat faces and straight edges between crystal faces. The pores in the 1100 C calcines of both materials are beginning to show straight sides as crystal growth begins.

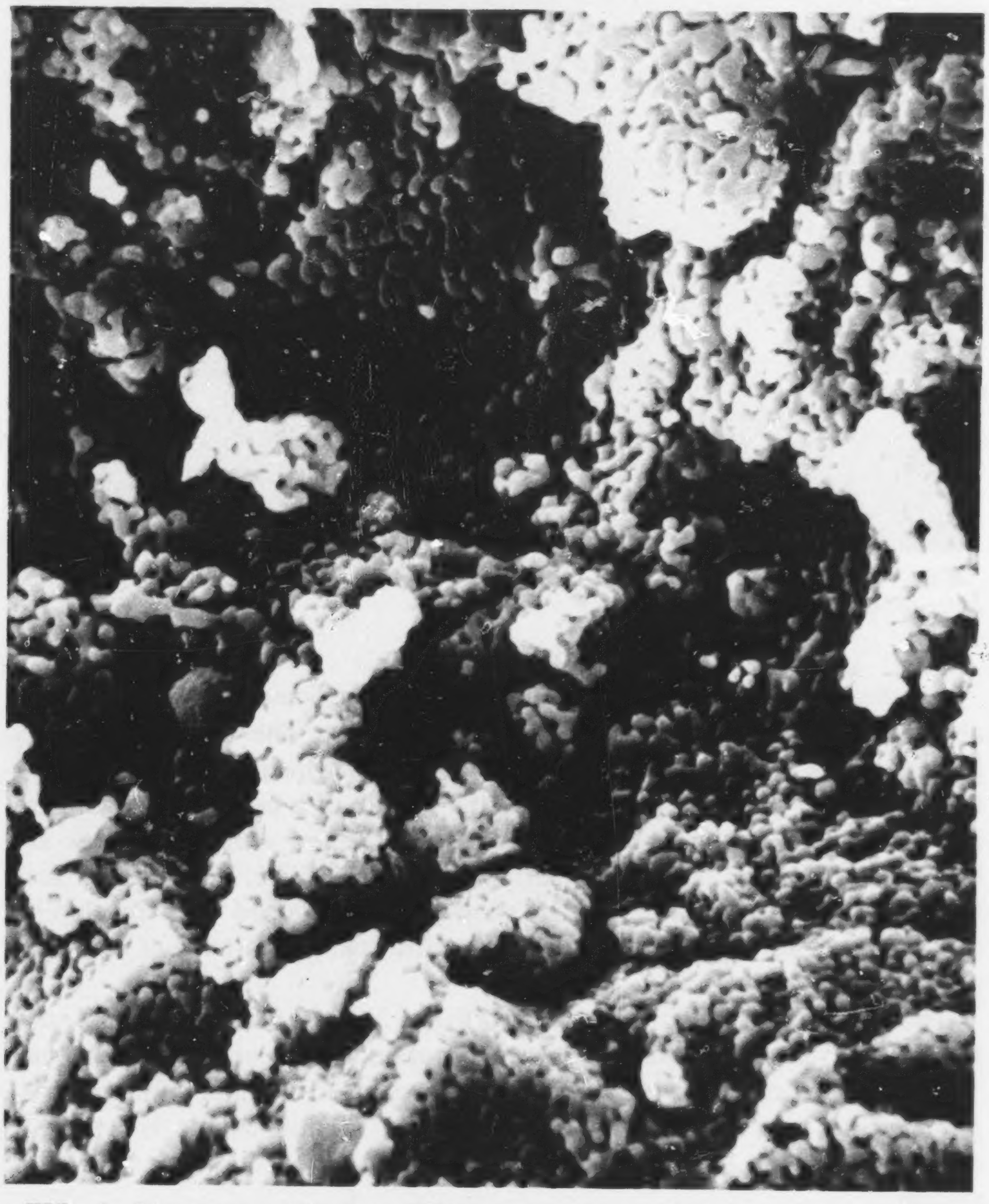

FIG. 6—*Limestone calcined at 1000 C showing completion of pore growth by coalescence (×2888).*

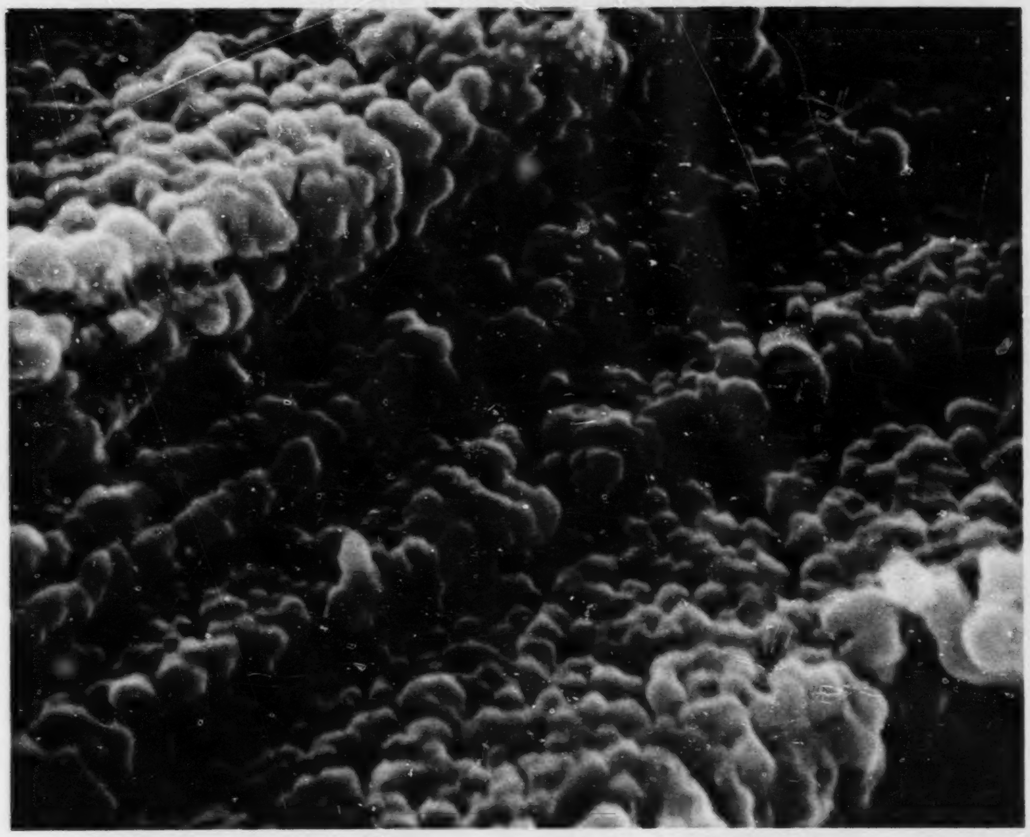

FIG. 7—*Iceland spar calcined at 1000 C showing the pores and individual lime units (×36,450).*

As shown in Fig. 10, the 1200 C limestone calcine is quite compact, and the porosity is confined to a few large pores. The figure contains a good example of a residual cleavage fragment on which typical features of the calcine are clearly apparent. Epitaxial growth of a potential crystal face is noticeable on six or seven oxide units, and the few remaining pores are large and contribute little to the surface area of the lime. The 1200 C Iceland spar calcine in Fig. 11 also shows well-developed and developing crystal faces and has the compact, nearly pore-free appearance of extended points of contact.

The 1300 C Iceland spar calcine (Fig. 12) has a very compact and practically pore-free surface texture with abundant growth loops. A very well-developed oxide crystal appears at the right of the figure. This photograph shows why the calculated surface area of this sample is only 0.2 m^2/g and why the surface would be considered unreactive in a solid-fluid system.

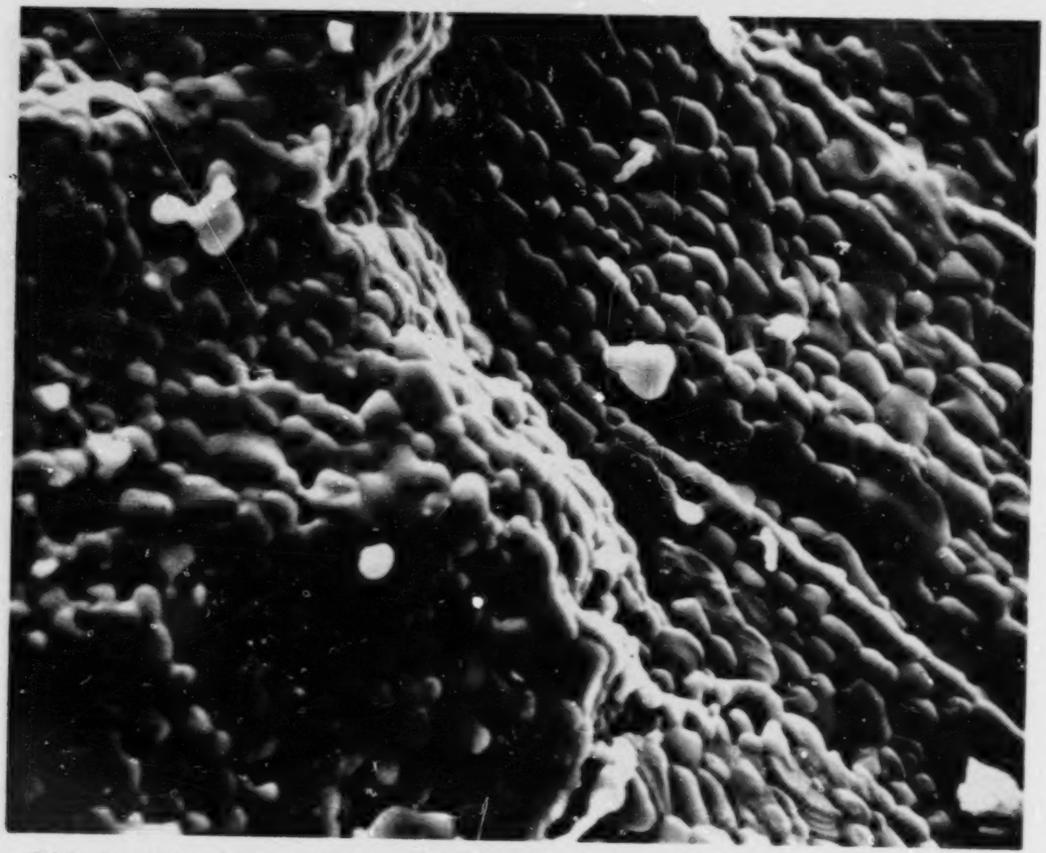

FIG. 8—*Limestone calcined at 1100 C showing sintering texture and growth spiral (×1350).*

Discussion of Results

The application of scanning electron microscopy to the study of limestone calcines demonstrates the meaning of pore volume, pore distribution, and surface area more clearly than other techniques. The evolution of both solids and pores as the temperature of calcination is raised can be observed directly rather than imagined by conceptual models as required in the past. These studies illustrate the access that pores provide reactant gases to the surface area of the calcines.

The calculation of surface areas from porosimeter measurements provides an insight into the physical characteristics of the calcines that is not provided by inspection of the pore-volume data alone. The calculated areas were essentially the surface areas generated by the pores observed in the scanning electron microscope studies. The surface area calculated for the 750 C Iceland spar calcine should be considered a low approximation because the data were calculated only for pores approximately 0.035 μm

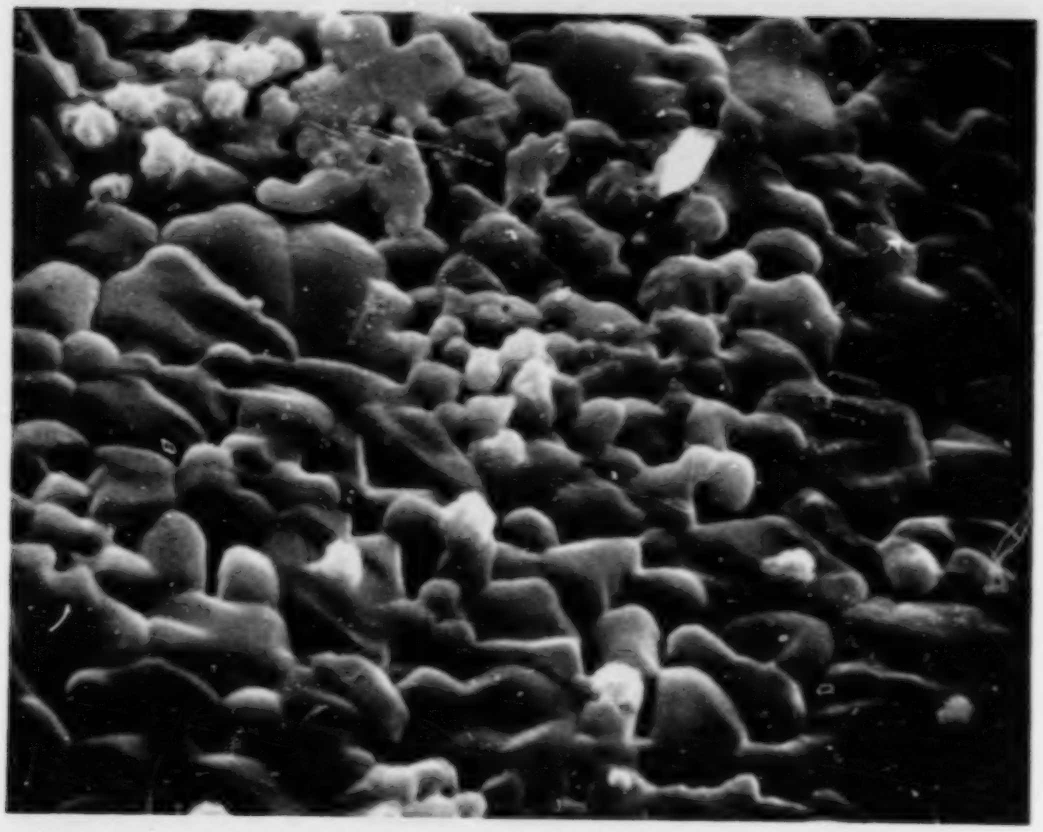

FIG. 9—*Iceland spar calcined at 1100 C showing developing crystal faces and geometric pores (×9720).*

or larger. Because of this restriction there was no plateau in porosimeter pore volume as in the other calcines, indicating that this calcine had pores smaller than 0.035 μm and would have a surface area larger than 63 m^2/g.

Potter [*5*] concluded from his studies of calcines sulfated in fixed-bed tests that pores in the range 17.5 to 0.3 μm are most important in the sulfation reaction and that smaller pores require diffusion times too long to be effective when dry limestone is injected into a power plant furnace. The porosimeter data show that 4 m^2/g of the 36 m^2/g of the surface area of the 750 C calcine and 9 m^2/g of the 20 m^2/g of the surface area of the 850 C calcine of sample 89 are accounted for by pores in the effective range, and that rising temperature increases the fraction of pores in this size range. In contrast, the Iceland spar calcines have only 0.1 m^2/g of the 1.1 m^2/g surface area contributed by pores in this size range at 1100 C and 1.1 m^2/g of the 2.0 m^2/g surface area at 1200 C. This study has shown that both the porosity and the physical condition of the lime in the calcines prepared at temperatures up to 1000 C were influenced strongly by the nature of the starting materials. The Iceland spar calcines had

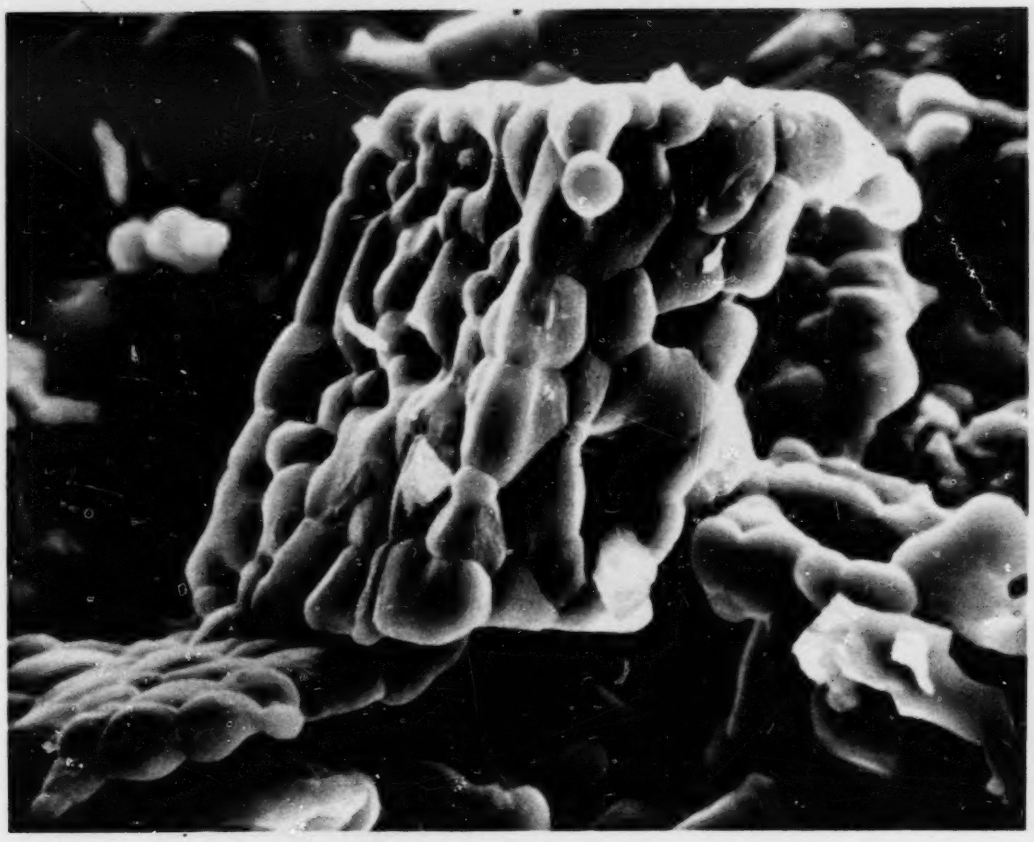

FIG. 10—*Limestone calcined at 1200 C showing epitaxial growth of crystal faces on cleavage fragment (×2183).*

smaller mean pore diameters and larger surface areas than the corresponding calcines of sample 89. Calcination at higher temperatures decreases the porosity and sinters the oxide of both materials so that the reactivity is decreased.

The Iceland spar calcines have a distribution of pores that is unfavorable for sulfation reactions, and sintering has occurred at temperatures at which suitable pores begin to develop, with a resultant decrease of surface area and potential reactivity.

This interpretation is consistent with the observations of McClellan et al[3] on the relative reactivities of limestone and Iceland spar calcines with sulfur dioxide in fixed-bed tests. They found that the limestone calcines were superior reactants under all the experimental conditions tested and concluded that unfavorable pore distribution and poor properties of the lime accounted for the relative inactivity of the Iceland spar calcines. Eades and Sandburg[5] drew similar conclusions from a series of limes on which they measured hydration reactivity. Their data showed that a developed pore structure of the limes was necessary for satisfactory hydra-

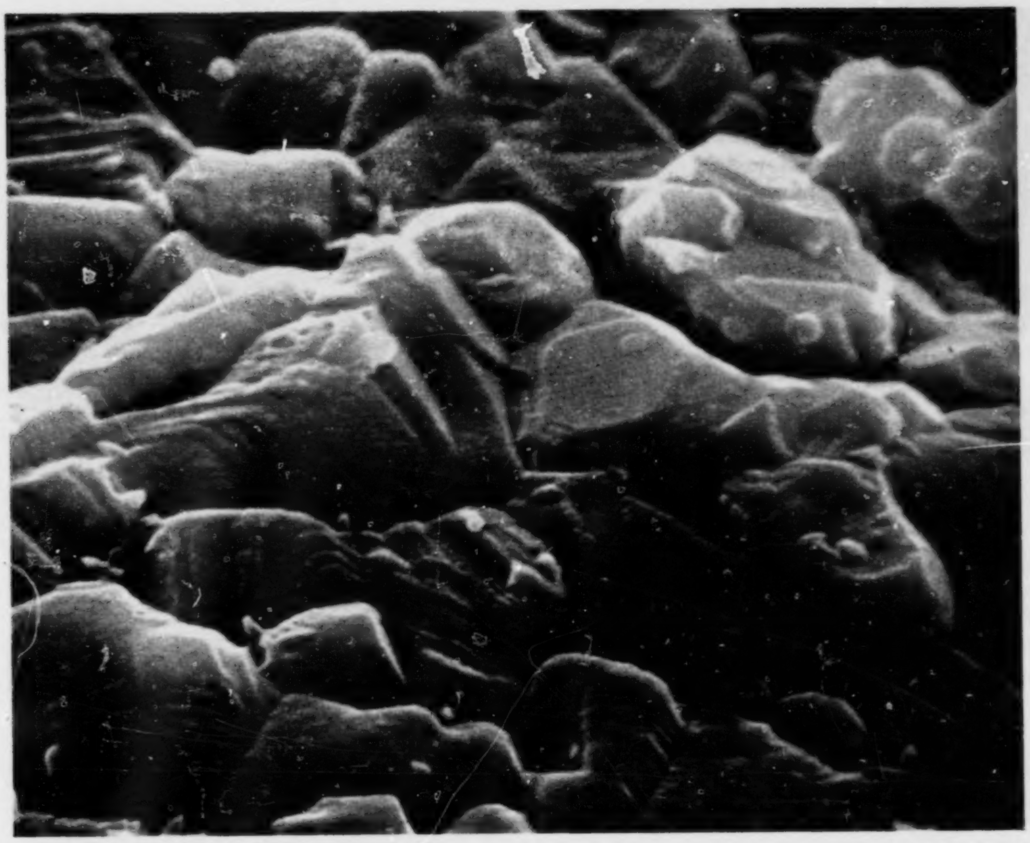

FIG. 11—*Iceland spar calcined at 1200 C showing well-developed crystal growth (×9315).*

tion of the surface, and that softer burned stones without suitable pore structure but with larger surface areas were less reactive.

Murray et al [*3*] have shown that the time required for a coarsely crystalline limestone to reach 920 C during its calcination has a significant effect on the porosity and activity of the lime produced. If the time is too short, the porosity and activity are quite low. If the time is too long, porosity develops satisfactorily, but the activity decreases slowly with prolonged exposure. Fischer [*6*] found similar results for the densities of a stone he shock calcined at different temperatures. McClellan et al[3] measured bulk densities of shock-heated limestone and Iceland spar calcines prepared in the temperature range studied by Fischer. The bulk densities of sample 89 shock-heated calcines were consistently lower than those of the corresponding Iceland spar calcines. The nature of the starting material again appears to influence the physical properties of the calcine, even though the rate of heating prior to and during calcination, as well as the maximum temperatures, were the same within experimental error for corresponding samples of both materials.

The differences in physical properties of equivalent calcines of Iceland spar and limestone 89 may reflect differences in the difficulty of removing carbon dioxide from the calcite structure of the materials [7]. The crystallite size of the Iceland spar measured by X-ray line broadening was 0.71 μm, whereas the crystallite size of sample 89 was 0.39 μm. This is the only difference in physical properties measured on the starting materials.

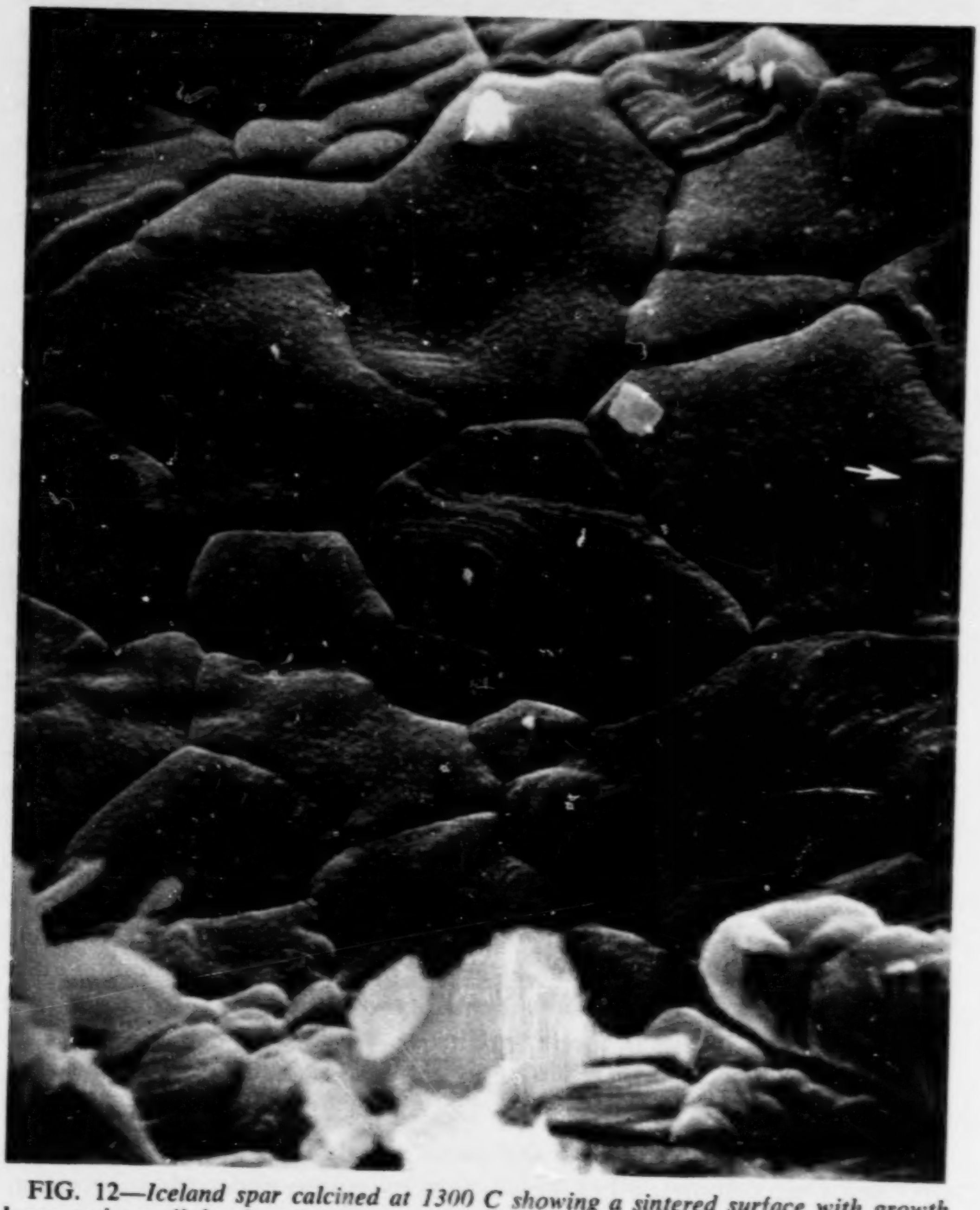

FIG. 12—*Iceland spar calcined at 1300 C showing a sintered surface with growth loops and a well-developed single crystal (arrow) (×4042).*

Perhaps the larger crystallite size of the Iceland spar inhibits the migration of carbon dioxide from the crystal structure.

The results of this study show that the texture of limestone calcines evolves in two distinct steps. Pores form initially as carbon dioxide is released during calcination. Raising the calcination temperature causes the pores to grow by coalescing (that is, big pores grow at the expense of small pores). This textural feature predominates in materials calcined below 1100 C. At about 1100 C, the change in the physical characteristics of the calcium oxide predominates as the limes become compact as a result of sintering and crystal growth of the calcium oxide. These changes are accompanied by a marked decrease in porosity as the calcination temperature is raised. Both stages of textural development may be present in a single particle if the external surface and edges are calcined before the center, as reported in the literature [*6,7*].

Summary and Conclusions

Results of scanning electron microscope and mercury porosimeter studies of the calcines confirm several general observations, among which is the fact that the nature of the uncalcined carbonates influences the properties of their calcines. The larger crystallite size of the Iceland spar confers undesirable physical characteristics on its calcines.

Raising the temperature of calcination causes a systematic evolution of texture in the calcines that is characterized by stages dominated by pore growth and later by sintering and calcium oxide crystal growth. The rate and nature of these changes also are influenced by the characteristics of the starting material. The undesirable pore size distribution of the Iceland spar calcines indicated that its properties were similar to those of some shock-calcined, coarsely crystalline materials that are described in the literature. Properties of calcines prepared from limestone 89 compare favorably with those of some of the reactive limes described [*6*][3].

It can be inferred from these results that solid-fluid reactivity is correlated with pore distribution and surface area.[3,5] The pores provide the reactant fluid with access to the surface area. If diffusion of the gas in small pores is slow [*5*], then each stone has some optimum time and temperature of calcination for development of a favorable pore size distribution and surface area that results in a reactive lime.

Acknowledgment

R. C. Mullins contributed to this paper through discussions of the pore sizes and pore volumes, all of which were measured under his supervision.

References

[1] Mayer, R. P. and Stowe, R. A., "Physical Characterization of Limestone and Lime," *Azbe Award No. 4,* National Lime Association, ~~Washington~~, D. C., 1964.

[2] Goldsmith, J. R. and Graf, D. I., "Relation Between Lattice Constants and Composition of the Ca-Mg Carbonates," *American Mineralogist,* Vol. 43, 1958, pp. 84–101.

[3] Murray, J. A., Fischer, H. C., and Sabean, D. W., "The Effect of Time and Temperature on the Properties of Quicklime Prepared from Calcite," *Proceedings,* American Society for Testing and Materials, Vol. 50, 1950, pp. 1263–1277.

[4] Rootare, H. M. and Prentzlow, C. F., "Surface Areas from Mercury Porosimeter Measurements," *Journal of Physical Chemistry,* Vol. 71, No. 8, 1967, pp 2733–2736.

[5] Potter, A. E., "Sulfur Oxide Capacity of Limestones," *U. S. Public Health Service Symposium on Limestone-Sulfur Dioxide Reaction Kinetics and Mechanisms,* National Air Pollution Control Authority, Cincinnati, Ohio, 1969 (abstract).

[6] Fischer, H. C., "Calcination of Calcite: I. Effect of Heating Rate and Temperature on Bulk Density of Calcium Oxide," *Journal of the American Ceramic Society,* Vol. 38, 1955, pp. 245–251.

[7] Hyatt, E. P., Cutler, I. B., and Wadsworth, M. E., "Calcium Carbonate Decomposition in Carbon Dioxide Atmosphere," *Journal of the American Ceramic Society,* Vol. 41, 1958, pp. 70–74.